Università degli Studi di Padova
Dipartimento di Scienze Chirurgiche, Oncologiche e Gastroenterologiche

SCUOLA DI DOTTORATO DI RICERCA IN
ONCOLOGIA E ONCOLOGIA CHIRURGICA

CICLO XXV

Role of CYBR, a cytohesin binder and regulator scaffold protein, in cell-mediated immune response in vivo

Direttore della Scuola : Ch.ma Prof.ssa Paola Zanovello
Supervisore :Dott. Antonio Rosato

Dottoranda : Dott.ssa Melania Frenati

INDEX

RESULTS

SUMMARY

Cybr (Cytohesin binder and regulator) is an adaptor protein involved in the assembly and recruitment of protein complexes associated with intracellular trafficking and signaling. Cybr has attracted attention as a potential key contributor to molecular mechanisms governing cells of the immune system due to its exclusive expression in cells of hematopoietic origin. Cybr interacts with members of the ADP ribosylation factor (ARF)-activating cytohesin family, mainly cytohesin-1, and it is involved in the cytohesin-1-mediated adhesion of LFA-1 to ICAM-1. Cybr expression is highly and rapidly responsive to, and regulated by, many cytokines and other soluble effectors of the immune system suggesting a potential functional role in the vesicle formation, endocytic trafficking, regulation of TCR signalling and regulation of dendritic cell (DC)/T cell interaction during the antigen presentation. To characterize the *in vivo* physiological role of this molecule, a *Cybr*-deficient mouse strain was created. *Cybr* deletion does not profoundly affect the development of the immune system, but *Cybr*-KO mice display a reduced or delayed capacity to respond to different stimuli and in stress conditions.

This project aimed at investigating the biological function of Cybr in cell-mediated immune response to tumors induced by the retroviral complex constituted by the Moloney murine sarcoma virus/Moloney murine leukemia virus (M-MSV/MuLV, hereafter indicated as M-MSV). Intramuscular injection of M-MSV in immunocompetent C57BL/6 (B6) mice causes sarcomas that spontaneously regress because of a strong immune reaction primarily mediated by cytotoxic T lymphocytes (CTL) specific for viral antigens. Conversely, *Cybr*-deficient mice injected with M-MSV developed larger tumors than B6 mice, which additionally regressed with a slower kinetics. To disclose the biological bases of this behavior, M-MSV-injected *Cybr*-deficient and wild type mice were characterized for the lymphocyte phenotype and function in tumors, lymph nodes and spleens at the peak of tumor growth (day 11 to 15). We found a reduced number of CD4$^+$ and CD8$^+$ T cells, as well as of antigen-specific CTL, in the tumor infiltrating cells (TIL) of *Cybr*-deficient mice. However, this defect was recovered after a short temporal shift.

Similarly, a three-day delay was also reported in the onset of lytic activity in *Cybr*-deficient respect to wild type CTLs. On the contrary, wild type or *Cybr*-deficient memory T cells from tumor regressor mice did not show any difference in terms of lytic activity. Overall, these data indicate that *Cybr* deficiency has a significant impact on the activation of naive T cells and expansion of primed T cells, but do not clarify whether Cybr mostly influence priming and/or cell adhesion or trafficking and migration of immune system cells. To address this issue, we transferred naive *Cybr*-KO or wild type GFP T cells in tumor-bearing RAG2-/- γc-/- mice, that lack T, B and NK cells and

do not spontaneously regress M-MSV-induced tumors. Despite T cell transfer, tumors continued to growth indicating that transferred naive T cells were not able to mount a fully effective immune response in this setting. This was probably due to a suboptimal recruitment and priming phase in lymph nodes, that were found to be hypoplastic. To provide a mechanistic insight, reconstitution of nu/nu athymic B6 mice with T cell-depleted bone marrow from either wild type or *Cybr*-KO mice, followed by adoptive transfer of naive or memory T cells from *Cybr*-KO/GFP or B6/GFP animals, will provide the appropriate experimental set up to assess the role of Cybr in the APC or T cell compartments.

Taken together, outlined results indicate that Cybr deficiency has a significant impact on antigen-specific immune response, but further studies have to be performed to fully dissect the role played by this molecule in the priming phase and in the delayed onset of lytic activity.

RIASSUNTO

Cybr (cytohesin binder and regulator) è una proteina adattatrice coinvolta nell'assemblaggio e nel reclutamento di complessi proteici associati con il trafficking intracellulare e la trasduzione del segnale. Grazie alla sua esclusiva espressione in cellule di origine ematopoietica, Cybr ha attirato l'attenzione come potenziale proteina chiave nei meccanismi molecolari che controllano le cellule del sistema immunitario. Cybr interagisce con i membri della famiglia delle citoesine attivanti gli ADP ribosylation factors (ARF), specialmente con citoesina-1, e regola l'adesione citoesina-1 mediata di LFA-1 a ICAM-1. La sua espressione è rapidamente regolata da molte citochine e da altri effettori solubili del sistema immunitario. Alcuni ruoli funzionali proposti per questa molecola sono la partecipazione nella formazione delle vescicole, nel trafficking endocitico, nella regolazione del signaling del TCR e nell'interazione tra cellule dendritiche e cellule T durante la presentazione dell'antigene. Al fine di caratterizzare il ruolo fisiologico di questa molecola *in vivo*, è stato creato un ceppo di topi deficienti per *Cybr*. Questi topi, nonostante un normale sviluppo del sistema immunitario, mostrano una ridotta o ritardata capacità di rispondere a diversi stimoli e in condizioni di stress.

Questo progetto di ricerca si è prefisso di investigare la funzione biologica di Cybr nella risposta immunitaria cellulo-mediata nei confronti di tumori indotti dal complesso retrovirale costituito dai virus sarcomatogeno e leucemogeno murini di Moloney (M-MSV/MuLV, in seguito indicato come M-MSV). L'inoculo intramuscolare di M-MSV in topi C57BL/6 (B6) immunocompetenti causa lo sviluppo di sarcomi che regrediscono spontaneamente grazie ad una forte risposta immunitaria mediata principalmente da linfociti T citotossici (CTL) specifici per gli antigeni virali. Al contrario, topi *Cybr*-deficienti inoculati con M-MSV sviluppano tumori di dimensioni maggiori e che regrediscono più lentamente rispetto ai controlli. Per comprendere i motivi di questo diverso andamento, dopo l'inoculo del complesso retrovirale in topi *Cybr*-deficienti e wild type, sono stati caratterizzati a livello fenotipico e funzionale i linfociti presenti nei tumori, nei linfonodi drenanti e nelle milze al momento della massima crescita tumorale (giorni 11-15). Abbiamo riscontrato un ridotto numero di linfociti T CD4$^+$ e CD8$^+$ e di CTL antigene specifici nella popolazione infiltrante il tumore nei topi *Cybr*-deficienti. Tuttavia questa differenza si è ridotta alla fine del periodo analizzato.

Inoltre, un ritardo simile è stato riportato nello sviluppo dell'attività litica nei CTL provenienti da topi *Cybr*-KO rispetto a topi wild type. Al contrario, linfociti T memoria wild type e *Cybr*-KO non hanno mostrato nessuna differenza in termini di attività litica. Complessivamente, questi dati indicano che la deficienza di Cybr ha un significativo impatto nell'attivazione delle cellule T naive

e nella loro espansione dopo il priming, ma non definiscono se questa proteina influenzi maggiormente la fase di priming e/o adesione cellulare o il trafficking e la migrazione delle cellule del sistema immunitario. Per chiarire questi aspetti, sono stati trasferiti linfociti T naive provenienti da topi *Cybr*-KO/GFP o B6/GFP in topi RAG2-/- γc-/- inoculati con il complesso retrovirale. Questi topi mancano di cellule T, B e NK e non regrediscono spontaneamente i tumori M-MSV indotti. Nonostante l'infusione di cellule T, i tumori hanno continuato a crescere, indicando che le cellule T naive non sono state in grado di montare una risposta immune pienamente efficace in questo modello, un aspetto probabilmente dovuto ad un reclutamento e priming sub ottimali nei linfonodi, che sono risultati ipoplastici. Al fine di rispondere a questi quesiti biologici, topi B6 nu/nu atimici ricostituiti con tessuto midollare depleto di linfociti T provenienti da topi wild type o *Cybr*-KO e successivamente infusi con linfociti T naive o memoria provenienti da topi *Cybr*-KO/GFP o B6/GFP, dovrebbero costituire un modello sperimentale ottimale per investigare il ruolo di Cybr sia nel comparto T che nel comparto APC.

Nell'insieme, i risultati ottenuti indicano che la deficienza di Cybr ha un significativo impatto nella risposta immune antigene-specifica, ma studi addizionali devono essere condotti al fine di definire con maggior precisione il ruolo di Cybr nella fase di priming e nel ritardo dello sviluppo dell'attività litica.

INTRODUCTION

1. The immune system: innate and adaptive immune responses

The immune system evolved under selective pressure imposed by infectious microorganisms through various defense mechanisms that have the capacity to be triggered by infection and to protect the host organism by destroying the invading microbes and neutralizing their virulence factors. It is composed by two main arms, the innate and the adaptive immune response. The innate immune system is the first line of host defense against pathogens and is characterized by receptors with a fixed germline-encoded specificity, which recognizes a genetically-determined set of ligands. One key group of innate receptors is the pattern recognition receptor (PRR) superfamily which recognizes evolutionary-conserved pathogen-associate molecular patterns (PAMPs) [1]. Moreover, Toll like receptors play the major role in pathogen recognition and in inflammatory initiation of the immune responses [2]. Cells of the innate immune response include neutrophils, monocytes, macrophages and dendritic cells (DC), which react rapidly to control pathogen growth and promote inflammation [3]. However, remains unclear the molecular mechanism between the polymorphonuclear (PMN) cells and tumor cells. It is know that FcγR on PMN interacts with antibody-coated antigens on tumor cells, leading to the release of cytokines and chemokines which influence the recruitment and the activation of DC and macrophages in tumor site [4]. Macrophages can efficiently eliminate apoptotic tumor cells by phagocytosis. Furthermore, they express FcγR that, when is activate, stimulate cytotoxicity to tumor cells [5]. Nevertheless, the macrophages are the major contributors to a chronic inflammation that affords an immune suppression environment in the tumor milieu, that can benefit its growth [6]. The DC are professional antigen presenting cells (APC) and are the interface between the innate and adaptive immune response. When DCs encounter a pathogen, mature and process the antigen, increasing the Major Histocompatibility Complex (MHC) molecule expression, and migrate to the lymph nodes where they can prime the naive T cells [7].

Normally the innate immune system responds with a rapid mechanism without recourse to the adaptive immunity; however, sometimes the innate system required this cross-talk with the adaptive immune response to deal with the infections [1]. Therefore, adaptive immunity is triggered in vertebrates when a pathogen evades the innate immune system and generates a threshold level of antigen [8]. An antigen (short for *anti*body*gen*erator), is defined as any substance (in particular, proteins and many polysaccharides) capable to bind to a specific antibody and elicit the adaptive immune response [9]. The parts of the antigen that interact with an antibody molecule or lymphocyte receptor (namely, BCR- B cell receptor, and TCR- T cell receptor, respectively) are called epitopes. Most antigens contain a variety of epitopes and can stimulate the production of antibodies by B cells, specific T cell responses, or both. BCR and TCR possess variable regions created by a complex process of somatic gene segment rearrangement. This mechanism allows a small number of genes to generate a vast number of different antigen receptors, which are then uniquely expressed on each individual lymphocyte and also account for the varying and random specificities of immune cells. The variable-region receptors of the adaptive immune system respond to particular pathogen structures, with BCRs directly recognizing peptide sequences on pathogens, such as components of bacterial cell membranes, and TCRs recognizing peptide sequences only in the context of the MHC. As a result, B cells play a large role in the humoral immune response, whereas T cells are intimately involved in cell-mediated immune responses [10].

The efficiency of the adaptive immune response relies on the capacity of immune cells to distinguish between the own body cells from unwanted invaders. The adaptive response is thus triggered only after recognition of non-self antigens. This ability is acquired during maturation processes in the thymus by T cells or bone marrow by B cells. In these organs, immature lymphocytes undergo positive and negative selection phases. In particular, in the thymus, immature T lymphocytes, harboring misfolded TCR or TCR that is unable to bind with self MHC molecules, are committed to die by apoptosis. Whereas, lymphocytes that recognize MHC complexes with the right avidity are selected (positive selection). During negative selection, T cells that strongly interact with MHC coupled with endogenous peptides are committed to die [10].

Finally, only naive lymphocytes able to recognize exogenous peptides in the context of self MHC can exit the thymus and reach lymph nodes, spleen and damage tissues. In the lymph nodes and spleens, lymphocytes interact with and are activated by mature dendritic cells only if their antigen receptors bind with the peptide presented by the DCs and they receive co-stimulatory signals from the DCs. Hence, naive T lymphocytes first undergo an intense period of proliferation, termed clonal expansion and then differentiate into either several classes of effector T lymphocytes or memory T lymphocytes. In the lymph node, DCs display non-self antigens on their surface by coupling them to MHC molecules (also known in humans as Human Leukocyte Antigen –HLA [9]. Although some exception does exist (cross-presentation process and autophagy), exogenous antigens are usually displayed on MHC class II molecules, which activate $CD4^+$ helper T cells while endogenous antigens (from viral or mutated proteins), are typically displayed on MHC class I molecules, and activate $CD8^+$ cytotoxic T cells. As well as activating T cells, DCs are important inducers of peripheral tolerance to self antigens, that are captured by DCs in the periphery and presented to T cells in the lymph nodes. Presentation of self antigens under steady state pathogen-free conditions induces tolerization through T cell apoptosis or anergy [7],[11],[12].

2. T cells

2.1 Helper T cells

T cells contribute to immune defenses in two major ways, by directing and regulating the immune responses and by directly attacking infected or cancerous cells. CD4$^+$ lymphocytes, as called also helper T cells, are all variously involved in the regulation of immune responses, through the action of cytokines that either stimulate or inhibit the function of other lymphocytes and APC and furthermore lead to co-stimulation or direct inhibition through cell-to-cell interactions. These cells can also display direct cytotoxic activity [13], but primarily they manage the immune response by directing other cells to kill infected and cancerous cells or clear pathogens.

CD4$^+$ T lymphocytes can be grouped into different subsets according to functional properties and cytokines secretion patterns. Originally, these cells were simply classified as Type 1 (Th1) and Type 2 (Th2) helper T cells. The differentiation of Th1 is primarily driven by interleukin-12 (IL-12) and interferon-γ (INF-γ). Th1 regulates delayed type hypersensitivity reactions, cell-mediated immunity to intracellular pathogens and tumor cells by producing high levels of IFN-γ, tumor necrosis factor-α (TNF-α), and IL-2. Conversely, Th2 cells are characterized by IL-4, IL-5, IL-10, and IL-13 production, operate in coordinating humoral immunity, eosinophilic inflammation, and are also involved in the control of helminthic infections.

In the last few years, new distinct subsets of CD4$^+$ T cells have been identified. A lineage distinct from Th1 and Th2 was recently described as Th17 cells, a CD4$^+$ T cell subset that selectively produces the IL-17 cytokine, in addition to TNF-α, IL-6, IL-21, and IL-22. The autocrine production of IL-21, together with IL-1 and low doses of IL-12, were shown to antagonize the Th1 differentiation in favor of Th17. Moreover, IL-23, whose action is inhibited by IFN-γ and IL-4, is necessary for the maintenance of Th17 and IL-17 production. Th17 are supposed to coordinate tissue inflammation and autoimmunity and protect against extracellular bacteria and fungi [14],[15]. More recently, a population of CD4$^+$ T cells secreting IL-22, but neither IL-17 nor IFN-γ, was isolated from human skin-homing memory T cells, and, therefore, identified as Th22 [16],[17]. The differentiation of this subpopulation of helper T cells, that show a potential role in skin homeostasis and diseases [18], may be promoted by stimulation of naive T cells in the presence of IL-6 and TNF or by the presence of plasmacytoid dendritic cells [16],[19].

In addition to helper cells, CD4$^+$ T lymphocytes also include a heterogeneous population of cells endowed with regulatory functions, namely regulatory T cells (Tregs). In particular, Tregs are of pivotal importance in the homeostatic control and suppression of immune responses, thus constituting an important mechanism in controlling the autoimmune diseases development. Tumor

Growth Factor-β (TGF-β)-induced, naturally occurring or peripherally-induced Tregs derive from the thymus and express high levels of CD25, glucocorticoid-induced TNF receptor, and the transcription factor forkhead box protein 3 (FoxP3). These cells mediate immune suppression through a cell-to-cell contact-dependent mechanism and, once activated, they are able to induce suppression in an antigen-independent fashion [20],[21].

2.2 CD8$^+$ T lymphocytes and cytotoxicity

Cytotoxic T lymphocytes (CTL) are a sub-group of T cells whose role is to monitor all the cells in the body, and are ready to destroy any that is considered to be a threat to the integrity of the host; for example, CTLs kill virally infected cells, preventing them from being the source of more viral pathogen [22]. Moreover, CTLs are also thought to provide some degree of protection against spontaneous malignant tumors, by virtue of their ability to detect quantitative and qualitative antigenic differences in transformed cells. In this regard, transformation results in an altered protein repertoire that can be sensed by CD8$^+$ T cells through binding of peptide-MHC class I complexes [23].

Naive CD8$^+$ T cells are activated into effector cells when their TCR strongly interacts with a peptide-bound MHC class I molecule and concomitantly receive costimulatory and IL-2 mediated signaling. Once activated, CTL undergo a process called clonal expansion in which it gains functionality, and divides rapidly, to produce an army of effector cells, that display cytotoxic activity upon encounter of an infected or mutated target cell in an inflammatory milieu. CTLs may kill target cells by one of, at least, three distinct pathways, two of which involve direct cell–cell interactions between effector and target cells. The third is mediated by cytokines, such as IFN-γ and TNF-α, that differently impact on target cells (Fig. 1a). In particular, TNF-α engages its receptor on the target cell and triggers the caspase cascade, leading to target-cell apoptosis. IFN-γ, however, induces transcriptional activation of the MHC class I molecules and Fas in target cells, leading to enhanced presentation of endogenous peptides, and increases Fas-mediated target-cell lysis. Cytolytic activity, requiring direct cell–cell contact which results in apoptosis of target cells, can be mediated by two different mechanisms. In one case, the Fas ligand, expressed on the surface of CTLs, binds to the Fas receptor (Fas, CD95) on the target cell (Fig. 1b) and triggers apoptosis through the classical caspase cascade [24]. In the other case, the CTL releases perforin and granzymes into the intercellular space (Fig. 1c) which are highly cytotoxic, but CTLs have elaborated a mechanism to protect themselves and neighboring cells from being killed accidentally. Firstly, the majority of the cytotoxic proteins are pre-synthesized, and so ready to be used in killing upon encountering a target cell. The regulated secretory organelles, in which the lytic proteins are stored, mobilize themselves to the cell surface and expose their content only upon contact with a target. CTLs use their lysosomes as regulated secretory organelles, which are often referred as secretory lysosomes [25]. Secondly, the secretory lysosomes do not exocytose their content randomly, but are mobilized to a defined point in the plasma membrane that is immediately opposite the target cell, termed secretory domain of the immunological synapse (see below). Thirdly, the secretory lysosomes release their content into a defined space, or “cleft,” that is formed between the otherwise tightly opposed CTL and the target-cell membranes, thus sparing innocent neighboring bystander cells. This organization therefore, concentrates the cytotoxic proteins for maximum impact and confines them to the environment of the target cell. The entry of the granular material in target cell causes cell death in a caspase-dependent or –independent manner [26].

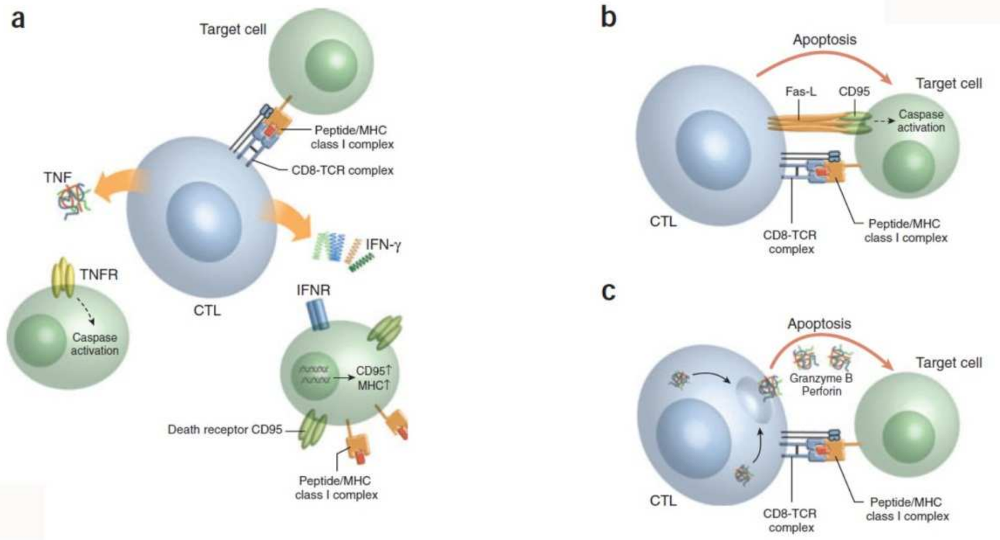

Figure 1. CTL-mediated cytotoxicity. (**a**) Indirect killing of target cells by release of tumor necrosis factor-α and IFN-γ. (**b**) Induction of apoptosis in target cells via death receptor triggering. (**c**) Direct killing by release of granzyme B and perforin into the intercellular space between CTL and target cell. TNF, tumor necrosis factor; TNFR, tumor necrosis factor receptor; IFNR, IFN receptor; Fas-L, Fas ligand. Modified from [22].

Upon infection resolution, most of the effector cells die by apoptosis due to prolonged activation (AICD, activation-induced cell death) and cytokines starvation or undergo a state of functional exhaustion [27]. Only a few of these antigen-specific cells are retained as memory cells [8]. Upon a later encounter with the same antigen, the memory cells quickly differentiate into effector cells, dramatically shortening the time required to mount an effective response and conferring thus a protective immunity to the host.

Progressive T cells differentiation from naive to effector and memory T cells is characterized by particular phenotypic, functional and transcriptional attributes [28]. Naive T cells (TN cells) are conventionally defined by the co-expression of the RA isoform of the transmembrane phosphatase CD45, the lymph node homing molecules L-selectin (CD62L) and CCR7, and the co-stimulatory receptors CD27 and CD28 [29]. These phenotypic characteristics facilitate T cell to entry into secondary lymphoid organs to probe APCs for cognate antigen and to respond to activating signals that give rise to more differentiated memory and effector progeny [30]. Among CD45RO-expressing T cells, two major subsets of memory T lymphocytes are defined on the basis of CD62L and CCR7 expression [31]. Similar to TN cells, CD62L and CCR7 expression is retained on central memory T (TCM) cells, whereas it is lost on more differentiated effector memory T (TEM) cells. Functionally, these phenotypic differences allow antigen-specific TCM and TEM cells to patrol the central lymphoid organs and the peripheral tissues, respectively [30],[31]. The co-stimulatory receptors CD27 and CD28 are also found in the majority of memory T cells; however, expression can be lost as cells become terminally differentiated by progressively acquiring inhibitory signaling molecules, such as killer cell lectin-like receptor subfamily G, member 1 (KLRG1) [32],[33] and through transition into senescence [32],[34]. In contrast to TN cells, memory T cells are capable to rapidly release of cytokines on restimulation [35]. Both subsets are capable to produce TNF-α, while TCM cells secrete IL-2 more efficiently. TEM cells have an increased capacity to IFN-γ release and cytotoxicity [32],[31]. All antigen-experienced T cells upregulate the common IL-2 and IL-15β receptor (IL-2Rβ) — conferring the ability to undergo homeostatic proliferation in response to IL-15 [36],[37] — and also display high amounts of CD95 [38], a receptor that provides either co-stimulatory or pro-apoptotic signals depending on the efficiency of CD95 signalling complex formation and on which particular intracellular signaling proteins are part of the complex31. Recently, CD95 and IL-2Rβ have been found to be expressed in a subset of phenotypically naive-appearing T cells [39]. These cells were observed in viral and tumor-reactive T cell populations and, similar to conventional memory T cells, displayed a diluted content of TCR excision circles, possessed the ability to rapidly release cytokines on activation and proliferation in response to IL-15 [39]. These cells, the least differentiated population of antigen-experienced T cells identified to date, were termed stem cell memory T (TSCM) cells by virtue of their enhanced capacity to self-renew and their multipotent ability to generate all memory and effector T cell subsets [39].

2.3 The immunological synapse

An immunological synapse (or immune synapse) is the interface between an antigen-presenting cell and a lymphocyte [40]. In the CTL–target cell junction, a cascade of activation signals causes rapid segregation of cell surface receptors into three concentric compartments, called the central, peripheral and distal supramolecular activation complex (SMAC) (Fig. 2) [41]. The peripheral SMAC (pSMAC) comprises Leucocyte Function Associated antigen 1 (LFA-1), clustered with the cytoskeletal protein talin on the CTL, and Intercellular Adhesion Molecule (ICAM) on the target cell. Within the pSMAC is the central SMAC, where TCR accumulates. This area is also enriched in TCR associated signaling proteins including TCRζ, Lck, ZAP-70 and PKCθ, CD2, CD4, CD8, CD28, Lck, and Fyn, and was assumed to be the site of TCR signaling. Beside it, there is a secretion domain where lytic granules fuse to release their content. The centrioles of the centrosome dock beside the cSMAC, which acts as a focal point for minus end microtubule-mediated delivery of lytic granules. Actin accumulation occurs in a distal SMAC (dSMAC) (Fig. 2) [42], [43].

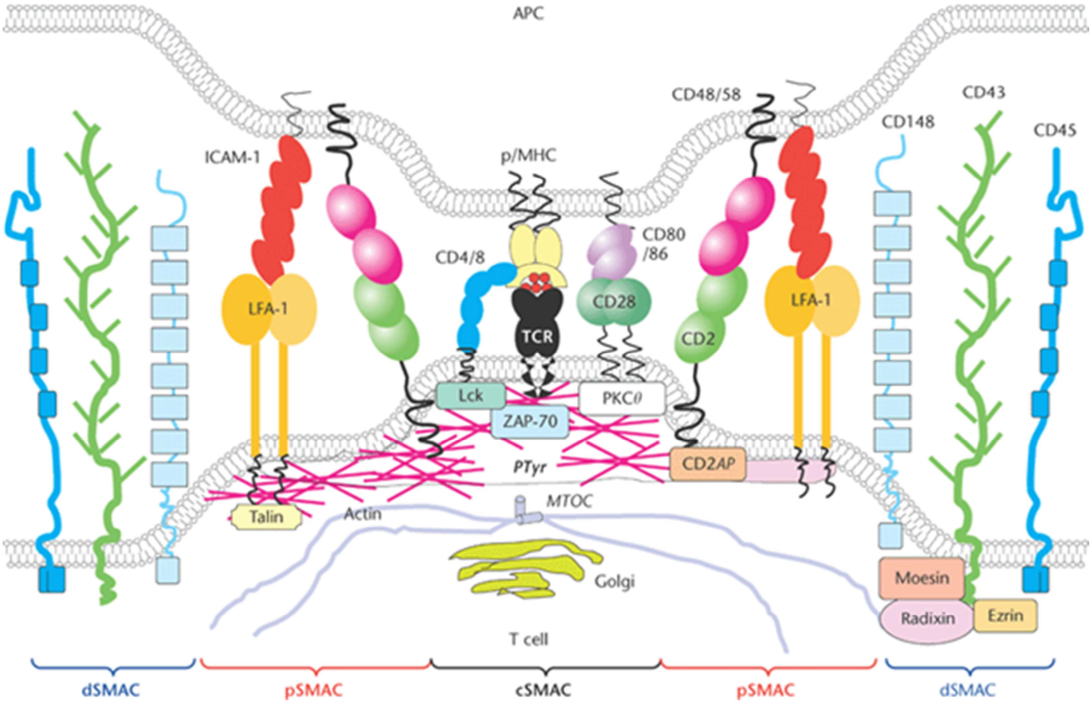

Figure 2. Schematic representation of the mature Immunological Synapse . The IS is composed of three major regions: the cSMAC containing TCR and accessory molecules, the pSMAC containing adhesion molecules and the dSMAC containing large and heavily glycosylated trans-membrane proteins. Intracellular signaling components and cytoskeleton components segregate in parallel with surface molecules within the three major zones of the IS. Modified from [44].

The central part in the immunological synapse is the TCR, a heterodimer molecule responsible for recognizing antigens bound to MHC molecules. The TCR is composed of two different protein chains that are expressed as a part of a complex with the invariant CD3 chain molecule. In 95% of T cells, this consists of an alpha (α) and beta (β) chain, whereas in 5% of T cells this consists of gamma and delta (γ/δ) chains. Each chain is composed of a Variable (V) region and a Constant (C) region. The Constant region anchors the TCR to the cell membrane and including a short cytoplasmic tail, while the extracellular Variable region binds to the antigen-MHC complex.

The Variable domain of both the TCR α-chain and β-chain have four hypervariable (HV) or complementarity determining regions (CDRs), that contact the antigen-MHC complex. TCRs possess unique antigen specificity, determined by the structure of the antigen-binding site formed by the alpha and beta chains [8], which are generated by V(D)J recombination. The unique combination of these segments, which corresponds to the CDR3 region, accounts for the great diversity in specificity of the T cell receptor for processed antigen.

The TCR associates with other molecules like CD3, which possess three distinct chains (γ, δ, and ε) in mammals and either a ζ_2 (CD247) or a ζ/η complex. These accessory molecules have transmembrane regions that are vital to propagate the signal from the TCR into the cell; the cytoplasmic tail of the TCR is extremely short, making unlikely to participate in signaling. The CD3- and ζ-chains, together with the TCR, form the T cell receptor complex. The TCR signal is enhanced by simultaneous binding to the MHC molecules by specific co-receptors, namely CD4 and CD8 molecules, which not only ensure the specificity of the TCR for an antigen, but also allow prolonged engagement between the APC and the T cell and recruit essential molecules (e.g., Lck) involved in the intracellular signaling of the activated T lymphocyte.

When the TCR engages antigens/MHC, the T lymphocyte become activated through a series of biochemical events mediated by associated enzymes, co-receptors, specialized accessory molecules, and activated or released transcription factors. The most common mechanism for activation and regulation of molecules beneath the lipid bilayer, is via phosphorylation/dephosphorylation by protein kinases. T cells utilize the SRC family of kinases in transmembrane signaling largely to phosphorylate tyrosines that are part of immunoreceptor tyrosine-based activation motifs (ITAM) [45].

In particular, when a T cell receptor is activated by contact with a peptide-MHC complex, CD45 dephosphorylates and activates Fyn, which in turn phosphorylates the ITAMs on the CD3 and ζ chains. This allows other kinases like ZAP-70 to bind on the ITAM near Lck, previously recruited and activated by CD4 or CD8. Lck phosphorylates ZAP-70, which in turn indirectly activate PLC-γ, resulting in gene transcription in the nucleus [46]. This is accomplished through an adaptor protein such as LAT, which brings together the activate ZAP-70 and PLC-γ. The recruitment of proximal signaling kinases like ZAP-70 and adaptor proteins, initiates a downstream signaling cascade events including activation of Rho family GTPases, Ras/MAPK, PLC, and Ca^{2+} mobilization [47],[48],[49]. The actin cytoskeleton reorganizes, the Golgi and the microtubule-organizing center (MTOC) reorient toward the target cell [50],[51]. Upon TCR ligation, cytolytic granules move via polarized microtubules to the region of the MTOC where they dock prior to release. The mechanisms regulating the docking fusion and the release process are not well understood. However, there is evidence to suggest important roles for the small GTPase Rab27A, and Munc13-4, a member of a family of proteins known for their roles in priming neuronal synaptic vesicles for fusion and release [52],[53]. In the CTL synapse, vesicle release appears to occur in a secretory domain distinct from the signaling domain containing the TCR complex [54],[55]. The close opposition and highly organized topography of the CTL synapse, allows the release of highly toxic components of secretory granules in a process that likely avoids damaging nearby cells. Tight control is critical since the contents of just a small number of granules are enough to elicit apoptosis in the target cell [54].

However, there are key differences between the synapse formed by active $CD8^+$ CTLs and $CD4^+$ T cells. A $CD4^+$ T cell interaction with its target may last many hours, prolonging signaling cascades necessary for gene activation, proliferation, and differentiation, while a CTL might only require minutes to initiate an irreversible apoptosis cascade to its target [54]. The antigen/MHC I recognition complex is a potent inducer of CTL cytotoxic activity. Remarkably, as little as one TCR/MHC I interaction may be all that is necessary to elicit a cytolytic response [56].

3. Trafficking and cell adhesion

3.1 Molecules involved and mechanisms

Trafficking and cell adhesion are key properties of both innate and adaptive immune responses. To facilitate T cell interaction with antigen-presenting cells, leukocytes that circulate as non-adherent cells, can be recruited to a specific site of infection or inflammation [57]. Cytokines (i.e. IL-4 or IFN-γ) released at the site of infection, create a chemotactic gradient to recruit T cells and inflammatory stimuli, activate vascular endothelial cells to express adhesion molecules and chemokines that physically engage circulating leukocytes and promote their adhesion to these vessels. The process of recruitment first involves T cells rolling along the surface of vascular endothelial cells, followed by the arrest and, finally, transendothelial migration (diapedesis) of T cells into tissue [58],[59],[60],[61]. The cell adhesion molecules (CAMs) involved in the initial steps of recruitment are E- and P-selectins, followed by L-selectin [62],[63]. The arrest process involves the tethering (adhesion) and spreading of T cells [64],[65]. Molecules that play a critical role in controlling this process are integrins, such as Very Late Antigen-4 (VLA-4), which is one of six identified β1 integrins, and LFA-1, a member of the β2 integrin family [66],[67]. The ligands for these integrins include VCAM-1 (Vascular Cell Adhesion Molecule-1) for VLA-4 and ICAM-1, -2, and -3 for LFA-1. In particular, LFA-1, a cell surface receptor found on leukocytes, is composed by αL- and β2-subunits, which are designated as CD11a, and CD18, respectively. The αL-subunit of LFA-1 contains an I- (inserted) domain that is essential for binding to ICAM-1. ICAM-1, a member of the immunoglobulin superfamily (IgSF), is a transmembrane glycoprotein that has five immunoglobulin-like domains (D1–D5); mutational studies have revealed that domain-1 (D1) contains residues that are crucial for binding to LFA-1 [68],[69]. ICAM-1 is found at the cell surface of endothelial and epithelial cells, leukocytes, dermal fibroblasts, melanocytes, and many carcinoma cell types; its expression is up-regulated by cytokines such as IFN-γ, IL-1, and TNF-α, leading to a selective recruitment of leukocytes in a variety of pathological states [70],[71].

The secure adhesion of T cells to epithelial or endothelial cells represents the demarcation point that allows T cells to complete extravasation into the surrounding tissue. When ICAM-1/LFA-1 interact, the adhesion mediated by VLA-4 and -5 decreases, indicating that a hierarchy exists in which LFA-1 plays a predominant role over VLA-mediated T cell migration [72]. By inhibiting ICAM-1/LFA-1 interaction, T cells are prevented from firm adhesion to epithelial, endothelial, or APC cells and are thus prevented from taking part in the immune response.

The ICAM-1/LFA-1 interaction plays also a critical role during the priming phase. Indeed, naive T cells require both an antigen-specific and a co-stimulatory signal (namely, Signal-1 and Signal-2, respectively) to be fully activated during the interaction with the APC [40]. This co-stimulatory signal is provided by interactions of several different pairs of molecules at the interface between T cells and APC, including LFA-1 on T cells and ICAM-1 on the APC or B-7 (found on B cells) and CD28 (found on T cells). The TCR-MHC-antigen binding in the absence of the Signal-2, not only fails to activate the cell, but also leads to a state called anergy, in which the T cell becomes refractory to activation. A high density of TCR–MHC-antigen complexes cannot compensate for the lack of a co-stimulatory signal such as ICAM-1/LFA-1 interaction for CD4$^+$ T cell activation [73]. Moreover, the source of this secondary signal can influence the type of response generated by T cells. For example, blocking CD28/B-7 inhibits IL-4 and IL-5 (Th2 cytokines) production, while blocking ICAM-1/LFA-1 leads to a significant increase in Th2 cytokines [74].

Another study demonstrated that co-stimulation by ICAM-1/LFA-1 strongly inhibits IL-10 production, which may favor the development of Th1 rather than Th2 cells [75].

3.2 Integrin regulation

Integrins participate in T cell activation and effector functions by promoting T cell contact with APCs during antigen recognition and priming [76]. Moreover, they are important in the migration and retention of T cells in different microenvironments in the body. Naive T lymphocytes exhibit a high rate of motility that facilitates rapid movement into and through secondary lymphoid organs [77],[78], where they are continually exposed to integrin cognate binding partners. Consequently, integrin receptors expressed on unactivated T cells exhibit a low basal state of functional activity that does not promote strong adhesion between T cells and relevant counter-receptors and extracellular matrix ligands. However, upon TCR ligation, the functional activity of integrins is rapidly enhanced following stimulation of the antigen-specific CD3/T cell receptor (TCR) complex; it results in robust increases in integrin-mediated adhesion of T cells to purified integrin ligands and to antigen-laden APCs [79],[80],[81] and reduced motility *in vitro* [82], and enhanced interaction with APCs in lymphoid organs during antigen stimulation *in vivo* [77],[78]. Thus, integrin activation provides a mechanism by which T cells can enhance their interactions with the extracellular environment in order to receive and integrate extracellular signals critical for optimal antigen-dependent T cell activation and differentiation [83]. In this so-called outside-in signaling, cytohesins have been implicated as possible signaling intermediates. Integrin activation initiated by TCR occurs within minutes following T cell stimulation and is one of the earliest detectable changes in the behavior of T cells following activation. Increased integrin-mediated adhesion following TCR stimulation does not require changes in levels of integrins on the T cell surface. Consequently, alterations in integrin function following TCR signaling involve either qualitative alterations in integrin conformation or enhanced clustering of integrins on the T cell surface. Changes in the redistribution of integrins in response to TCR signaling have been well documented, the most notable examples is the movement of the LFA-1 and a4b1 integrins to the periphery in the contact site between activated T cells and APC [41],[84],[85]. However, changes in integrin conformation in the context of antigen stimulation of T cells, particularly *in vivo*, are incompletely understood. In the case of T cells, analysis of LFA-1 function using fluorescence photobleaching recovery and single-particle tracking has shown that LFA-1 mobility (regulated by cytoskeletal attachment) and conformation are clearly linked [86]. These experiments indicate that multiple conformations of LFA-1 exist on the T cell surface, each with a unique diffusion profile. On resting T cells, both inactive and active conformations of LFA-1 are mobile, while intermediate conformations of LFA-1 are tethered to the cytoskeleton and thus are immobile (Fig. 3).

Stimulation of T cells with the phorbol ester phorbol-12-myristate-13-acetate (PMA), which activates protein kinase (PK) C, releases cytoskeletal constraints on the intermediate LFA-1 receptors, thereby promotes receptor–ligand interactions. In contrast, LFA-1 in the active conformation, becomes immobile following stimulation to stabilize adhesion, and this cytoskeletal attachment is further enhanced following ligand engagement. Thus, changes in the distribution of the LFA-1 various conformations between mobile and cytoskeleton-attached immobile pools provides a dynamic mechanism by which T cells can regulate their adhesive potential. The ability to rapidly modulate integrin function in response to external signals is common to many hematopoietic cells. In particular, the control of the activation status of LFA-1on DC may be a key mechanism by which these cells regulate their interaction with T cells [87].

Early during the T cells priming, a scanning process takes place, connecting the antigen-presenting cell with the T cell for a limited time. [78],[88]. The initial contact between T cells and DCs is antigen independent, [89] and only if antigen recognition occurs, the interaction is productive, leading to a strengthening of the conjugate, synapse formation and finally activation of antigen-specific T cells. Otherwise, the interaction between T cell and DC is loose and transient [90],[77],[43]. In both cases the connection release between the two cell types is necessary to continue the process of immune response, either to allow the clonal expansion of activated T cell or to continue the scanning process. Although many molecules are known to build cell conjugates, the termination of them was not equally studied. Given the importance and the calculated incidence of DC–T cell contacts during the scanning process, which ranges between 500 and 5000 encounters per hour [78], it is well assumable that this process is actively regulated. For example, the scaffold protein Cybr is an emerging candidate regulator of LFA-1 activity in both dendritic and T cells [87].

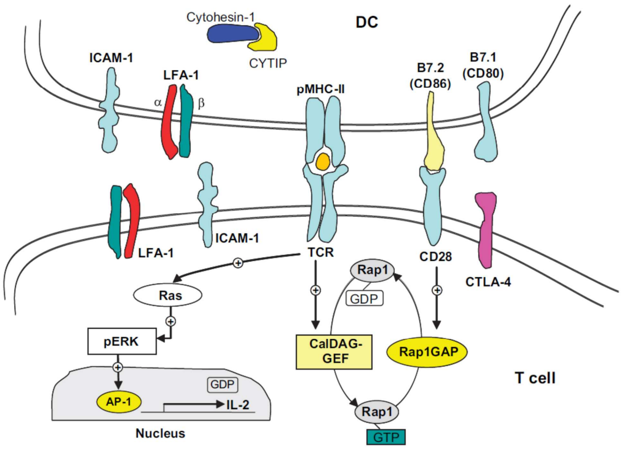

Figure 3. A hypothetical scenario of signaling events underlying contact formation of T cells and antigen-specific DCs. Notice the cycle between guanosine diphosphate (GDP)-bound inactive Rap1 and guanosine triphosphate-bound active Rap1. The induction of the active form is mediated through the Ca2+ and DAG-guanine exchange factor (CalDAG-GEF), whereas the GTPase activity of Rap1 is initiated by the Rap1-GTPase-activating protein (Rap1GAP). Modified from [91].

4. The scaffold protein Cybr

4.1 Discovery of *Cybr* gene

Cytohesin binder and regulator (Cybr) is a novel adaptor protein that participates in the assembly and recruitment of protein complexes associated with intracellular trafficking and signaling. Owing to its exclusive expression in cells of hematopoietic origin, Cybr is consider a potential key contributor to molecular mechanisms governing cells of the immune system [92]. The *Cybr* cDNA was originally cloned and sequenced by Dixon and Pohajdak group in the early 1990s from a subtractive hybridization of human natural killer (NK) cell-enriched transcripts minus those of a T helper cell line [93]. Of the several hundred clones obtained, 13 were new, previously undiscovered gene transcripts. In 1998 the cDNA sequence for this protein named cytohesin-binding protein HE has been deposited in the Genbank with the accession number AF068836. It was similar to the sequence of a protein termed B3-1 with the L06633, submitted by Dixon and colleagues [93], which today corresponds to a slightly truncated *Cybr* cDNA. On the basis of its deduced amino acid sequence, B3-1 was classified as a non-secreted non-membrane-bound protein containing an unusually long leucine zipper, a putative nuclear targeting sequence, and a motif found in many oncogenes, transcription factors and interleukins. The full transcript was finally elucidated based on genomic clones and the human genome sequencing project, and the 29 kb gene was ultimately assigned to the human Chromosome 2 band q11.2 and renamed *PSCDBP* (Pleckstrin homology Sec7 and coiled coil domains binding protein) [94], also known as *Cybr*, *CASP* (cytohesin-associated scaffolding protein,[95]) and *CYTIP* (cytohesin interacting protein,[96]). The *Cybr* gene comprises eight exons giving a transcript with a 1077 bp open reading frame, and corresponds to a polypeptide of 359 amino acids.

4.2 Expression profile, transcriptional activation and transcript properties

The expression profile of Cybr in Unigene (NCBI) reported high expression in the lymph, lymph nodes, blood, bone marrow, spleen and thymus and was supported also by northern analysis of a panel of cell lines, such as showed in lymphoid cells (NK/T cell) stimulated with PHA/PMA (phytohemagglutinin/phorbol 12-myristate 13-acetate) and/or interleukin (IL)-2. In particular, Cybr mRNA was found to increase 2-fold in NK/T cells upon stimulation with IL-12 and 25% upon stimulation with PHA/PMA [93]. Cybr expression has also been found in the lymphoblastoid cell line 721, in the T helper cell line Jurkat (increased upon stimulation with PHA/PMA) and in CD14$^+$ monocyte-derived dendritic cells. Moreover, Cybr mRNA levels were dramatically higher in mature DCs (20-fold increase) when compared to immature cells.

Cybr expression is also highly regulated in T cells, and several microarray studies and northern analysis have shown that induction of Cybr expression is affected by the stage of development of T cells; more differentiated CD3$^+$ thymocytes express reduced Cybr levels than the less differentiated CD3$^-$ cells. Microarray, northern analysis and real-time PCR studies have demonstrated that Cybr in T cells is at least double expressed in Th1 polarized conditions compared to Th2 [92]. Cybr was later found to be overexpressed in T cells (Jurkat) following T cell receptor engagement, and to have effects on T cell receptor-dependent downstream events, such as enhancement of nuclear factor of activated T cell (NFAT). This aspect confers a role for Cybr to participate in the TCR signalling by regulating Vav phosphorylation and enhancing JNK and p38 MAPK upon CD3 crosslinking [97]. *Cybr* expression not only increases NFAT activity but also NFAT may act on the *Cybr* promotor, since the upstream region of the *Cybr* gene contains numerous potential binding sites for NFAT as well as for several lymphoid-specific transcription factors. This sets up a potential positive feedback loop between *Cybr* and *NFAT* transcription during T cell activation and proliferation. *Cybr* expression also enhances AP-1 activation, that leads to enhance AP-1 transcriptional activity and involves co-operation with NFAT·AP-1[97].

Overall, Cybr is widely accepted as a hematopoietic cell-specific transcript and it appears to be differentially regulated and specifically controlled within this lineage. Expression is basally low in many of these cell types, but is highly and rapidly responsive to, and regulated by, many cytokines and other soluble effectors of the immune system. In T cells and DCs, *Cybr* expression is readily inducible by specific stimulation of each respective cell type. This attribute is surely a clue to the nature of *in vivo* Cybr protein function.

4.3 Protein interactions, intracellular localizations and functional activities

Cybr is a 40 kDa adaptor protein, since it contains multiple protein-protein interaction domains and motifs (namely, an N-terminal PDZ domain or PSD-95/Dlg/ZO-1, an unusually long central coiled-coil motif or leucine zipper and a C-terminal PDZ-binding motif or PDZbm) that participate in the assembly of larger protein complexes (Fig. 4) [98]. The coiled-coil motif mediates the interactions with cytohesin-1 (B2-1), the first Cybr binding partner discovered. The cytohesins are a ubiquitous group of proteins that have been variously implicated in several biological roles, including intracellular trafficking and signaling, through ARF (ADP-ribosylation factor) activation, cytoskeletal rearrangement, endocytic trafficking and cell adhesion through β2 integrin signaling. The intracellular Cybr function is particularly influenced by the interaction with cytohesin-1 (Fig. 4), described using a yeast two-hybrid system, and further confirmed by *in vitro* protein-binding assays and *in vivo* using transfection and immunoprecipitation experiments. These studies also showed that Cybr could interact with other members of the cytohesin/ARNO family of guanine-nucleotide exchange factors (ARNO/cytohesin-2 and ARNO/GRP1/cytohesin-3), demonstrating that Cybr may act as an adaptor for all members of this family.

Another Cybr binding partners is represented by sorting nexin 27 (SNX27), a molecule with an active role in the polarization during lymphocyte migration and tumor cell engagement. Cybr interacts with SNX27 through PDZ-PDZbm interaction, thus bringing together members of the cytohesin/ARNO family to SNX27, as demonstrated *in vivo* in lymphocytes with co-immunoprecipitation studies. Moreover, the co-localization of Cybr and SNX27 in early endosomal compartments implicates a function of this molecules in endocytic trafficking and/or signaling [99] (Fig.5). Finally, it is also possible that other proteins interact with the respective coiled-coil motif and the PDZbm, as these motifs can be promiscuous and interact with several distinct proteins.

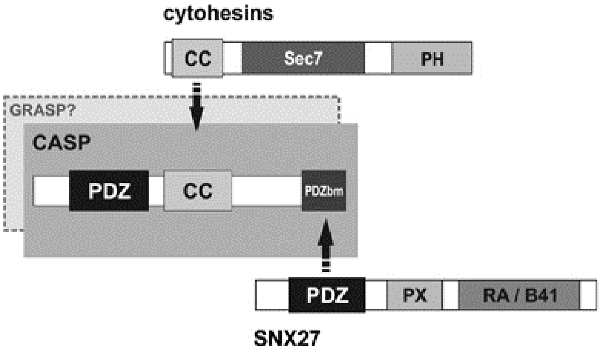

Figure 4. Domain and motif architecture in the Cybr interactome. Protein domain distributions of Cybr, the cytohesin/ARNO family and SNX27. All four members (cytohesin-1, ARNO, ARNO-3 and cytohesin-4) of the mammalian family are identical in domain distribution. SNX27 exists as two isoforms with modified C termini. GRP1-associated scaffolding protein (GRASP), with a domain composition the same as CASP, may also play a role in potential redundant pathways. Domains: PDZ: PSD-95/Dlg/ZO-1; CC: coiled-coil; PH: pleckstrin homology; PX: phox homology; Sec7: guanine-nucleotide-exchange factor (GEF) activity with similarity to S. Cerevisiae SEC7 protein; RA: Ras-associated; B41: component of FERM. Modified from [98].

With regard to the intracellular localization, in the first experiments with transfected COS-1 cells, full-length Cybr construct showed a perinuclear localization, but failed to display co-localization with Golgi or endoplasmatic reticulum related proteins or markers. Moreover, Cybr was shown to be recruited by cytohesin-1 to separate subcellular locations, including the cytoplasm and membrane, dependent upon cytohesin-1 related signals [95].

Cybr localization, investigated in Jurkat cells, demonstrated that Cybr shows a cytoplasmatic and vesicular localization , and also it's associated with the cortex with a cytoplasmatic domain directly below to the plasma membrane (Fig. 5). In cells co-expressing cytohesin-1 and Cybr, Cybr acts on, and sequester, cytohesin-1 from the membrane/cortex to the cytoplasm. The detachment of the Cybr-cytohesin-1 complex from the plasma membrane in turn induces the inhibition of the cytohesin-1-mediated adhesion of LFA-1 to ICAM-1 [96]. The relationship between the cytohesin/ARNO family and Cybr is found to be dynamic and differentially regulated. Indeed, while certain stimuli appear to cause cytohesin-1 recruitment of Cybr to the membrane (Epidermal Growth Factor-EGF and cell adhesion-associated events), others (PMA) induce Cybr to recruit cytohesin-1 away from the membrane/cortex to the cytoplasm. The regulation likely relies on both intracellular signaling and the particular cytohesin family member, as well as further protein components (such as Cybr-PDZ-binding partners, ARFs, and others), is associated with the particular complex implicated.

In DCs, Cybr is localized in the cytoplasm in a very diffuse distribution. It was observed that normal immature DCs (characterized by low endogenous *Cybr* expression) adhere more effectively than mature DCs (characterized by high endogenous *Cybr* expression), but Cybr silencing, using small interfering RNA, enhanced the adherence of mature DCs to fibronectin, indicating a role for Cybr in reducing DC adherence. Moreover, Cybr accumulates at the contact zone between dendritic cells and T cells when co-cultured [100]. Cybr silencing in dendritic cells inhibited their ability to efficiently detach from T cells during *in vitro* T-cell priming assays. In this way DCs keep longer contacts with T-cells and the stimulatory capacity for antigen-specific CD8$^+$ T cells is diminished, indicating a possible role of Cybr in the de-attachment of T cells from dendritic cells [100] (Fig. 5).

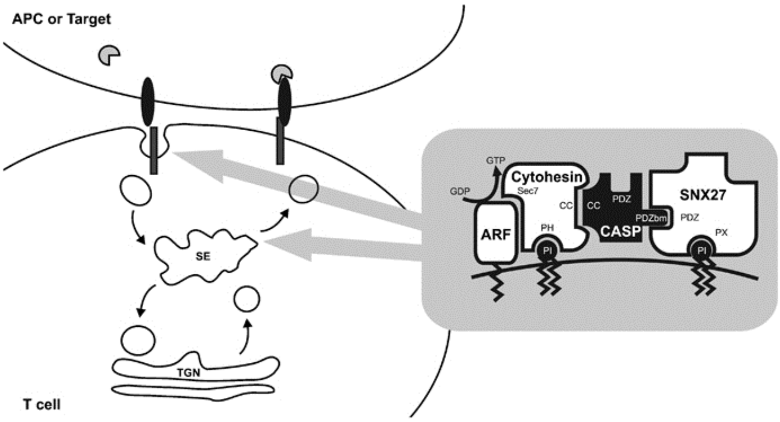

Figure 5. A model implicating Cybr/CASP in putative novel polarized hematopoietic endosomal sorting events. A Cybr/CASP-mediated link between members of the cytohesin/ARNO family and SNX27 gives this novel complex a dynamic affinity for phosphoinisitides enriched both at the plasma membrane (through the PH domain of cytohesins) and endosomal compartment (through the PX domain of SNX27). Likely, dependent on the cytohesin/ARNO implicated, vesicle initiation may take place on either membrane (for example with cytohesin at the plasma membrane or with ARNO at endosomal compartments). While shown from the T cell side, this complex may well support a parallel mechanism on the APC (antigen-presenting cell) side. SE: sorting endosome; TGN: trans Golgi network; PI: phosphoinositol. Modified from [98].

Altogether, Cybr's localization has emerged as dynamic and varied. Endogenous Cybr localization has been shown to be both endosomal and cytoplasmatic, depending on the cell-type examined. Cybr can translocate to and from the plasma membrane and/or cell cortex upon stimulation in a variety of contexts (for example EGF, PMA, cell adhesion, immune synapse formation) (Fig. 5). This localization pattern suggested functional roles of Cybr in ARF vesicle formation [101], endocytic trafficking and/or signaling [99], regulation of TCR signaling [97] and regulation of dendritic cell-T cell interaction times during the screening process for antigen-specific T cells [100]. In particular, the Cybr translocation in DCs to the immunological synapse is critical for efficient cell-cell interaction and detachment, allowing DCs to rapidly contact and subsequently leave T and B cells in their search for a T or B cell receptor corresponding to the presented antigen.

A reduction in the efficiency of these interactions, leading to longer and less cell-cell interactions in each case, would cumulatively promote a delayed and reduced migration of immune cells to appropriate tissue sites [102]. Indeed, reduced Cybr expression in DCs, leads to a longer interactions due to a reduced detachment during presentation to lymphocytes, and *in vivo* setting, this would wreak havoc on the process of screening naive lymphocytes to an efficient activation and proliferation [100],[102] (Fig. 6).

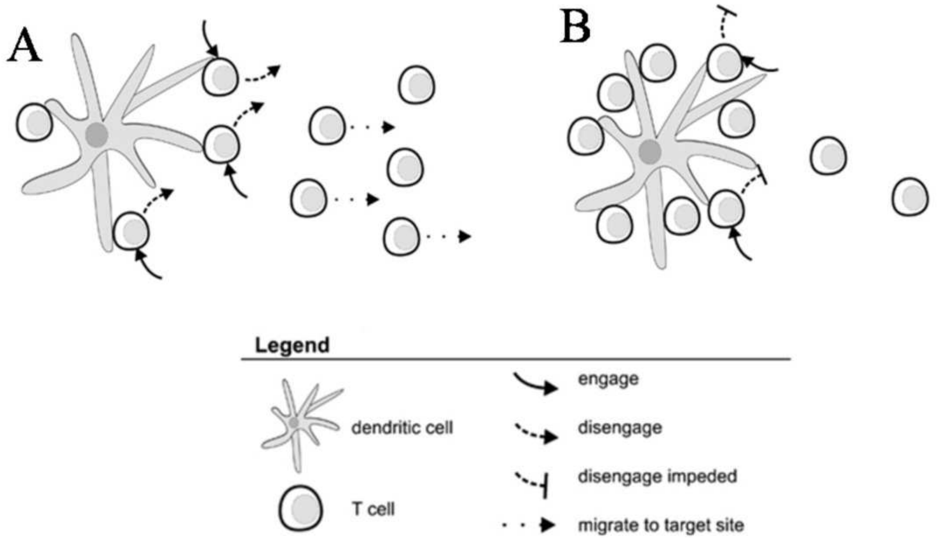

Figure 6. A model depicting the role of Cybr expression in antigen presentation by dendritic cells. A) In normal conditions, antigen presentation at the lymph node involves interactions between DCs and T cells which include engagement, presentation and disengagement, followed by proliferation and migration of activated T cells. B) In the absence of Cybr, active disengagement is impeded, resulting in a bottleneck effect where ultimately fewer T cells are being primed, activated and exiting the lymph node and blood stream, as evidenced in several distinct studies [103],[104],[96] examining Cybr knockouts from both the T cell and DC side. Modified from [98].

4.4 Functional characterization in the context of immunity: insights from *Cybr*-knockout mouse models

For *in vivo* characterization of Cybr, two *Cybr*-deficient mice were created, one by replacing parts of exon 2 and exon 3 by enhanced EGFP-encoding sequence [103], the other by the removal of exon 1 using the cre-lox system [104]. In both mouse models, the lack of Cybr only marginally affects the development of the immune system. A minor developmental of *Cybr*-deficient hematopoietic stem cells relative to wild-type cells in a bone marrow competitive repopulation model, was interpreted as not substantial, thus the role of Cybr was rated as nonessential, possibly due to functional redundancy with other proteins [103].

However, *Cybr*-deficient mice older than 6 months display fewer circulating white blood cells and lymphocytes in the inguinal lymph nodes [104]. With regard to functional activity, leukocytes trafficking was only impaired in stress conditions, namely Th1-polarized milieu. In an aseptic peritonitis model, *Cybr*-KO mice showed a significantly lower number of peritoneal inflammatory cells than wild type controls and only a limited reduction in the number of circulating WBC, due to the fact that neutrophils fail to efficiently exit the bloodstream. Moreover, the CD8-mediated immune response to Moloney murine sarcoma virus (M-MSV) is significantly delayed, in accordance with the impaired trafficking capacity of lymphocytes [104], and the finding that Cybr-silenced human dendritic cells show a reduced stimulatory capacity for antigen-specific CD8 positive T-cells [100].

Contrasting results were obtained by Heib and colleagues [105] in a contact hypersensitivity model in *Cybr*-KO mice. Indeed, in deep contrast with human DC, they found that murine *Cybr*-KO dendritic cells display a greater ability to activate T cells [105]. Differences in the mouse model used and technical procedures can account for this discrepancy, but also a different Cybr expression between humans and mice has to be considered. Indeed, real-time PCR has shown that normal Cybr expression in mice is markedly lower than in humans, particularly in the thymus (~ 7-fold) and lymph node (~ 20-fold) [103].

Overall these observations point to a role for Cybr in a number of critical aspects of the immune response. Indeed, Cybr deficiency may affect lymphocyte interaction with vascular endothelial cells during rolling and extravasation in homing to tumor and infection sites and/or lymphoid organs, efficient migration and presentation of antigen by DCs to lymphocytes, and cytotoxic T lymphocytes interaction with cells targeted for destruction. Despite the fact that, due to the presence of redundant proteins, Cybr may not be essential in immunity under normal conditions, but it turn out to be a streamlined protein that greatly ameliorates the efficiency of the immune system under circumstances of significant stress.

5. Tumor immunity and tumor antigens

5.1 Cancer immunoediting: from immunosurveillance to immunoescape

Cancer immunology is the study of interactions between the immune system and cancer cells. Progresses in the knowledge of the cell-mediated immune response function and of the tumor's biology disclosed that a competent immune system has a key role in the prevention and treatment of cancer. The immune system has the ability to recognize antigens continuously generated by genetic and epigenetic events in the tumor [106],[107] and carry out humoral and cell-mediated responses directed against tumor cells, potentially inhibiting the tumor development. The discovery of over 1000 human tumor antigens and clinical evidences supported the fundamental concept of cancer immunosurveillance, developed first in 1957 by Burnet and Thomas. They proposed the theory that lymphocytes act as sentinels in recognizing and eliminating continuously arising, nascent transformed cells. Cancer immunosurveillance appears to be an important host protection process that inhibits carcinogenesis and maintains regular cellular homeostasis [106]. Important proofs came from studies conducted on immunodeficient mice and in particular in mice lacking B and T lymphocytes and STAT-1 (the transcription factor that mediates the IFN-γ-signaling) in which it was demonstrated a higher incidence of adenomas and adenocarcinomas compared to immunocompetent control mice. In human malignant tumors, the presence of leukocytes with specific properties of inhibiting the establishment and growth of tumor cells, was known since the 1970 [108],[109]. Moreover, recent observations indicate that the infiltration of tumor by T cells is an important predictive marker of survival in several cancer types (e.g. ovarian and colorectal cancer) [110], [111].

During the tumor growth, continuous interactions between tumor cells and immune system take place at tumor site and at tumor draining-lymph node. In the initial phases of tumor development, even few antigenic differences between normal and mutated cells and the disruption of tissue homeostasis could activate local innate immune responses, mediated by macrophages, natural killer T cells (NKT) and natural killer cells (NK) [112]. Local inflammation recruits dendritic cells and promotes their maturation and migration to lymph nodes, where they become able to activate B and T cells, the effectors cells of the specific anti-tumor immune response. In tumors there is a synergy between the innate and adaptive immune response that maintain the malignant growth under control in a dynamic equilibrium. However, under the immunological pressure, some tumors could acquire mechanisms to evade or suppress the immune attack, thus surviving in the immunocompetent host [113].The tumor evolution in immunocompetent hosts is therefore associated with the selection of scarcely immunogenic cells and/or cells which are able to escape the immune-mediated effector mechanisms that could allow the tumor reject, as proposed by Dunn, Old and Schreiber [114],[115],[116] in the concept of *immunoediting*. The tumor immunoescape include alterations of immune effector mechanisms and/or acquisition by tumor cells of the resistance against the immune response. There are different mechanisms of tumor immune escape, for example the loss of components of the processing and presentation of antigen system, such as large multifunctional protease (LMP) and transporter associated with antigen processing (Tap), the downregulation of expression of MHC and co-stimulatory molecules as well as tumor antigens, especially the most immunogenic [117]. Furthermore, tumor cells could acquire a resistance to CTL lysis [118], and the capacity to produce cytokines that inhibit T-cell responses, such as TGF-β or IL-10 [119], or could induce the apoptosis of T lymphocytes [120]. Tumor microenvironment, moreover, could supply signals that block the development of the innate immune response and consequently the inflammatory reaction [121]. In addition, tolerance or suppression of T lymphocytes can be induced by recruitment of myeloid-derived suppressors cells (MDSC) or other suppressors cells as NKT or T regulatory cells [122],[21].

5.2 Tumor antigens

Tumor antigens are produced in tumor cells, and they can trigger an immune response in the host. The first proof of the presence of immunogenic molecules on tumor cells was demonstrated in chemical tumorigenesis studies, in which sarcomas methylcholanthrene-induced and then surgically removed, were rejected when transplanted in original hosts, while caused death in syngeneic previously untreated mice. Further studies revealed that the tumor rejection was related to the recognition of molecules present in the surface of transformed cells, called tumor antigens, by the host immune system. Tumor antigens were broadly classified into two categories based on their pattern of expression: Tumor-Specific Antigens (TSA), which are present only in tumor cells and not in normal cells and Tumor-Associated Antigens (TAA), which derive from not mutated proteins, are specific for particular cell lineages and are present in tumor cells but also in normal cells, even if at lower levels [117],[123].

Three classes of TAA can be distinguished:

- **Oncofetal antigens.** These proteins are normally expressed in the early stages of embryonic development and disappear when the immune system is fully developed in adult tissues. α-fetoprotein (AFP) and carcinoembryonic antigen (CEA) are well characterized oncofetal antigens. AFP is a α-globulin that is normally produced in the yolk sac and liver during fetal development, and successively is replaced by albumin. A relevant increase of AFP levels can be a symptom of a tumor mass presence in the liver or in germinal cells [124]. CEA is a membrane protein that belongs to Ig family, principally expressed in the gut, pancreas and liver during the first six months of gestation. The increase of CEA concentration is associate with colon tumors. The oncofetal antigens are not immunogenic, but they can be used for diagnosis and to monitor an anti-tumor therapy and prognosis [125].

- **Cancer/Testis antigens.** Cancer/testis (CT) antigens are a category of tumor antigens with normal expression restricted to male germ cells in the testis but not in adult somatic tissues. In malignancy, this gene regulation is disrupted, resulting in CT antigen expression in a proportion of tumors of various types [126]. Characteristics commonly shared by CT antigens, aside from the highly tissue-restricted expression profile, include existence as multigene families (namely MAGE, BAGE, GAGE, RAGE, NY-ESO-1), frequent mapping to chromosome X, heterogeneous protein expression in cancer, likely correlation with tumor progression, induction of expression by hypomethylation and/or histone acetylation, and immunogenicity in cancer patients [127].

- **Tissue-specific or differentiation antigens.** These antigens are encoded by genes expressed in tissue-specific manner which, in particular differentiation stages of cell cycle or tissue development, and can induce a T cell response. Among these antigens, melanocyte differentiation antigens (gp100 protein, MART-1/MELAN-A and tyrosinase) are important, as they were first identified in melanoma, but also in normal melanocytes [128]. Other examples are components of clusters of differentiation (CD) on lymphocytes, such as CD10 or CALLA (Common Acute Lymphoblastic Leukemia Antigen), a molecule expressed on normal pre-B lymphocytes and on mature neoplastic B lymphocytes [129], and the Prostate-Specific Antigen (PSA), a serine protease synthesized in epithelial cells of prostatic and vesical cancer, thus used as humoral marker for prostatic carcinoma [130].
- **Altered cell surface glycolipidic and glycoproteic antigens.** This class of antigens includes gangliosydes, mucins, glycolipids and glycoproteins expressed at unusually high levels on cell surface of several tumors. It is presumed that their presence can promote the invasion of surrounding tissues and the metastatic process. They can be used as anti-tumor vaccines for their ability to stimulate the production of IgM and IgG against tumor cells.

The group of Tumor Specific Antigens comprises:

- **Antigens encoded by mutated oncogenes and tumor suppressor genes.** Two groups of genes are included in this category: proto-oncogenes, which normally are silent and when activated or overexpressed become oncogenes and tumor suppressor genes involved in the regulation of cell cycle, which inactivation determines the production of mutated or the absence of proteins. Mutations of oncogenes are recurrent, for example the p53 protein that if mutated is recognized by specific CTLs [131]. However, also the native form of p53, as the protein encoded by Her2/Neu oncogene, is able to generate a specific CTL response, if produced in large amounts compared to normal levels [132].

- **Oncogenic viruses encoded antigens.** Both DNA and RNA viruses can be involved in tumors development, in animal models and humans [133]. Several viruses own in their genome well-known oncogenes inducing therefore tumors and are defined as “acutely transforming viruses”, for example the Rous sarcoma virus and the Kirsten murine sarcoma virus. On the contrary, other viruses do not contain oncogenes in their genome, but are also able to induce tumors several months or years after the infection and are known as “chronically transforming viruses”. They can induce tumors not only by insertional mutagenesis, but also by expressing proteins that interfere with the activity of cellular genes and proteins involved in the growth, the differentiation or the transcription in normal cells. Examples of human oncogenic virus are represented by EBV (Epstein-Barr Virus), HTLV-1 (Human T-lymphotropic type I Virus), HPV (Human Papilloma Virus), HBV (Hepatitis B Virus), HCV (Hepatitis C Virus) and KSHV (Kaposi’s Sarcoma Herpes Virus).

  Among murine tumor viruses, we focused our attention on the Moloney murine sarcoma virus/Moloney murine leukemia virus retroviral complex (M-MSV/MuLV), described in depth in the next Section, as a model in which characterize antigen-specific T cell responses. Indeed, from an immunological and immunotherapeutical point of view, viral tumor antigens represent a privileged group of antigens; indeed, due to their non-self origin, they are potentially able to induce even strong immune responses without the need to break tolerance.

6. Experimental model: the M-MSV/M-MuLV retroviral complex

Moloney murine sarcoma virus (M-MSV) is an acutely transforming type C murine retrovirus, containing the oncogene *mos* in its genome. *Mos* encodes for a kinase protein that is responsible for the transformed phenotype. The oncogene insertion in the viral genome determined the deletion of envelope-encoding sequences; therefore, M-MSV is replication-defective and needs the helper activity of the chronic transforming Moloney murine leukemia virus (M-MuLV). Consequently, M-MSV particles as well as the virus-infected cells have the antigenic specificities associated to the helper virus M-MuLV. M-MuLV genome is constituted by *gag*, *pol* and *env* genes, by the LTR sequences and the encapsidation sequence E; the *gag*, *pol*, and *env* genes encode for the viral core proteins, for the reverse transcriptase enzyme and for the viral envelope, respectively (Fig. 7).

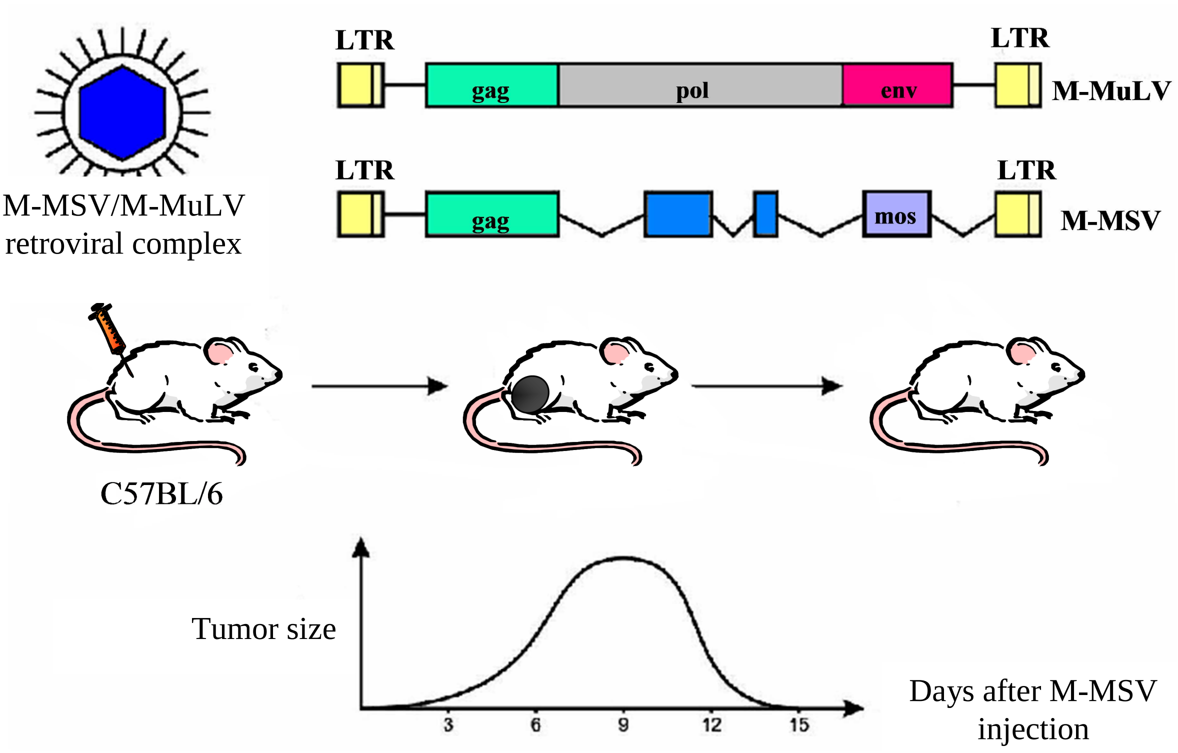

Figure 7: Experimental model of the viral oncogenesis. Intramuscular injection of the M-MSV/M-MuLV retroviral complex in immunocompetent C57BL/6 (B6) mice causes sarcomas to develop at the inoculation site, followed by subsequent spontaneous tumor regression.

The *gag* gene contains the information for two principal precursors, the 65 kDa ($Pr65^{gag}$) protein that is phosphorylated and cut in smaller proteins respectively of 15, 12, 30 and 10 kDa (p15, p12, p30 and p10), which constitute the viral capside proteins, and the 80 kDa (gPr80^{gag}) protein that contains a N-terminal additional portion and is glycosylated starting from a 75 kDa precursor (Fig. 8). gPr80^{gag} has no function for the replication of M-MuLV *in vitro*, but it is necessary for the efficient diffusion of viral infection and for the pathogenesis *in vivo*. The translation of this second precursor does not begin from the ATG of Pr65^{gag} (located at base 621 of the viral genoma), but from the upstream CTG, so determining the translation of an additional region in respect to the N-terminal of the protein [134].

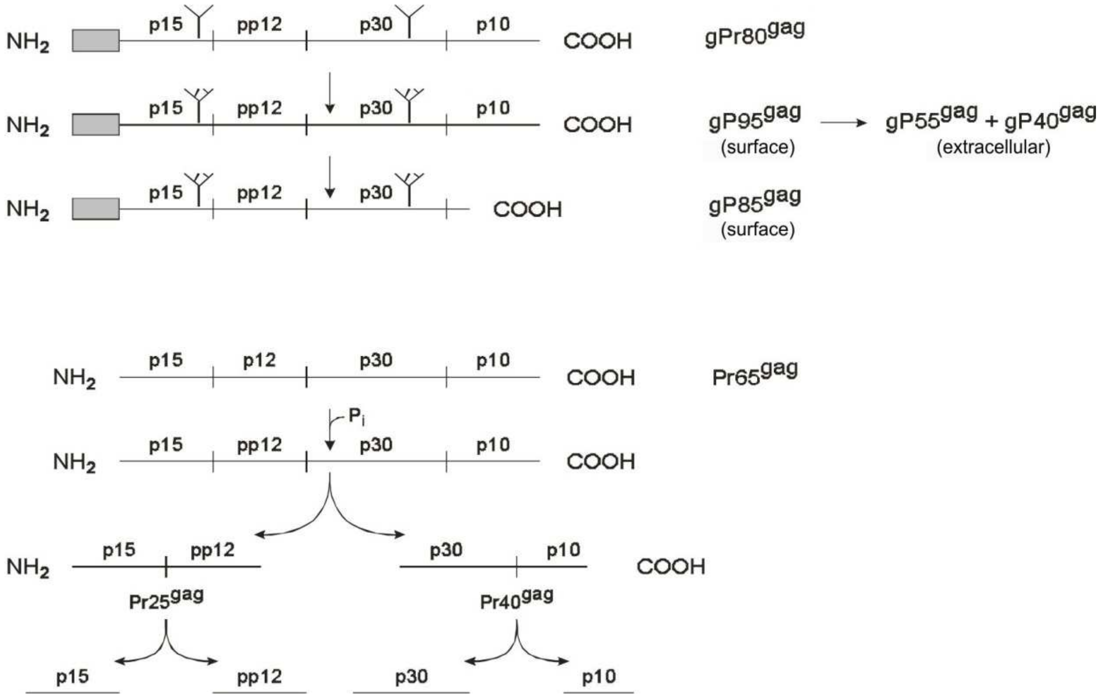

Figure 8: Synthesis and post-translational modifications of the Gag polyproteins in the leukemia murine viruses (MLV). The scheme represents the metabolic pathways of glycosylated and non glycosylated MLV Gag polyproteins. The aminoacidic sequences of the two forms are identical, except for the N-terminal region, showed in grey. The localization of the glycosydic groups is indicated by the branched structures. Moreover, the phosphorylation and the proteolysis of the 65 kDa precursor are represented. The proteolysis produces the internal structural proteins of the mature virion. The numbers indicate the protein molecular weight expressed in kDa (pp12 = phosphoprotein of 12 kDa).

The *env* gene encodes for a 80 kDa (gPr80^{env}) precursor, that is glycosylated and cut in two proteins: gp70^{env} that is involved in the entry of the virus in the cell, and p15^{env}, the most hydrophobic protein of the viral particle that can be found associated to the virion and infected cell membrane.

Intramuscular injection of the M-MSV/M-MuLV retroviral complex in immunocompetent C57BL/6 (B6) mice, not older than 10-12 weeks, causes sarcomas to develop at the inoculation site after a short period of latency. Sarcomas reach the maximal growth about 10-12 days after the injection; subsequently, tumors regress spontaneously until they completely disappear [135]. Studies previously conducted in our laboratory demonstrated that this spontaneous regression is due to the induction of a strong virus-specific immune reaction, primarily mediated by CTLs specific for viral antigens. The T population integrity was demonstrated to be crucial in contrasting the M-MSV tumors development, and in operating their regression [136].

Using different approaches, two works led to the definition of two M-MuLV specific antigenic epitopes, one from $gPr80^{gag}$ and the other one by $gp70^{env}$. The first one, namely Gag_{85-93} (CCLCLTVFL) presented in the context of $H\text{-}2D^{b}$ allele, was identified as the immunodominant epitope by Chen and colleagues [137]. They studied the response generated by the immunization of B6 mice with FBL-3 cell line, a murine leukemia originally induced by the Friend leukemia virus. The Friend leukemia virus and the Moloney virus belong to the same group and share an elevated Gag sequence homology. The second peptide was described by Sijts e colleagues [138]. It is an optameric epitope, situated in position 189-196 of the $gp70^{env}$ aminoacidic sequence (SSWDFITV) and is presented in association with the $H\text{-}2K^{b}$ allele.

Previous experiments carried out in our laboratory confirmed the immunodominance of Gag_{85-93} peptide in terms of frequency of Gag-specific-pCTL in mice that regressed a M-MSV/M-MuLV induced sarcoma, as assessed by limiting dilution analysis (LDA) technique. The majority of the tumor-specific CTL response is therefore directed against this epitope while the pCTL frequency that recognize $Env_{189-196}$ is conversely much lower (8%) in regressors mice [139].

AIM OF THE PROJECT

Cybr is a scaffold protein mainly expressed in the hematopoietic cells and involved in the assembly and recruitment of protein complexes associated with intracellular trafficking and signaling. These characteristics place Cybr in a crucial position to control cell adhesion, cell-cell interactions, and migration of cells of the immune system.

This research project aimed at characterizing *in vivo* the physiological role of Cybr in the cell-mediated immune response in a mouse model of sarcoma induced by the M-MSV retroviral complex. By taking advantage of a *Cybr*-deficient mouse strain, we focused our attention principally on T cells dynamics in tumors, spleens and lymph nodes. In particular, we compared the phenotype, the antigen specificity and the lytic activity of *Cybr*-KO and wild type T cells at the peak of tumor growth and after its spontaneous regression. Furthermore, we investigated the priming phase and the tumor homing capacity of naive *Cybr*-deficient/GFP T cells adoptively transferred in M-MSV tumor-bearing Rag2-/- γc-/- mice.

MATERIALS AND METHODS

1. Mice

All mouse strains were housed in our Specific Pathogen Free (SPF) animal facility. Procedures involving animals and their care were in conformity with institutional guidelines that comply with national and international laws and policies (D.L. 116/92 and subsequent implementing circulars). The experimental protocols were approved by the local Ethical Committee of Padua University (CEASA). Mouse strains used for this study are reported as follows:

C57BL/6 (B6) mice. 6–8-week-old female C57BL/6 (B6) mice (H-2^{b}) were purchased from Charles River Laboratories (Calco, Como, Italy).

C57BL/6-Tg (UBC-GFP) mice. These transgenic mice were purchased from Charles River Laboratories and are hereafter indicated as as B6/GFP mice. They express the enhanced Green Fluorescent Protein (eGFP) under the transcriptional control of the human ubiquitin C promoter. Mice homozygous for the transgene are viable, fertile, normal in size and do not display any gross physical or behavioral abnormalities. Some hematopoietic cell types display distinct expression levels of GFP, allowing identification of different cell types by cytometry analysis. GFP expression is uniform within a cell type lineage and remains constant throughout development. T cells have a 2-fold higher GFP expression than CD19^{+}B220^{+} B cells or peripheral blood cells.

***Cybr*-deficient mice**. This strain was generated and kindly provided by Coppola and colleagues [104]. The Cybr-specific targeting vector was obtained by DNA recombinant technology. Briefly, an 8.8-kb DNA fragment containing Cybr exon 1 (EX1) was retrieved from BAC 265C23 (ResGen; Invitrogen Corp., Huntsville; AL) and inserted into the targeting vector. Subsequently, by recombination in the DY380 bacterial strain, a loxP site was introduced 83 bp upstream of EX1. Finally, a cassette containing the neo resistance gene flanked by both loxP and Frt sites was placed 63 bp downstream of EX1. *Cybr*-mutant mice were generated by a standard gene-targeting approach using the CJ7 embryonic stem cell line, as previously described. Removal of EX1 was accomplished by crossing the offspring of chimeras with the targeted allele to a Cre deleter strain. Resulting mice were negatively selected for the presence of Cre and backcrossed with B6 mice for nine generation in the original animal facility, and up to generation 22 after being imported in our facility, before being used for experiments.

***Cybr*-deficient/GFP mice.** The *Cybr*-deficient/GFP mice were obtained by crossing *Cybr*-deficient mice with UBC-GFP mice for 8 generations. The colony was screened at each generation by PCR to detect the homozygosity of the mutated form of Cybr, and by flow cytometry analysis to detect the homozygosity of GFP expression in the blood cells.

C57BL/6 Rag2-/- γc-/- mice. These mice were purchased from Taconic (Laven, Denmark). The common gamma chain knockout (γc-/-) mouse lacks functional receptors for many cytokines including IL-2, IL-4, IL-7, IL-9, and IL-15. As a consequence, lymphocyte development is greatly compromised. The mouse lacks natural killer (NK) cells and produces only a small number of T and B cells. To eliminate the residual T and B cells, this mouse was crossed to the Rag2 (recombinase activating gene 2) deficient mouse. The double knockout lacks T cells and B cells, due to the inability to initiate V(D)J rearrangement, and lack NK cells. Double knockout mice were found to appear normal except for thymuses, spleens and lymph nodes, that were small and hypoplastic. No detectable alterations were observed in other tissues tested. In the Results section they are referred to as Rag2-/- γc-/- mice.

2. Mouse DNA extraction

Genomic DNA was obtained from mouse whole blood collected by retrorbital puncture under isofluorane/oxygen anesthesia and purified by using Puregene Blood Kit (Qiagen, Milan, Italy). After treatment with EDTA (pH 8, 0.5 M) as anticoagulant, erythrocytes were lysed using RBC (Red Blood Cells) lysis solution 1X (Qiagen). White blood cells (WBC) were lysed with an anionic detergent (Cell Lysis Solution, Qiagen), and RNA was removed by treatment with a RNase A solution (Qiagen). Other contaminants, such as proteins, were removed by salt precipitation (Protein Precipitation Solution, Qiagen). Finally, the genomic DNA was recovered by precipitation with isopropanol, washed with ethanol and resuspended in sterile water. The DNA was stored at -20°C.

3. PCR for Cybr-deficient mouse screening

Genomic DNA samples extracted from WBCs of *Cybr*-deficient/GFP mice were tested by PCR in order to detect the mutant form of *Cybr* gene. *Cybr*-deficient DNA was used as positive control. The following primers were used:

A) 5’-GAGTATCAAACTCTATGTTCCGGCTG-3’

B) 5’-GGAATAAGGCTGGTAGTCAAAG-3’

C) 5’-GAGAGGGGCGGATCAATTCATAACT-3’

PCR conditions were the followings:

1) 96°C 2 min;
2) 94°C 1 min;
3) 53°C 1.5 min;
4) 72°C 3 min;

Steps from 2 to 4 were repeated for 40 cycles;

5) 72°C 10 min;
6) 4°C hold.

The expected resulting fragments were 600 bp corresponding to the wild type gene, and 340 bp corresponding to the *Cybr*-KO gene. PCR-amplified DNA samples were then electrophoretically run on a 2% agarose gel.

4. Preparation of blood samples for flow cytometric analysis of *Cybr*-deficient/GFP mice

Mouse blood samples were collected in a tube with EDTA to avoid blood coagulation. RBCs were lysed for 7 minutes at 37°C with 0.83% NH_4Cl (Sigma, Milan, Italy) and then washed with PBS. This procedure was repeated twice. WBCs obtained were resuspended in 250 µl PBS and flow cytometry analysis was performed to detect GFP^+ cells.

5. Tumor cell lines

MBL-2, a T cell leukemia cell line ($H-2^b$) derived from a M-MuLV-infected B6 mouse, were cultured in Dulbecco’s modified Eagle’s medium (DMEM) supplemented with 2 mM L-glutamine, 10 mM HEPES, 20 µM 2-mercaptoethanol, 150 U/ml of streptomycin, 200 U/ml of penicillin and 10% of heat-inactivated fetal bovine serum (FBS). All reagents were purchased from GIBCO BRL (Monza, Italy).

6. Virus preparation and M-MSV tumor induction

The cell extracts containing defective M-MSV copelleted with its natural helper M-MuLV (M-MSV/M-MuLV) were prepared from primary sarcomas induced by serial passages in 1-week-old

BALB/c mice, which had an *in vitro* M-MSV titer of 3 × 10^5 PFU/ml on 3T3/FL cells. M-MSV extract (100 µl) was injected intramuscularly in the thigh region of adult mice, which developed sarcomas at the site of injection that underwent spontaneous regression within 15-20 days. Tumor growth was monitored daily by caliper measurements starting 6 days after inoculation when sarcomas become apparent and until day 20 when tumors disappear.

7. Histological analysis

To study the infiltrating cell population in M-MSV-induced tumors of *Cybr*-KO and B6 mice, animals were sacrificed at different days. Tumors were excised, formalin-fixed (PFA 1%, Thermo Scientific, Milan, Italy) for 1 hour and then transferred in PBS 20% sucrose (Sigma) for the hematoxylin and eosin (H&E) staining. Alternatively, they were frozen in OCT (Bio-Optica, Milan, Italy) for the immunohistochemical (IHC) analyses. Thigh muscles from normal B6 and *Cybr*-KO mice were used as negative controls. The H&E and IHC stainings were performed in collaboration with the group of Professor P. Musiani, Department of Medicine and Aging Science, University of Chieti, Italy. For the IHC staining, the sections were incubated with the following primary antibodies: rat anti-mouse CD4 (clone H129.19), CD8α (clone 53-6.7), CD11b (clone M1/70), Ly-6G and Ly-6C (clone RB6-8C5), CD45R/B220 (clone RA3-6B2) (all from BD Pharmingen, Buccinasco, Italy), CD68 (clone FA-11; Abcam, Cambridge, UK), FoxP3 (clone FJK-16s; eBioscience, Milan, Italy) mAbs; Armenian Hamster anti-mouse CD11c mAb (Clone HL3, BD Pharmingen). After incubation with the appropriate secondary antibodies, immunocomplexes were detected using Bajoran Purple Chromogen System (Biocare Medical, Concord CA, USA), and Vulcan Fast Red (Biocare Medical).

8. TIL isolation

Tumors excised at different time points after M-MSV injection were dissociated using a combination of mechanical tissue disruption and enzymatic digestion with a mixture of DNAse I (270 U/ml), Collagenase (200 U/ml) and Ialuronidase (35 U/ml) for 40 min at 37°C (all reagents were from Sigma). Cells suspensions were then washed twice and the tumor infiltrating lymphocytes (TIL) were analyzed at FACSCalibur (BD).

9. Mixed Leukocyte Tumor Cell Cultures (MLTC)

Mouse spleens were removed at different time points after M-MSV injection and MLTC cultures were set up by *in vitro* restimulation of 25 × 10^6 splenocytes with 10^6 syngeneic irradiated (60 Gy) MBL-2 cells. Cell cultures were maintained in DMEM, 10% FBS, in 25-cm^2 tissue culture flasks

(Falcon, Becton Dickinson) for 5 days at 37°C, 5% CO_2 and then tested for lytic activity in a ^{51}Cr release assay.

10. Peptides

The $Env_{189-196}$ (H-$2K^b$-restricted; SSWDFITV) peptide was obtained from Technogen (Naples, Italy). The Gag_{85-93} peptide (H-$2D^b$-restricted; CCLCLTVFL) was modified by replacing –SH groups with –OH groups, because it contains 3 cysteines forming disulfide bonds that avoid the correct biomonomer/tetramer folding. The modified peptide Abu-Abu-Leu-Abu-Leu-Thr-Val-Phe-Leu (Gag/Abu, α-aminobutyric acid [140]) was thus synthesized at the Centro Ricerca Interdipartimentale Biotecnologie Innovative (CRIBI) of Padua University. All peptides were purified by high-performance liquid chromatography (HPLC) reaching a purity of >95%. Lyophilized peptides were finally dissolved in DMSO at 10 mM (Sigma) and stored at -80°C.

11. MHC-biomonomer and MHC-tetramer preparation

The synthesis of MHC-peptide tetrameric complexes is based on the use of prokaryotic expression systems for MHC class I heavy chain and β2-microglobulin. The MHC heavy chain (H-$2D^b$ for Gag/Abu peptide and H-$2K^b$ for Env peptide) was modified by substitution of the transmembrane and cytosolic domains with a signal sequence containing a biotinylation site for the enzyme BirA. The MHC heavy chain, β2m and epitope peptide were subjected to a refolding *in vitro* in Tris-HCl pH 8, L-Arginin-HCl, NaEDTA, oxidized glutathione and reduced glutathione (Sigma). The complex was isolated through dialysis, concentrated and purified by HPLC to separate monomers from unconjugated components. Monomers were then enzymatically biotinylated by the enzyme BirA. The biomonomers obtained were purified and then quantified with a spectrophotometer. The tetramers were finally assembled with phycoerythrin (PE)-conjugated extravidin (Sigma) for the subsequent use of tetramers in flow cytometry analysis. The MHC-tetramers obtained were stored at 4°C. The correct volume of extravidin-PE and hence the efficiency of tetramerization was verified by ELISA. Briefly, 96-well plates (Maxisorb, NUNC, Rochester, NY, USA) were coated overnight (ON) at room temperature (RT) with rabbit anti-human β2 microglobulin antibody (1:5000 in PBS 1X; Genetex, Irvine CA, USA), that recognizes β2 microglobulin of free biomonomers. The coating was then removed and the assay buffer (AB: PBS 1X, 2% BSA, pH 7.4) was added for 1 hour at RT to saturate the aspecific sites. After three washes with wash buffer (WB: Tris HCl 50 mM, 0.2% Tween 20, pH 7.4), serial dilutions starting from 1 µg/ml of Gag or Env tetramers or the corresponding biomonomers were added for 1 hour at RT. The Gag and Env biomonomer solutions were used as positive controls. The plates were then washed three times with WB and Poly-

Horseradish Peroxidase-Streptavidin antibody (1:15000 in AB; Endogen, Rockford, IL, USA) was added for 1 hour at RT. After three washes with WB, OPD solution (*o*-Phenylenediamine dihydrochloride, Sigma) was added for 3-5 minutes for the detection of peroxidase activity. The reaction was finally stopped with HCl 3N and the absorbance was read at 490 nm in the ELISA plate reader (Victor X4 Multilabel Plate Reader; Perkin Elmer, Santa Clara, CA, USA).

12. Cell staining and flow cytometry analysis

To assess clonal dynamics *ex vivo*, fresh lymphocytes were isolated from lymph nodes, tumors and spleens at different time points, and labeled with D^b-Gag(Abu) or K^b-Env tetramer-PE (5 μg/ml) for 20 min at room temperature. Each sample was then stained with the APC-conjugated rat anti-mouse CD8a (clone 5H10; Invitrogen, San Giuliano Milanese, Italy) or the isotype control for 30 min at 4°C and then analyzed on a FACSCalibur. Data collected were evaluated with FlowJo software (TreeStar Inc., Olten, Switzerland). Cells from non-injected mice were used as negative controls, while Gag- or Env-specific cytotoxic T lymphocytes clones, previously obtained in our laboratory, were used as positive controls [141].

13. Cytotoxicity assay

The cytotoxic activity of MLTC was assessed in a 4h [^{51}Cr]-release assay after 5 days of culture. Briefly, MBL-2 cells were labeled for 1 hour at 37°C with 100 μCi of $Na_2{}^{51}CrO_4$ (DuPont, Boston, MA, USA), washed twice and added to the effectors cells plated in serial dilutions, starting from an effector/target (E/T) ratio of 100:1. Triplicates for each assay condition were set in round-bottom 96 well plates in a final volume of 200 μL/well. The supernatant was collected after 4 hours and radioactivity was assessed using a γ-counter (Cobra Gamma Counting System, Packard Instrument Company). The percentage of specific lysis was calculated as [(cpm experimental release − cpm spontaneous release)/ (cpm maximum release − cpm spontaneous release)] × 100. Where indicated, cytotoxic activity was expressed in terms of Lytic Unit $(LU)_{30}$ or LU_{15} (number of effectors in 1 x 10^6 of total effectors, which cause 30% or 15% of lysis).

14. Adoptive Cell Therapy (ACT)

Single-cell suspensions were obtained from spleens of UBC-GFP and Cybr-deficient/GFP donor mice. Naive T cells were isolated using Pan T cell isolation kit II (Miltenyi Biotec, Calderara di Reno, Bologna, Italy), according to the manufacturer instructions. Briefly, splenocytes were resuspended in staining buffer (PBS pH 7.2, 0.5% bovine serum albumin-BSA, and 2 mM EDTA) and incubated at 4°C for 10 min with the proper amount of Biotin-Antibody Cocktail. This cocktail comprises biotin-conjugated monoclonal antibodies against CD11b, CD11c, CD19, CD45R (B220), CD49b (DX5), CD105, MHC class II, and Ter-119. Microbeads conjugated to an anti‒biotin mouse mAb were then added for additional 15 min. After washing, purified naive T cells were obtained by magnetic negative separation using a LS column. The isolated populations were stained with APC-conjugated rat anti-mouse CD8a (clone 5H10, Invitrogen), CD19 (PeCa1; Immunotools, Friesoythe, Germany), F4/80 (clone BM8; Biolegend, London UK), and PercP-conjugated rat anti-mouse CD4 (clone GK1.5; Biolegend), and Armenian Hamster anti-mouse CD3e (clone 145-2C11, BD Pharmingen), to assess their purity by flow cytometry analysis. A total of 10 x 10^6 naive T cells were then injected into the tail vein of recipient RAG2-/- γc-/- mice after M-MSV injection. Mice were daily monitored for tumor growth by caliper measurement. Moreover, at different time points and until day 29 after the M-MSV and T cell injection, blood was collected and analyzed by flow cytometry. WBC were stained with the Armenian Hamster anti-mouse CD3e (clone 145-2C11, BD Pharmingen) or the isotype control for 30 min at 4°C and then analyzed on a FACSCalibur. At day 32, tumors, spleen and lymph nodes were collected and analyzed for the presence of GFP T cells. Each sample was labeled with D^b-Gag(Abu) or K^b-Env tetramer and then stained with the APC-conjugated rat anti-mouse CD8a (clone 5H10, Invitrogen) or the isotype control for 30 min at 4°C and then analyzed on a FACSCalibur. Data collected were evaluated with FlowJo software (TreeStar Inc.).

15. Statistical analysis

For the kinetics data, ANOVA for repeated measurements was performed to determine a significant difference between the tumor growth in control and *Cybr*-deficient groups. P< 0.05 (*) and P<0.01 (**) were considered to be statistically significant. Statistical differences between mean values of lymphocytes numbers, $CD8^+$, $CD8^+$/Gag^+ and $CD8^+$/Env^+ CTL expressions were calculated with the Student *t* test for independent samples.

RESULTS

1. Assessment of growth kinetics of M-MSV/M-MuLV-induced sarcomas in wild type and *Cybr*-deficient mice

To assess the potential role that Cybr could play in the immune response mediated by T lymphocytes, we took advantage of our knowledge of MSV mouse model, which had been previously characterized in depth in our laboratory. Briefly, the intramuscular injection of M-MSV causes sarcomas that develop at the inoculation site, after a short period of latency. Subsequently, tumors regress because of a strong immune reaction primarily mediated by CTL specific for viral antigens [141]. Thus, *Cybr*-deficient and wild type B6 mice were injected intramuscularly with the retroviral complex and the tumor growth was monitored up to day 20 after virus injection. The incidence of tumor development in *Cybr*-deficient mice appeared slightly higher (67 out of 76, 88%) compared to wild-type mice (64 out of 86, 74%). Notably, *Cybr*-deficient mice developed larger sarcomas that additionally underwent regression with a slower kinetics in contrast to that observed in control mice (P < 0.001; Fig. 1). Furthermore, we noticed, that such difference was more evident from day 11 to day 15 after virus injection, which corresponds to the phase where the tumors reached the maximum size.

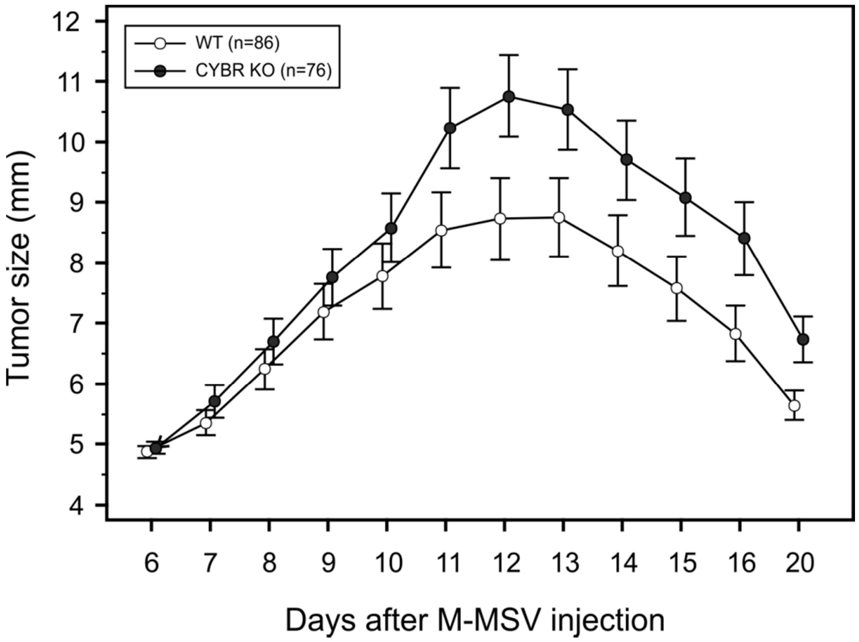

Figure 1: Analysis of M-MSV-induced tumor growth in *Cybr*-deficient mice. Cumulative kinetics of tumor growth in *Cybr*-knockout (filled circles) and wild type control littermates (open circles). Sixty-seven out of 76 (88%) *Cybr*-deficient and 64 out of 86 (74%) wild-type mice developed sarcomas after the intramuscular injection of M-MSV. Tumor size (in millimeters) was monitored up to day 20. P < 0.001 (ANOVA Repeated measures analysis of variance).

2. Histological and immunohistochemical analyses of *Cybr*-KO mouse tumors.

Based on the information of tumor growth kinetics in *Cybr*-deficient and wild-type mice, we decided to study the immune cells infiltrating the tumor site at different days during cancer development and regression. Indeed, our purpose was to detect any possible difference in the cell types infiltrating tumors between *Cybr*-deficient and B6 mice, to gain insight about potential mechanisms involved. Thus, mice were injected with the retroviral complex and sacrificed at different time points. Tumors were then collected and evaluated by H&E staining and by immunohistochemistry. Representative images of tumor sections from day 9 to 15 of H&E staining are reported in Figure 2.

We could not notice apparent differences in the overall amount of tumor cellular infiltrate between the two groups. In both of them, the infiltrate gradually increased from day 9 to day 13 to gradually decrease thereafter, as expected by the resolution of the inflammatory process. Conversely, the immunohistochemical analyses (Fig. 3) showed some differences in terms of the cellular types infiltrating the tumors. As it can be observed in representative tumor sections at day 12, the day of the maximal tumor growth, the rich inflammatory infiltrate appeared to be mainly constituted by cells of the myeloid lineage: neutrophils expressing Gr-1, macrophages expressing CD11b and, in a large percentage, also CD68. Only a few CD11c$^+$ dendritic cells were present. No significant differences in myeloid infiltrate were evident between the two strains (Fig. 3A). However, the number of infiltrating T cells was quite different between the two groups. Indeed, both CD4$^+$ and CD8$^+$ cells were less represented in *Cybr*-KO compared to wild-type mice. Notably, no Fox-p3 positive cells (regulatory T cells) were present and CD45R$^+$ B cells were scarcely represented in either strain (Fig. 3B).

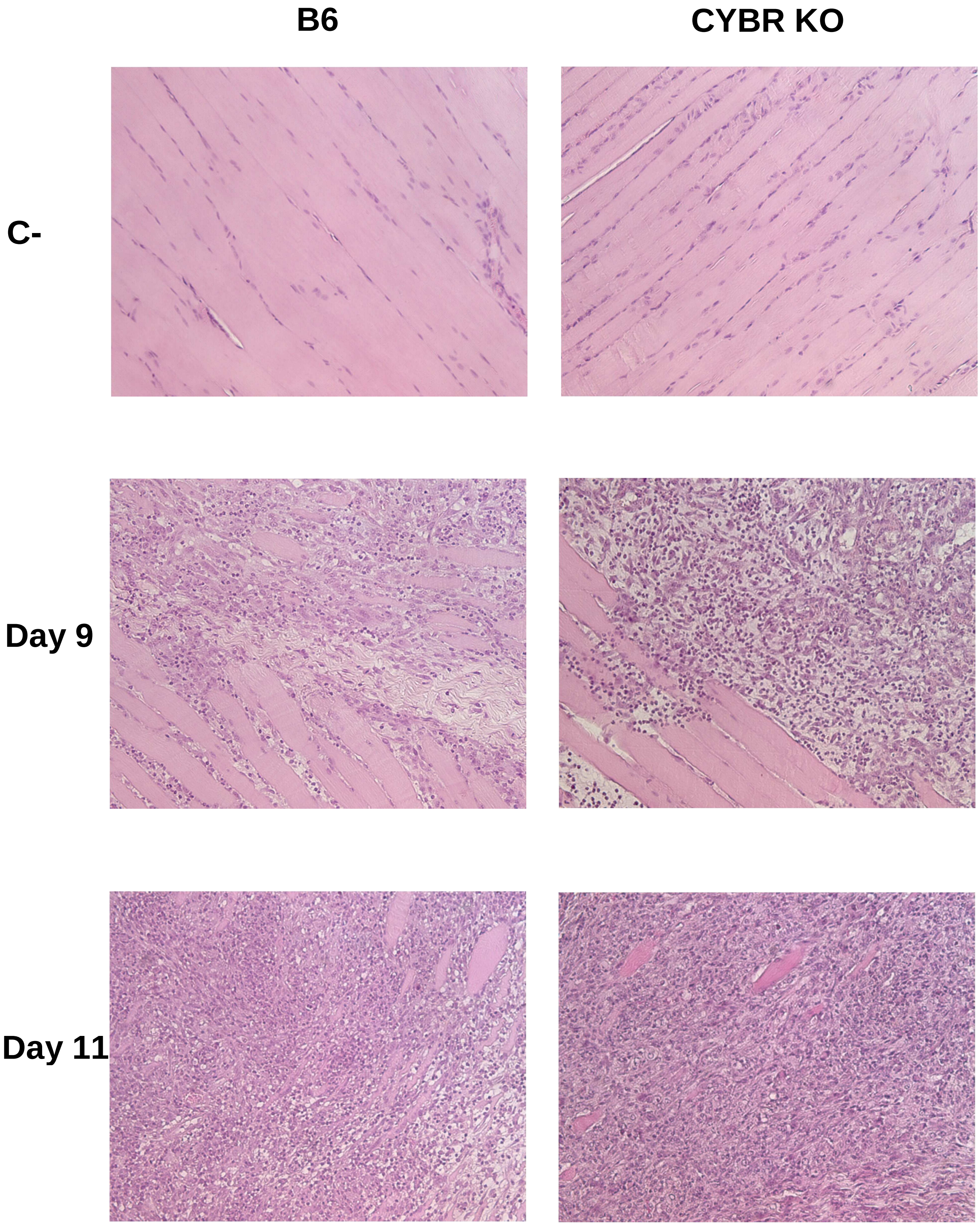
B6
CYBR KO
C-
Day 9
Day 11

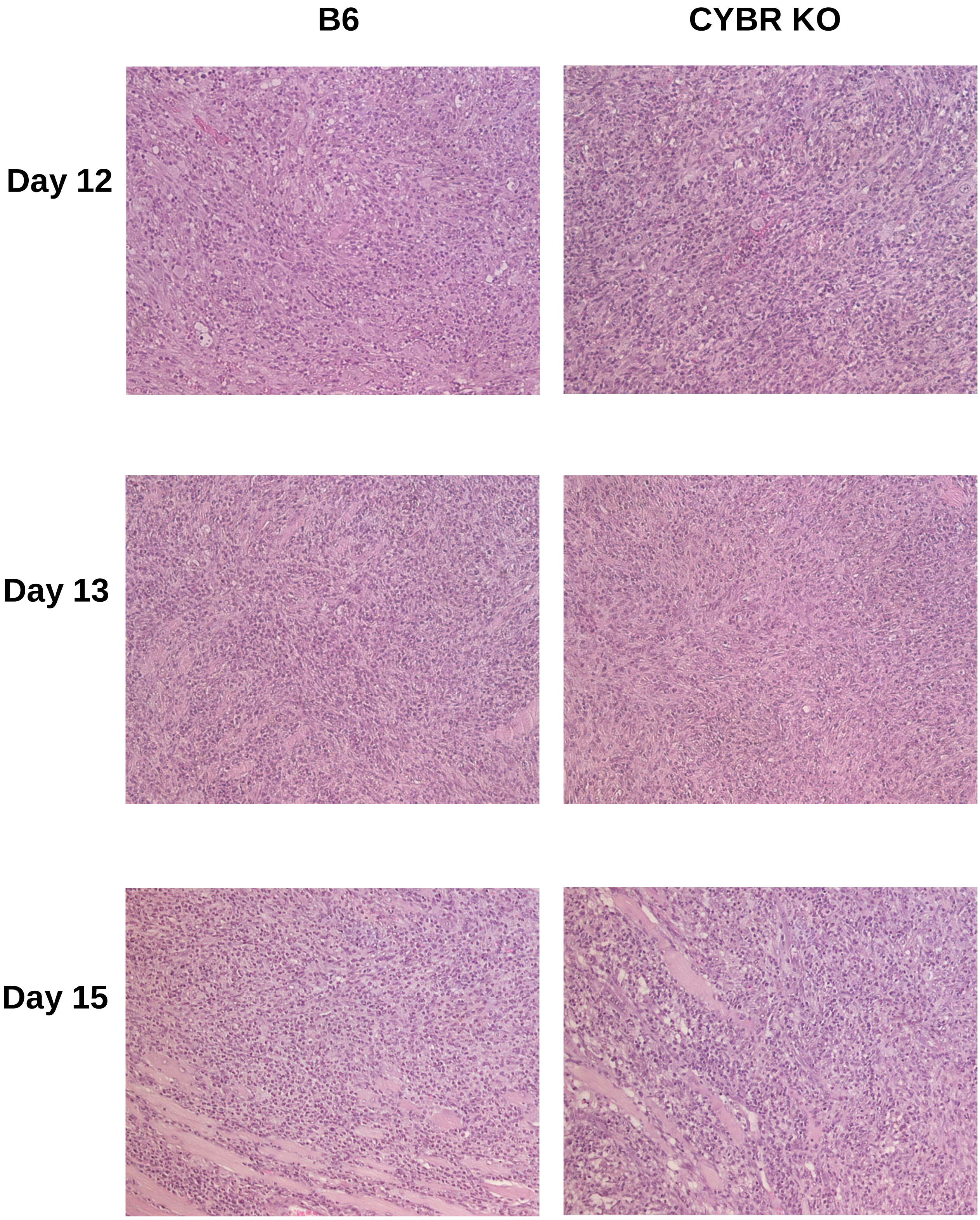
B6
CYBR KO
Day 12
Day 13
Day 15

Figure 2: Histological analyses of *Cybr*-KO and B6 mouse tumor sections. Representative images of tumor sections from day 9 to 15 in H&E staining (20X).

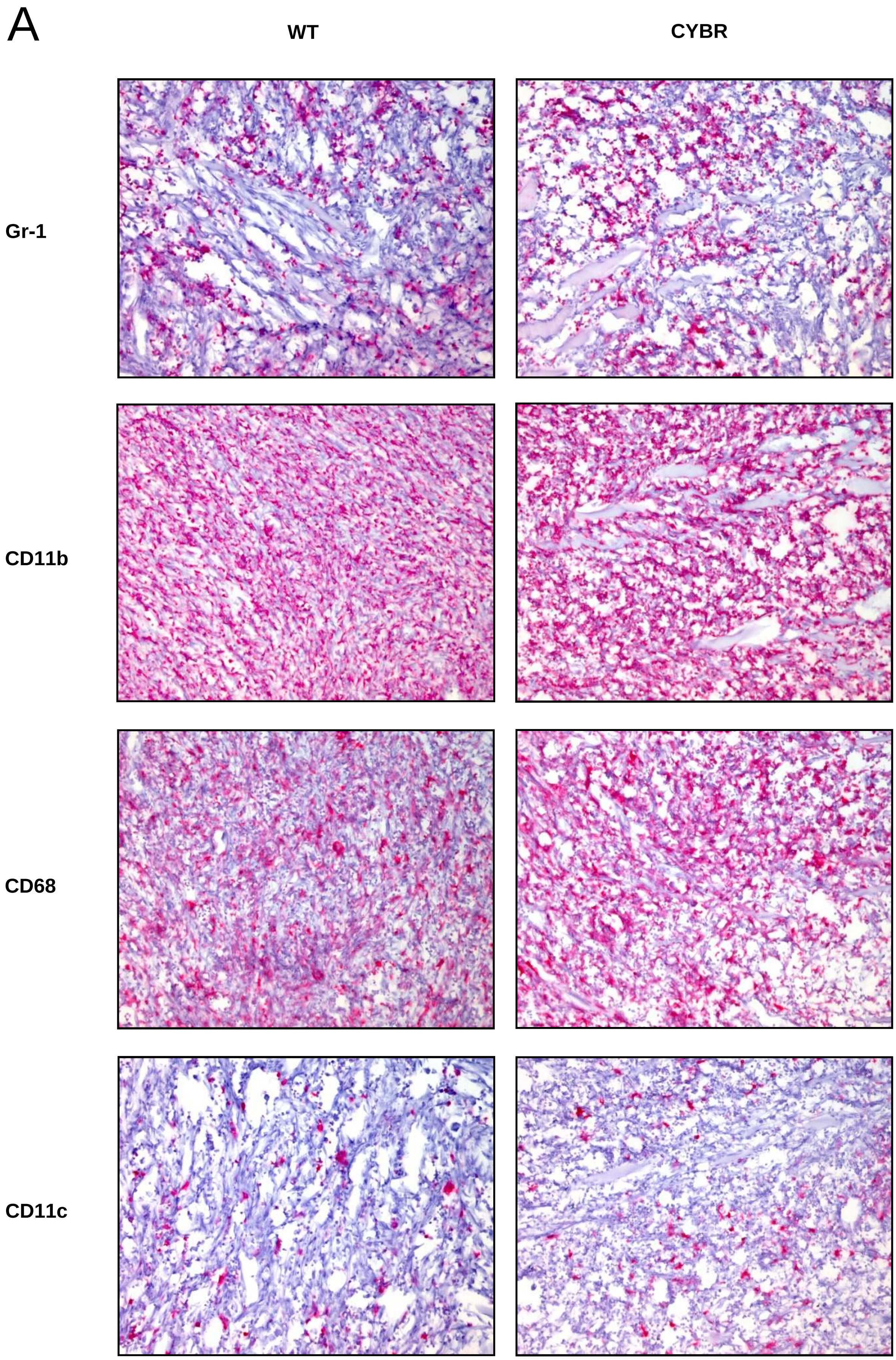

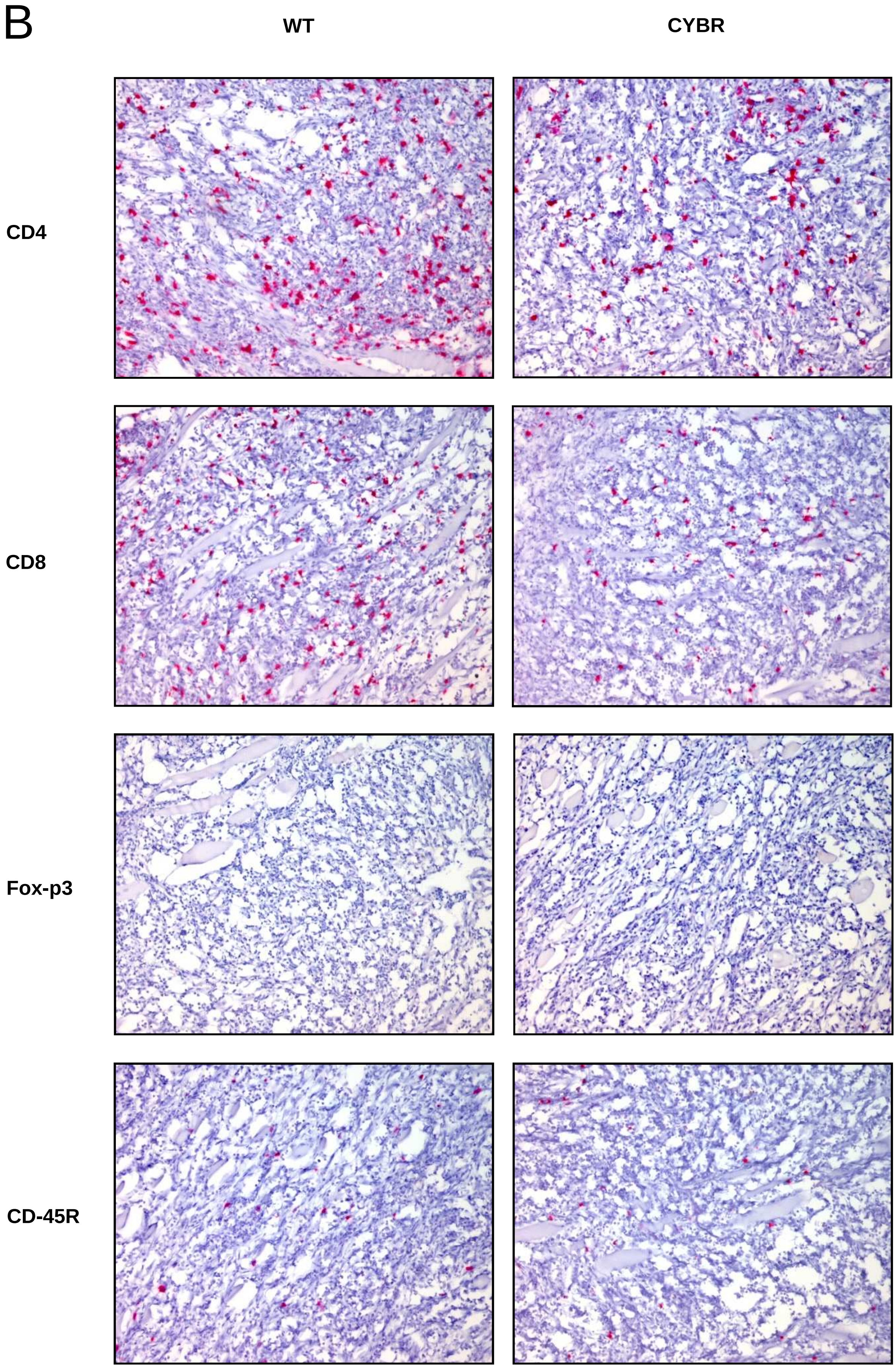
B
WT
CYBR
CD4
CD8
Fox-p3
CD-45R

Figure 3: Immunohistochemical analyses of *Cybr*-KO and B6 mouse tumor sections. Analyses of A) myeloid and B) T cells markers. Representative images of tumor sections at day 12, the day of the maximal tumor growth, are reported.

3. Evaluation of virus-specific CTL response in tumors, lymph nodes and spleens of M-MSV-injected wild-type and *Cybr*-deficient mice.

To assess the immunological features that may be responsible of the different tumor growth kinetics between *Cybr*-deficient and wild-type mice, animals of both groups were injected with the retroviral complex and sacrificed at the peak of tumor growth (day 11, 12, 13 and 15 after virus injection). Subsequently, tumors, spleens and tumor-draining lymph nodes were collected, the leukocytes isolated and finally analyzed by flow cytometry in order to evaluate the amount and specificity of the CD8$^+$ T cell populations directed to the *Gag* and *Env* viral antigens.

For this purpose, we took advantage of the tetramer technology in use in our laboratory. The Gag- and Env-specific tetramers were produced from the corresponding biotinilated biomonomers by the addition of Extravidin-PE, and subsequently were purified by HPLC. The tetramerization was carried out with good efficiency, as assessed by ELISA (Fig. 4A). Indeed, the presence of free biomonomers was negligible in both tetramer preparations, since the absorbance values obtained were markedly lower than the corresponding unlinked biomonomers. Then, the capacity of tetramers to stain specific T cell clones isolated from splenocytes of tumor regressor mice [139], was tested by flow cytometry. Results clearly showed that both tetramers were capable to stain 100% of cells with a relatively high intensity (Fig. 4B).

Cybr-deficient and wild-type B6 tumors were collected and processed with a cocktail of enzymes that digest tissues to obtain tumor infiltrating leukocytes (TIL) in suspension. Leukocytes were counted and normalized with the tumor volumes (Fig. 5A). Although no apparent differences were noticed at day 11, at day 12, the day of the maximal tumor growth in both groups of animals, the number of TIL was clearly lower in *Cybr*-deficient mice than wild type B6 animals ($P < 0.01$). Moreover, while the amount of TIL in B6 mice gradually decreased during the following days, the number of TIL in *Cybr*-deficient mice remained nearly constant and started to rise only by day 15. These data were further confirmed by flow cytometry analysis of the CD8$^+$ T cell populations in TIL, which disclosed a three day delay in the increase of lymphocytes in *Cybr*-deficient mice compared to wild type animals (Fig. 5B). To evaluate the amount of CD8$^+$ T cell populations specifically directed to the *Gag* and *Env* viral antigens, we subsequently stained the TIL with the specific tetramers. The results obtained are presented as number of lymphocytes positive for the specific tetramers (CD8$^+$/*Gag*$^+$ and CD8$^+$/*Env*$^+$) adjusted according to the tumor volume (Fig. 5C and D). Data confirmed the same trend observed previously, emphasizing the difference between B6 and *Cybr*-deficient lymphocytes especially at day 13, although they did not always reach statistical significance. In contrast, the number and the tetramer specificity of lymphocytes isolated from lymph nodes and spleens were not different between the two groups of mice (Fig. 6 and 7, respectively). Representative flow cytometry images of such experiments are presented in panel E and F of Figure 5, 6 and 7.

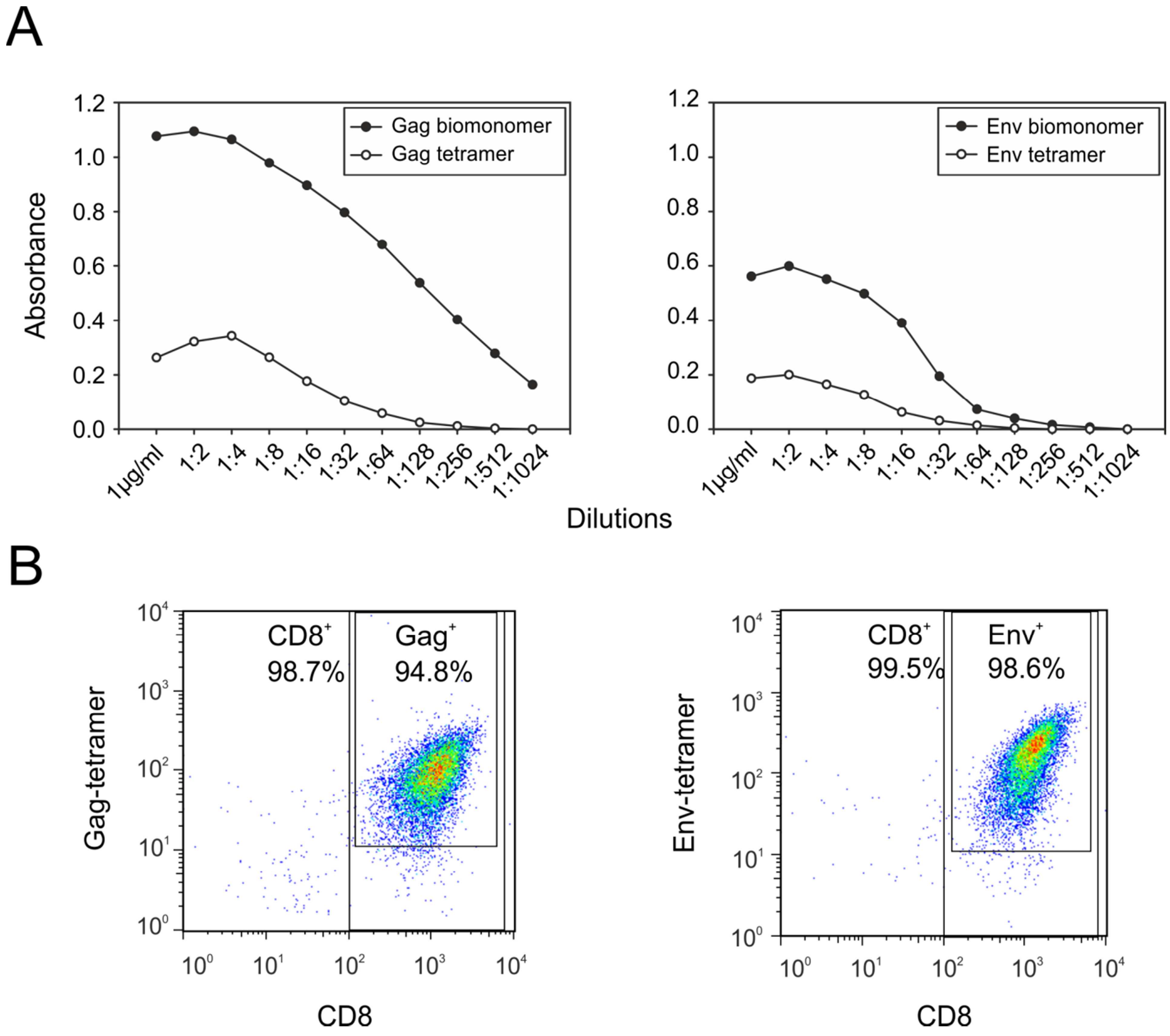

Figure 4. Evaluation of Gag- and Env-specific tetramers. A) Tetramerization efficiency of Gag-specific (left panel) and Env-specific tetramers (right panel), as assessed by ELISA. The absorbance of different dilutions (starting from 1µg/ml) of the tetramer preparations (open circle) and the respective biomonomers (filled circles) were compared. B) Flow cytometry analysis was performed to evaluate the capacity of tetramers to stain Gag-specific (left panel) and Env-specific (right panel) T cell clones.

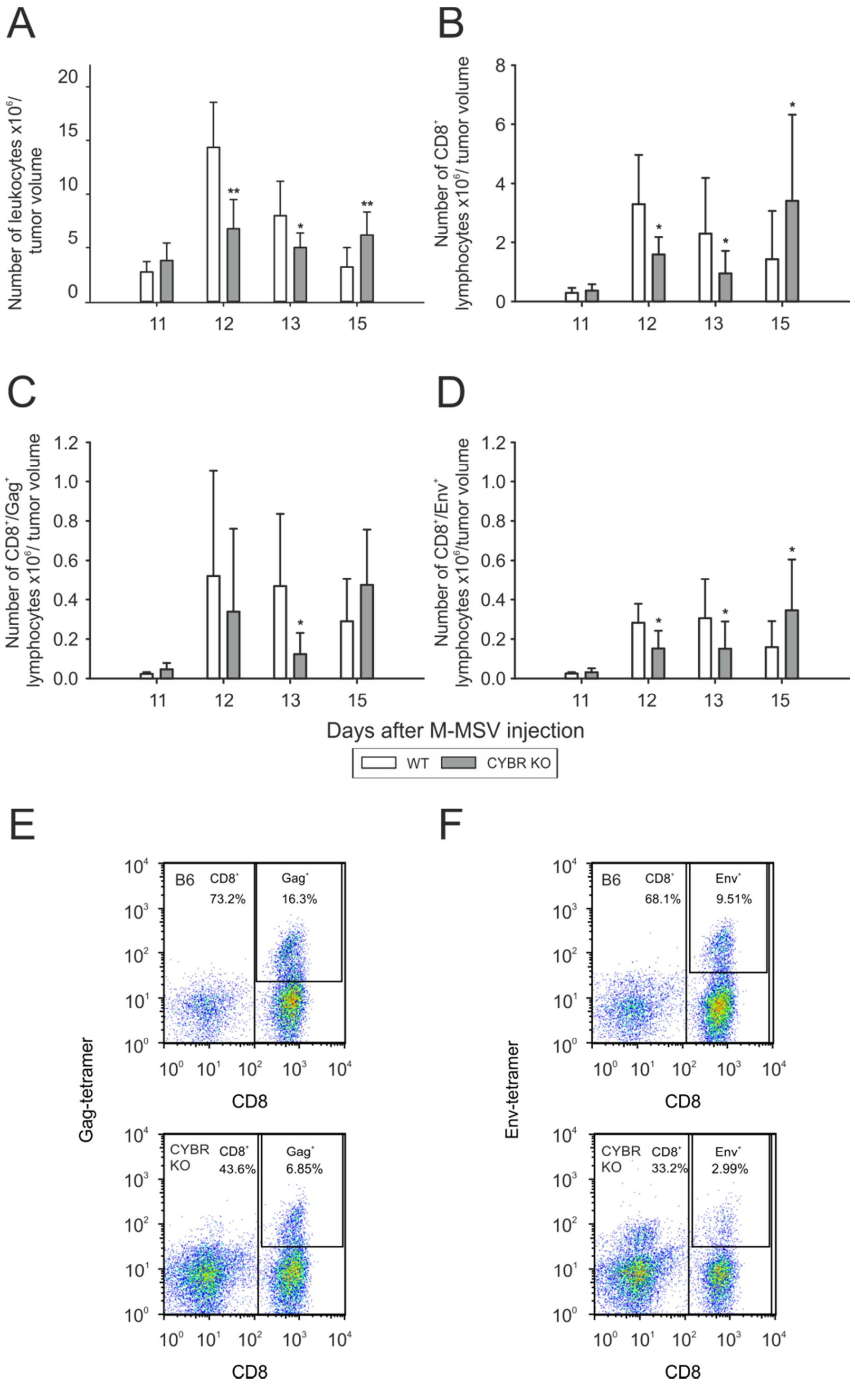

Figure 5. Analysis of leukocytes and specific CTL populations in tumors of *Cybr*-deficient and B6 mice at days 11-12-13-15 after M-MSV injection. A) Leukocytes numbers standardized with the correspondent tumor volume in *Cybr*-deficient and B6 mice. Figure shows mean + SD of 4 independent experiments (10-15 mice/day for each strain). B) $CD8^+$ T lymphocytes as analyzed by flow cytometry after correlation with leukocyte numbers shown in A. C) $CD8^+/Gag^+$ and D) $CD8^+/Env^+$ T lymphocyte analyzed by flow cytometry and correlated with leukocyte numbers shown in A. E, F) Representative images of flow cytometry analyses of $CD8^+/Gag^+$ (E) and $CD8^+/Env^+$ T cells population (F) in B6 and *Cybr*-deficient mice at day 13. * $P<0.05$ and ** $P<0.01$ versus wild type, Student's *t*-test for independent samples.

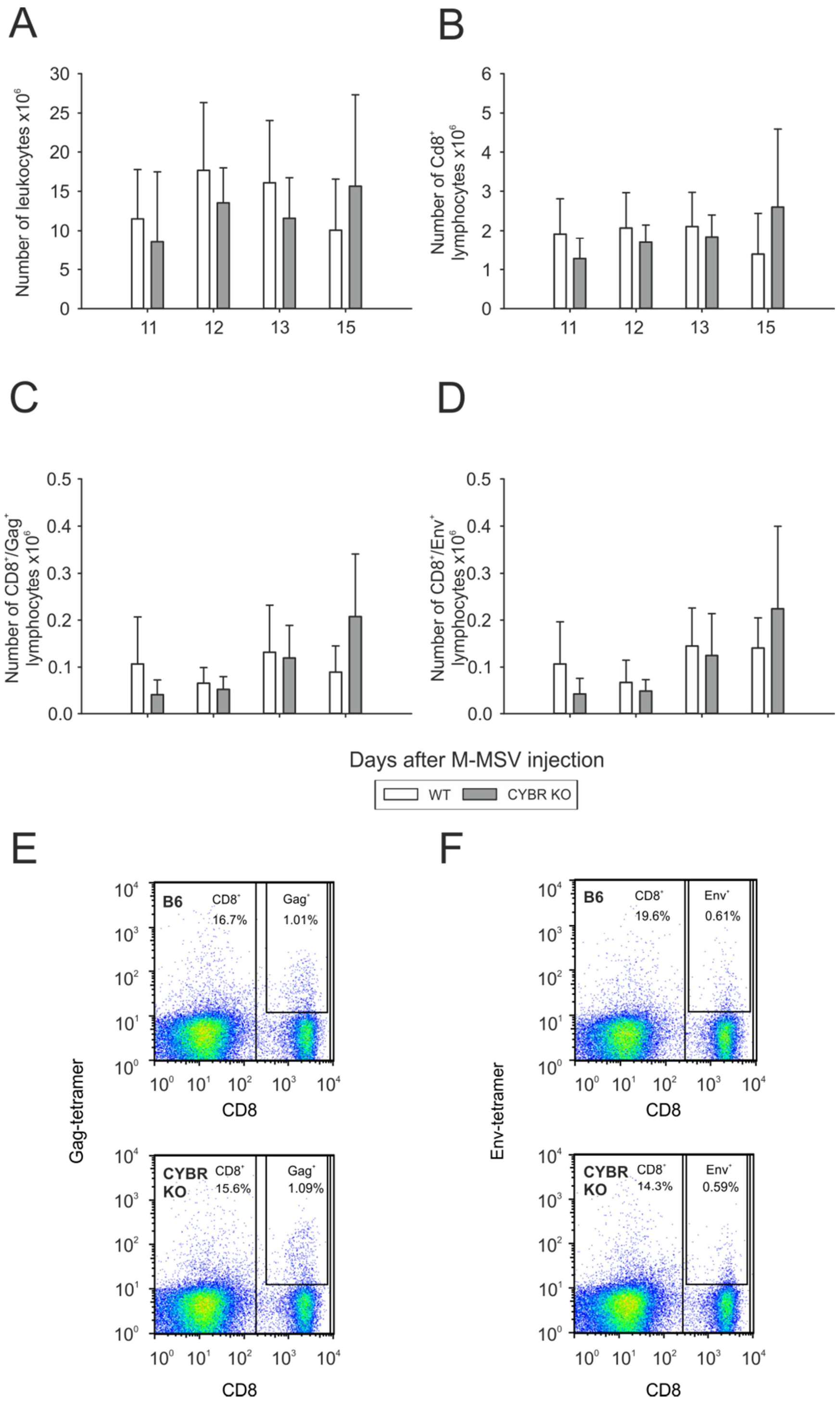

Figure 6. Analysis of leukocytes and specific CTL populations in lymph nodes of *Cybr*-deficient and B6 mice at days 11-12-13-15 after M-MSV injection. A) Leukocytes numbers in lymph nodes of *Cybr*-deficient and B6 mice. Figure shows mean + SD of 4 independent experiments (10-15 mice/day for each strain). B) CD8$^+$ T lymphocytes as analyzed by flow cytometry after correlation with leukocyte numbers shown in A. C) CD8$^+$/Gag$^+$ and D) CD8$^+$/Env$^+$ T lymphocyte analyzed by flow cytometry and correlated with leukocyte numbers shown in A. E, F) Representative images of flow cytometry analyses of CD8$^+$/Gag$^+$ (E) and CD8$^+$/Env$^+$ T cells population (F)in B6 and *Cybr*-deficient mice at day 13. * $P<0.05$ and ** $P<0.01$ versus wild type, Student's *t*-test for independent samples.

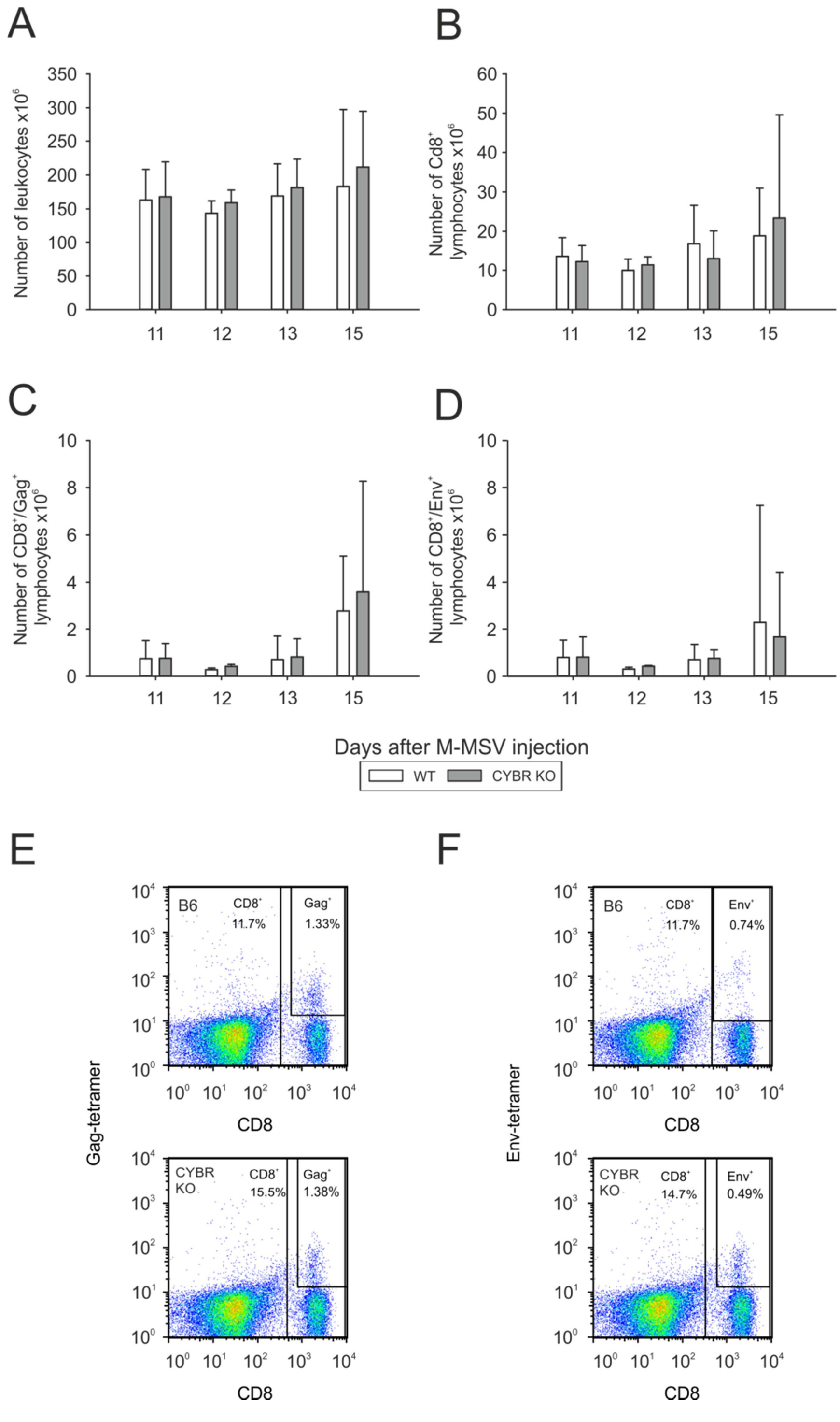

Figure 7. Analysis of leukocytes and specific CTLs populations in spleens of *Cybr*-deficient and B6 mice at days 11-12-13-15 after M-MSV injection. A) Leukocytes numbers in spleens of *Cybr*-deficient and B6 mice. Figure shows mean + SD of 4 independent experiments (10-15 mice/day for each strain). B) CD8+ T lymphocytes as analyzed by flow cytometry after correlation with leukocyte numbers shown in A. C) $CD8^+/Gag^+$ and D) $CD8^+/Env^+$ T lymphocyte analyzed by flow cytometry and correlated with the leukocyte numbers, shown in A. E, F) Representative images of flow cytometry analyses of $CD8^+/Gag^+$ (E) and $CD8^+/Env^+$ T cells population (F) in B6 and *Cybr*-deficient mice at day 13. * $P<0.05$ and ** $P<0.01$ versus wild type, Student's *t*-test for independent samples.

4. Functional characterization of CTL.

To functionally characterize and compare the CTL populations in *Cybr*-deficient and wild type mice, we analyzed the cytotoxic activity of MLTC set up from spleens of either strain. MLTC were obtained by co-culturing splenocytes collected at days 11, 13 and 15 after M-MSV injection with irradiated MBL-2 tumor cells expressing viral antigens. As shown in Figure 8A, *Cybr*-deficient CTLs displayed a significantly lower lytic activity than wild type CTLs at day 11 ($P<0.05$). The lytic activity difference between the two groups was observed also at days 13 and 15, although individual variability of cultures precluded the achievement of a statistical significance. By expressing the data in terms of LU_{30} (Fig. 8B), the differences between the lytic capacity of the two groups can be further better appreciated. At day 11, *Cybr*-deficient CTLs were confirmed to exert a significant lower cytotoxicity than effectors from wild type mice ($P<0.05$), while lytic function was recovered by days 13 and 15 and was similar to control CTLs.

To verify whether the lower lytic activity displayed by *Cybr*-deficient CTLs at day 11 was simply due to a reduced number of *Gag*- and *Env*-specific T cells in culture, we analyzed the percentages of virus-specific T cells in MLTC from mutant and B6 mice by tetramer staining before the cytotoxic assay.

Tetramer-specific $CD8^+$ T cells turned out to be more represented in MLTC from B6 than *Cybr*-deficient mice (day 13: 7.45 % *vs* 3.67% for B6 and *Cybr*-deficient cultures, respectively; day 15: 31.8% *vs* 11.85% for B6 and *Cybr*-deficient cultures, respectively), an exception being represented by day 11 when they appeared to be comparable (9.7% *vs* 6.6% for B6 and *Cybr*-deficient cultures, respectively). Therefore, data expressed in terms of LU_{30} were corrected for the percentage of specific CTLs to obtain more accurate information about the specific lysis of MLTC. Hence, *Cybr*-deficient specific CTLs disclosed a lower lytic activity only at day 11 (Fig. 8C), while they fully recovered and were even more cytotoxic than their wild type counterparts by day 15.

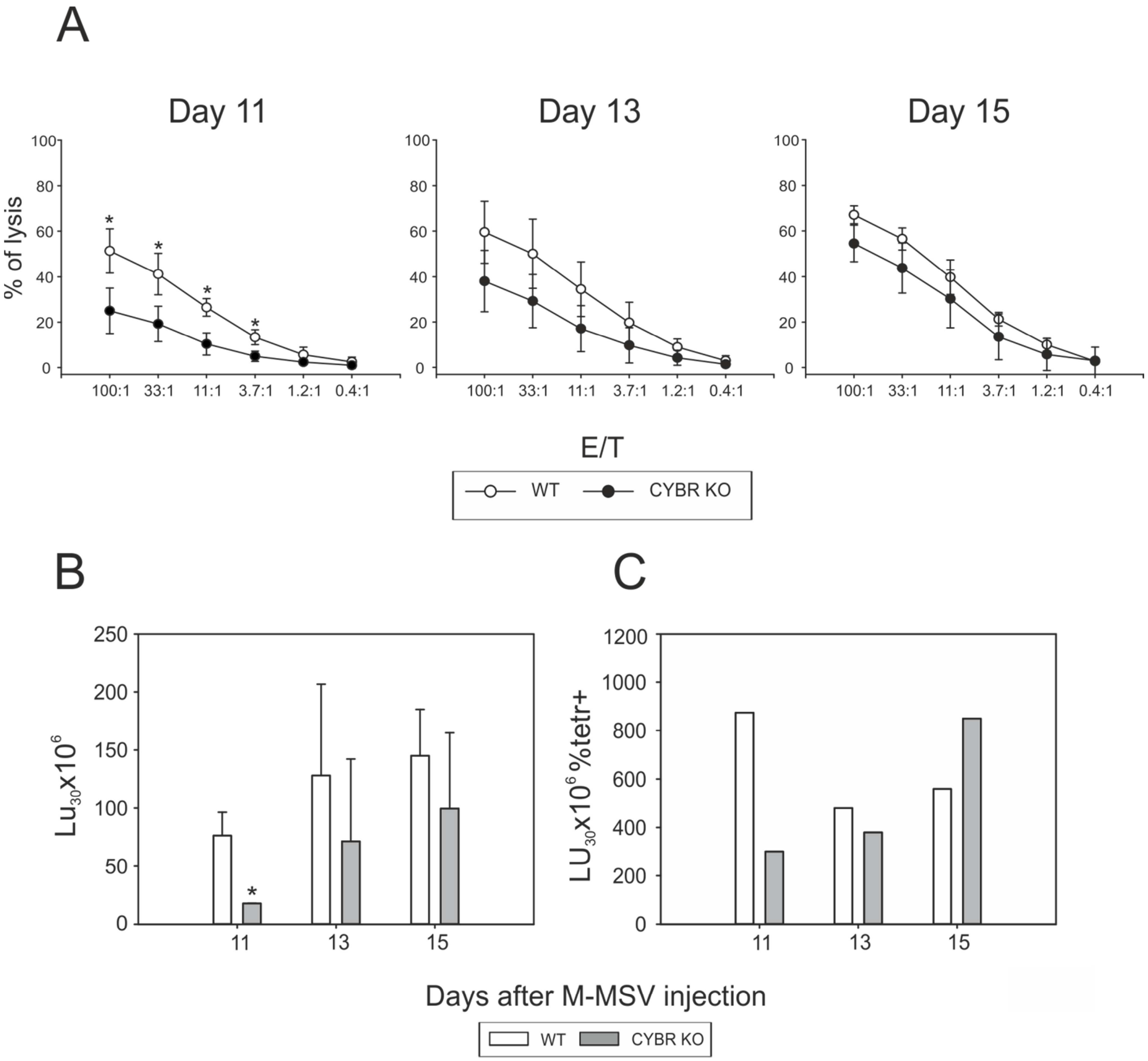

Figure 8. Analysis of lytic activity of *Cybr*-deficient and B6 CTL. A) Cytotoxic activity of *Cybr*-deficient and B6 MLTC, as assessed by standard 4h chromium release assay. MLTC were set up at days 11, 13, 15 after M-MSV injection and each MLTC was obtained from a pool of 4-5 animals. Figure shows mean +/- SD of four independent experiments. B) Cytotoxic activity as in (A) is reported in terms of LU_{30}. * refers to a statistically significant difference (P=0.018, Student’s *t*-test for independent samples). C) LU_{30} corrected for the percentage of $CD8^+$/tetramer$^+$ CTL populations, as obtained by flow cytometry analysis. Figure shows a representative experiment out of 4 carried out.

5. Assessment of lytic activity of *Cybr*-deficient and wild type CTLs from tumor regressor mice.

To compare the lytic activity of memory T cells from wild type and *Cybr*-deficient mice, splenocytes were isolated at day 40 after M-MSV injection, when mice of both strains had completely regressed the tumors, and MLTC were set up to be subsequently tested in a standard chromium release assay. As reported in Figure 9A, 6 weeks after retroviral complex injection CTLs from both *Cybr*-deficient and wild-type mice exhibited a fully overlapping lytic activity. These results are even more evident when data are expressed in terms of LU_{15} (Figure 9B) and also confirmed by the correction with the percentage of tetramer specific T cells (data not shown).

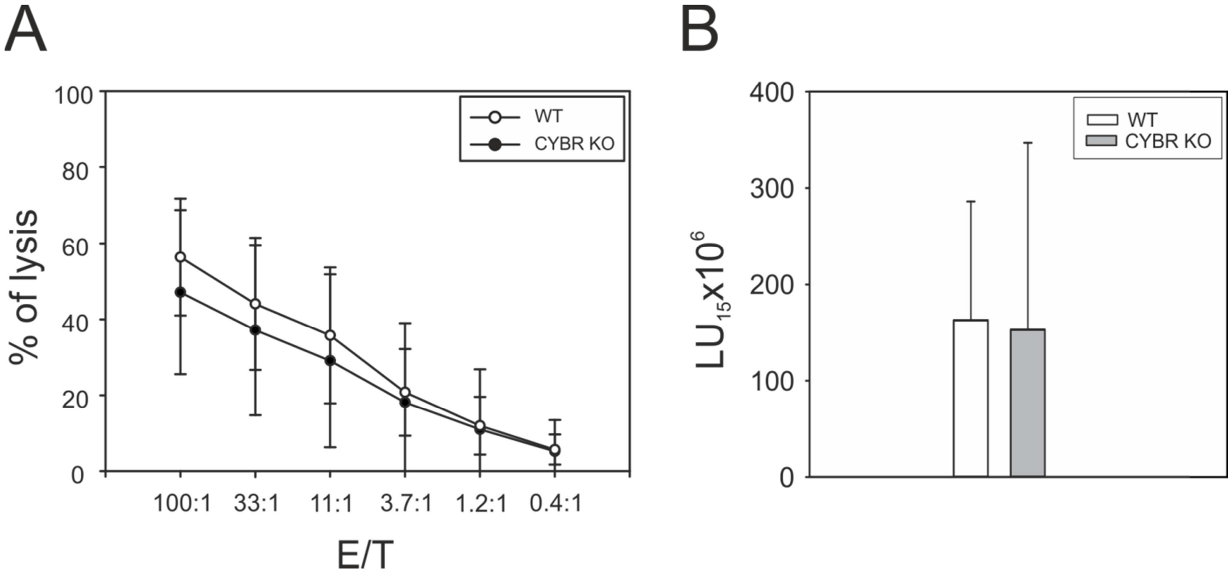

Figure 9. Analysis of lytic activity of *Cybr*-deficient and wild type CTLs from tumor regressor mice. A) Cytotoxic activity of *Cybr*-deficient and B6 MLTC as assessed by standard 4h chromium release assay. MLTC were set up from pools of 5 animals each 40 days after M-MSV injection. Figure shows mean +/- SD of four independent experiments. B) Cytotoxic activity as in A) was expressed in terms of LU_{15}.

6. Generation of *Cybr* knockout/GFP mice.

With the aim to develop a tool to track *Cybr*-deficient T cells in *in vivo* models after adoptive transfer experiments, we generated a *Cybr*-deficient/GFP mouse strain. Having in our animal facility the UBC-GFP mice, the Cybr-deficient/GFP mouse strain was obtained by crossing the eGFP-transgenic mice with *Cybr*-KO animals for at least 8 generations. The colony obtained was screened at each generation by PCR to detect the homozygosity of *Cybr* mutant gene (Fig. 10A) and by flow cytometry analysis to detect the GFP expression (Fig. 10B). Because of a dose-effect mechanism, the expression of GFP in homozygous and in hemizygous mice is characterized by a different intensity, thus allowing to clearly distinguish the two conditions.

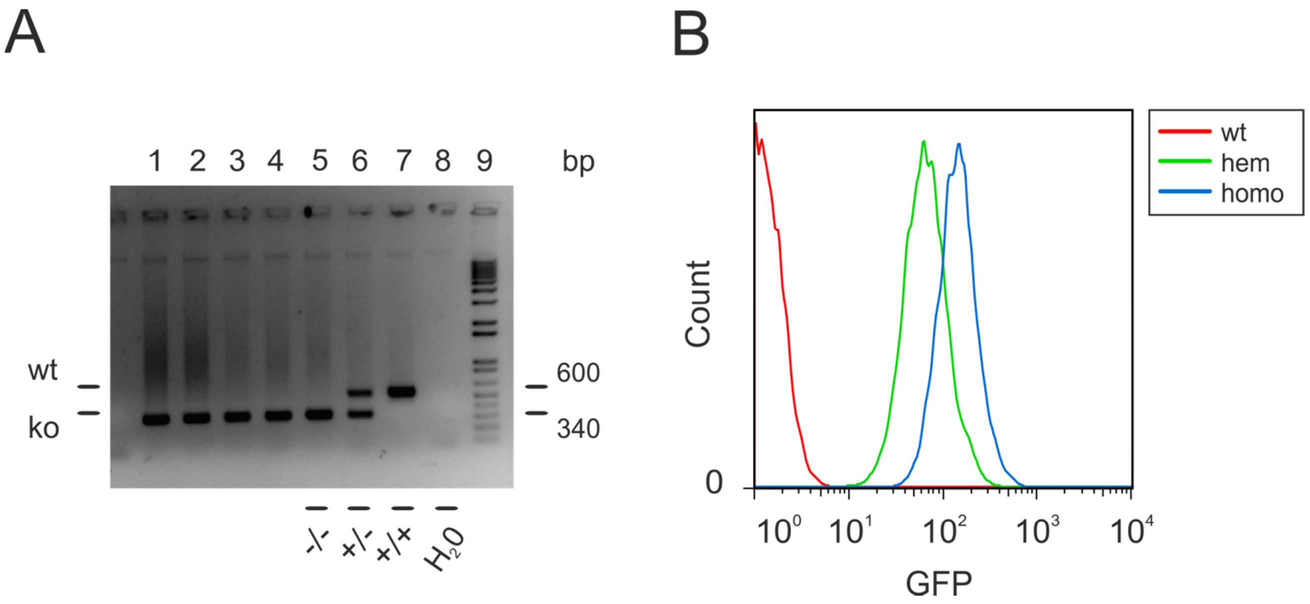

Figure 10. Analysis of *Cybr*-Knockout/GFP mice. A) Expression of *Cybr* mutant gene in genomic DNA extracted from peripheral blood of *Cybr*-KO/GFP mice. The samples were loaded for electrophoresis in the following order: lines 1 to 4, sample of homozygous mutant gene of *Cybr*-KO/GFP mice; line 5 homozygous mutant gene of *Cybr*-KO mice control; line 6, heterozygous gene of *Cybr*-KO/GFP mice; line 7, wild type gene of B6 mouse; line 8, water; line 9, base pairs ladder (bp). B) GFP expression, as assessed by flow cytometry analysis, in leukocytes obtained from peripheral blood of *Cybr*-KO/GFP mice. Blood from wild-type B6 mice (red peak) was used as negative control, while blood from UBC-GFP and from UBC-GFP x Cybr-KO F1 mice were used as homozygous (blue peak) and heterozygous (green peak) GFP expression controls, respectively.

7. Adoptive transfer of naive GFP-T cells from *Cybr*-deficient and B6 mice into Rag2-/- γc-/- animals.

To understand the mechanistic role of Cybr in the priming or effector phases of the immune response, further experiments were performed using the Rag2 -/- γc -/- mouse model, which lacks T, B and NK cells [142],[143]. First, M-MSV was injected into Rag2-/- γc-/- and the tumor growth was monitored (Fig. 11A). As expected because of the absence of T cells in Rag2-/- γc-/-, the tumors continued to grow without undergoing regression, as compared to the wild type mice. Then, ACT experiments were set up by transferring 10 x 10^6 purified naive T cells (96% CD3, 34% $CD3^+/CD8^+$, 62% $CD3^+/CD4^+$, 0,15% $CD19^+$, 0,35% $F480^+$) obtained from spleens of B6/GFP or *Cybr*-deficient/GFP mice, into M-MSV-injected Rag2-/- γc-/-, and tumor size was monitored daily by caliper measurement (Fig. 11B). Untreated M-MSV-inoculated RAG2-/- γc-/- were used as controls. Until day 10, mice treated with purified T cells from either strains did not developed tumors, which were conversely evident in RAG2-/- γc-/- control mice. From day 12 to day 18, RAG2-/- γc-/- mice receiving *Cybr*-deficient/GFP T cells presented neoplastic masses that were larger than those appearing in animals treated with B6/GFP T cells; nonetheless, tumors in mice undergoing ACT with T cells from either mouse strains were smaller than those of untreated RAG2-/- γc-/- mice, although the observed differences did not reach statistical significance. After the day 18, tumors continued to growth in all groups, suggesting that transferred naive T cells were not able to mount a fully effective immune response.

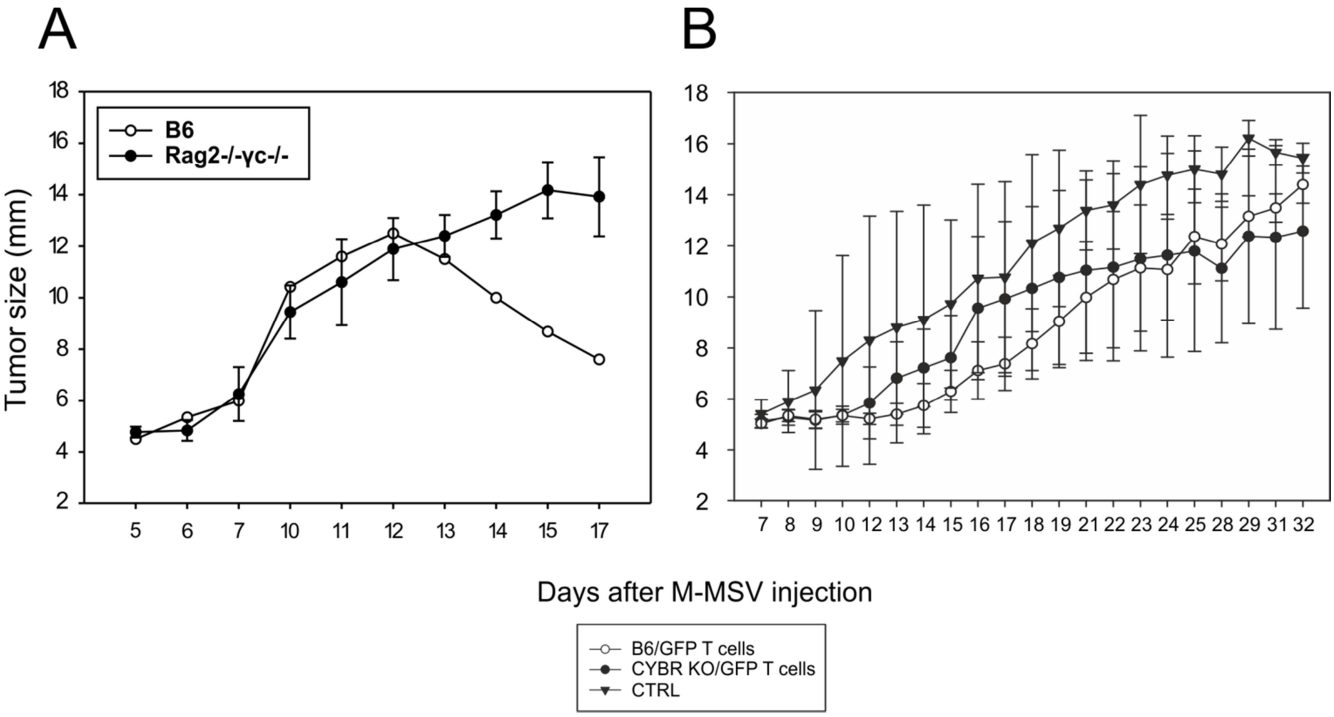

Fig.11. Analysis of M-MSV-induced tumor growth in Rag2-/- γc-/- mice. A) Kinetics of tumor growth in Rag2 -/- γc-/- mice injected with M-MSV (filled circles) is reported in comparison to that of wild-type control mice (open circles). All mice developed sarcomas, but Rag2 -/- γc-/- mice did not regress M-MSV-induced tumors. This preliminary experiment was set up with 5 animals for each group. B) Kinetics of tumor growth in Rag2 -/- γc-/- mice injected with M-MSV and receiving *Cybr*-deficient/GFP (filled circles) or B6/GFP T cells (open circles). For each group, 6 animals were injected while untreated Rag2 -/- γc-/- mice inoculated with M-MSV were used as control.

Moreover, blood samples were collected at different time points after ACT and the presence and amount of transferred GFP T cells were evaluated. In the peripheral circulation, the leukocyte counts were similar between the two groups (Fig. 12A). Blood specimens were further analyzed for the percentage of CD3$^+$/GFP$^+$ cells and a similar kinetic trend was observed, even though B6/GFP T cell-injected mice displayed higher percentages of GFP$^+$ T cells in the circulation (Fig. 12B). By expressing the obtained data in terms of fold-increase, with the post-injection value of both groups of mice considered as baseline (Fig. 12C), we found that the percentage of circulating *Cybr*-deficient T lymphocytes was significantly lower than that of wild type T cells only at day 7 (P=0.041). Moreover, based on the CD3$^+$/GFP$^+$ cell percentages and the number of counted leukocytes, we could extrapolate the absolute number of transferred T cells in the peripheral blood (Fig. 12D). Again, by expressing the results as fold-increase (Fig. 12E) it was confirmed that a significant difference (P<0.0001) was present only at day 7.

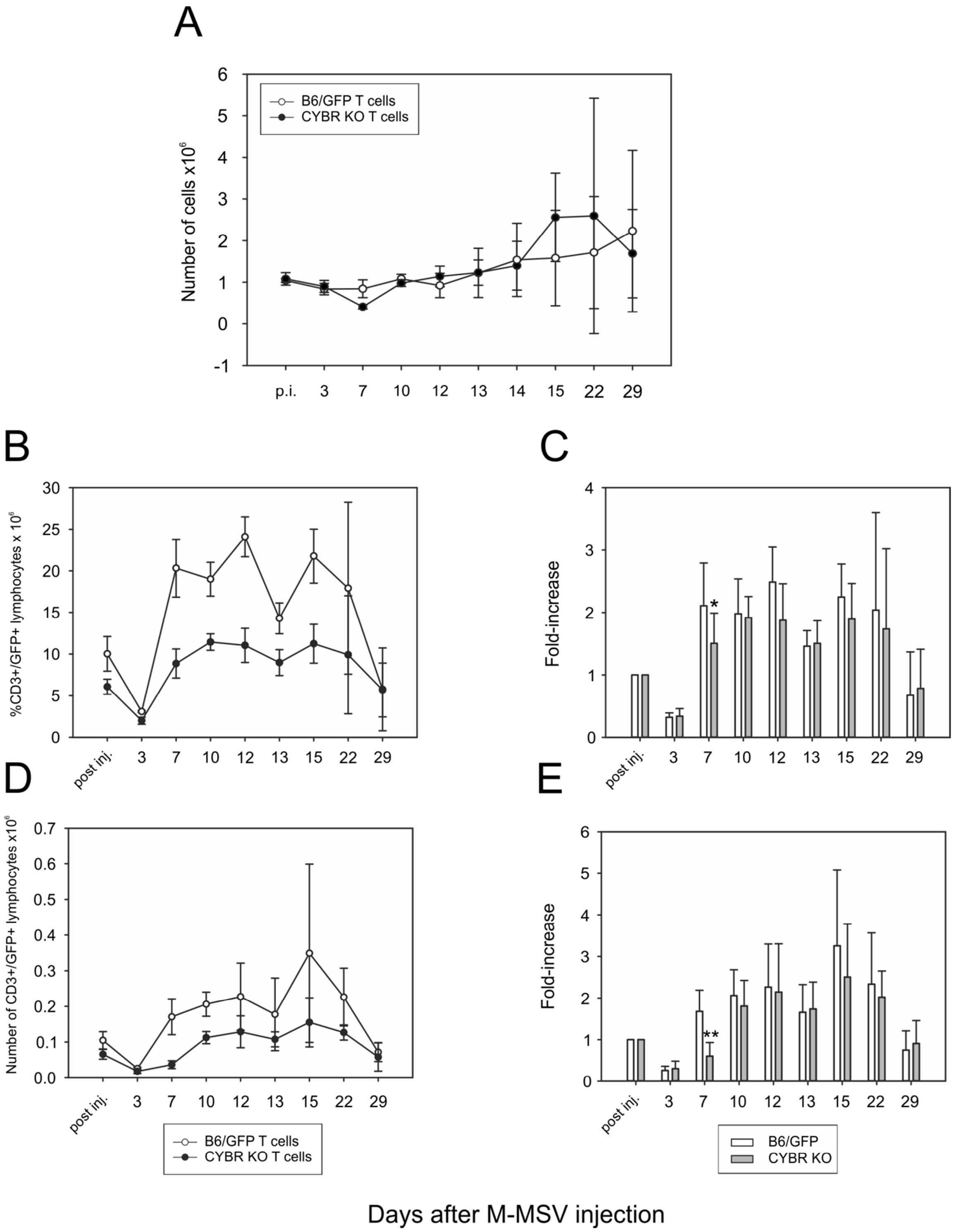

Figure 12. Assessment of *Cybr*-deficient/GFP and B6/GFP T cells adoptively transferred in Rag2-/- γc-/- mice. A) Number of peripheral blood leukocytes in Rag2 -/- γc-/- mice injected with M-MSV and receiving *Cybr*-deficient/GFP (filled circles) or B6/GFP T cells (open circles). B) Percentages (mean +/- SD) of CD3$^+$/GFP$^+$ T cells in peripheral blood at different time points after virus injection and ACT. C) Fold-increase of percentage data. * P=0.041, Student's *t*-test for independent samples. D) Number of CD3$^+$/GFP$^+$ T cells in peripheral blood calculated on the basis of leukocyte counts (A) and CD3$^+$/GFP$^+$ percentages (B). E) Fold-increase of CD3$^+$/GFP$^+$ T cells. ** P<0.0001, Student's *t*-test for independent samples.

Finally, mice were sacrificed at day 32 and leukocytes were isolated from the tumors, spleens and lymph nodes. Although no difference was found in the number of leukocytes isolated from tumors of either group of animals (data not shown), no CD8$^+$/GFP$^+$ T cells could be recovered from these samples. Tumor-draining lymph nodes were hypoplastic and were detected only in few animals, thus precluding a flow cytometry analysis of the CD8$^+$/GFP$^+$ populations. Moreover, differences were not found in the number of leukocytes isolated from spleens of Rag2-/- γc-/- mice injected with B6/GFP or *Cybr*-deficient/GFP T cells (Fig. 13A). The CD8$^+$/GFP$^+$ component was also similar in both groups (Fig. 13B and 13C), but Gag- or Env-specific CTLs could not be detected.

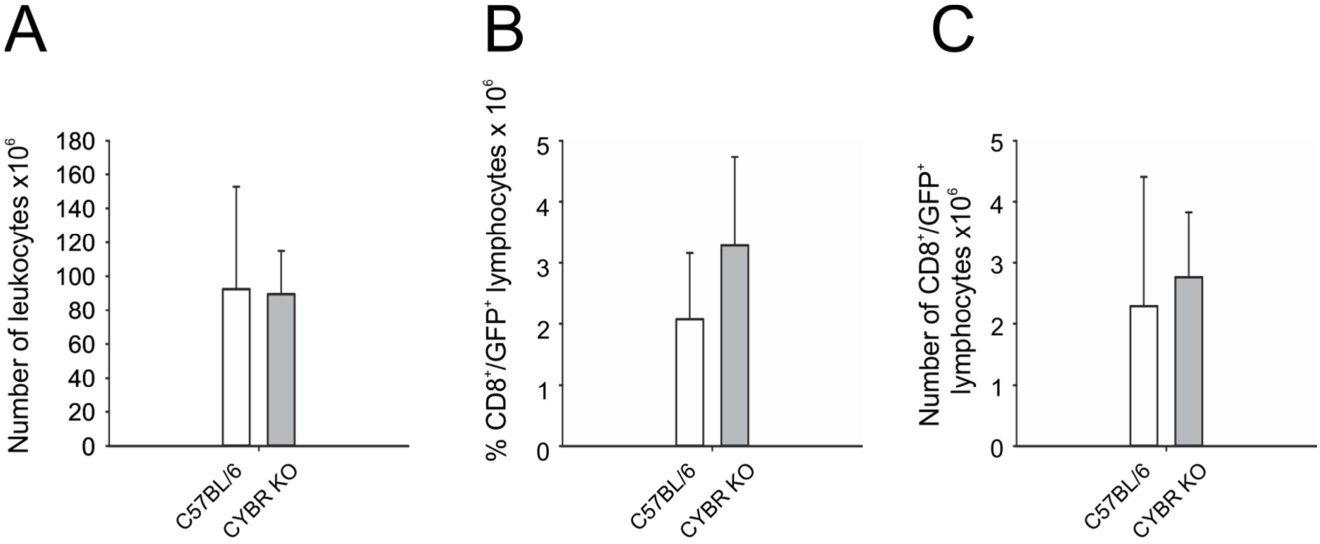

Figure 13. Spleen cell analysis at day 32 after adoptive transfer. A) Figure shows the number of leukocytes found in spleens of M-MSV-injected Rag2-/- γc-/- mice and inoculated with *Cybr*-deficient/GFP or B6/GFP T cells. B) and C) show the percentages and numbers of CD8$^+$/GFP$^+$ T cells, respectively. Data are the means + SD of 6 mice receiving B6/GFP or *Cybr*-deficient/GFP T cells.

DISCUSSION

Cybr is a scaffold protein highly expressed in the hematopoietic/immune system. Its interaction with members of the cytohesin family [95],[101] is interesting because of its ability to control ARF function and to regulate LFA-1-mediated cell adhesion in T cells [96],[100]. Specifically, Cybr diminishes stimulated adhesion of LFA-1 to ICAM-1 [96], and also regulates T cell attachment and detachment from contact zones to DCs [100],[87]. These findings place Cybr in a crucial position to control cell adhesion and trafficking of the immune system cells; however, the knowledge about this protein is still limited and mainly relies on *in vitro* studies.

First insights from the two available *Cybr*-deficient mouse strains [104],[103] showed that the development of the immune system is only marginally affected by the targeted deletion of Cybr, and that these mice display a reduced or delayed capacity to respond in stress conditions to different stimuli, namely Th1 polarized settings [104].

The purpose of this project was therefore to investigate the biological relevance of Cybr *in vivo* in a model of viral induced tumorigenesis, namely the M-MSV mouse model [144], taking advantage of the *Cybr*-deficient mouse strain described by Coppola and colleagues [104]. The intramuscular inoculation of the M-MSV retroviral complex in immunocompetent mice gives rise to sarcomas that rapidly undergo spontaneous regression, due to a strong immune reaction mainly mediated by CTL specific for viral antigens, in particular Gag and Env antigenic peptides [141].

In this setting, we found that *Cybr*-deficient mice developed larger sarcomas that additionally regressed with a slower kinetics in comparison to control mice. To characterize which subset of immune cells was affected in Cybr deficiency, we studied the immune cells infiltrating the tumors by H&E staining and by immunohistochemistry. As expected [144], tumors were characterized by a rich infiltrate mainly constituted by cells of the myeloid lineage (neutrophils, macrophages and CD11c$^+$ dendritic cells), without apparent differences between wild type and *Cybr*-deficient mice. However, with regard to TIL, *Cybr*-KO mice were characterized by a reduced number of both CD4$^+$ and CD8$^+$ T cells compared to wild type mice. The relevant presence of CD4$^+$ Fox-p3 negative T cells (comparable to that of CD8$^+$ T cells in both strains) underlines the important role of this subset in tumor immune response. Indeed, as previously reported [145], mice injected with depleting anti-CD4 antibody did not generate virus-specific cytotoxic T lymphocytes and ultimately died with progressing sarcomas at the inoculation site. Based on the increasing importance as effector cells in tumor immunity and the impact of Cybr on CD4$^+$ T cell function [146], the role of this subset in our model needs further investigation. However, in this work we mainly focused our attention primarily on CD8$^+$ T cells. Specifically, we characterized the CTL clonal dynamics in tumor, lymph nodes and spleen in correspondence of maximal tumor growth (day 11, 12, 13 and 15 after virus injection), by means of flow cytometry analysis and tetramer staining.

In line with immunohistochemistry analysis, we found an overall reduction in the number of lymphocytes infiltrating the tumor, as well as in the number of virus-specific CTLs in *Cybr*-deficient mice compared to the wild type mice. This difference was more evident at day 12 and 13, while at day 15 the number of TIL in *Cybr*-KO mice steadily rised and was comparable to values found in wild type mice. The delay in tumor cell infiltration is consistent with the hypothesis that Cybr-deficiency negatively affects leukocyte trafficking, especially in response to proinflammatory cytokines in stress conditions, as it happens in the response to the M-MSV-induced tumors. Moreover, in line with results of Coppola and colleagues [104], we found no differences in number and specificity of splenocytes in the two mouse strains. With regard to lymphocyte numbers in tumor-draining lymph nodes, a trend similar to that reported by Coppola and colleagues [104] was also observed, although our data did not reach statistical significance.

Additionally, we observed a delayed onset of the lytic activity in the *Cybr*-deficient specific CD8$^+$ T cell population. Indeed, *Cybr*-deficient CTLs displayed a lower cytotoxicity than wild type mice at day 11, while at day 15 they displayed a lytic activity comparable to that exerted by wild type CTLs at day 12. Thus, it appears that Cybr deficiency does not produce a strong immunodepression but is responsible of a mild immunodeficient phenotype, characterized only by a delay in the expansion of T lymphocytes in the tumor and also in the onset of their lytic activity, both defects being recovered in few days, an overall phenomenon that could be likely ascribed to the regulation of LFA-1 exerted by Cybr. Indeed, it was previously reported that the injection of anti-LFA-1 antibody enhanced tumor growth, delayed regression and also negatively impacted on the cytotoxic activity [147],[148]. Nonetheless, the involvement of Cybr in the events downstream the TCR engagement (namely, MAPK, JNK, p38, AP-1 and NFAT activation) [97] cannot be excluded in the delayed onset of lytic activity in *Cybr*-deficient CD8$^+$ T cells, and require further studies.

Interestingly, the increased tumor growth in *Cybr*-deficient mice appears to strictly correlate with the temporary impairment of CTLs, both in terms of overall number and lytic activity respect to wild type CTLs; as soon as these defects were recovered, tumors finally regressed in both groups of mice. Indeed, at day 40 after retroviral complex injection, *Cybr*-deficient and wild type CTLs from tumor regressor mice, displayed a fully overlapping lytic activity. These data suggest that naive T cell activation and the expansion of primed T cells are primarily affected by the influence of Cybr's regulatory activity.

Collectively, our data indicate that Cybr deficiency has a significant impact on antigen-specific immune response, but it is still not clear whether Cybr mostly impacts on priming and/or cell adhesion, or in trafficking and migration of cells in the immune system.

In an attempt to answer the biological question whether Cybr deficiency plays a major role in the priming or in the effector phase of the T cell cytotoxic response, we set up a series of experiments of adoptive cell therapy in Rag2-/- γc-/- mice with a H-2^b background; because of the lack of T, B and NK cells, in this immunodeficient strain the M-MSV injection leads to the development of sarcomas that do not spontaneously regress. Moreover, we took also advantage of a new mouse strain (*Cybr*-KO/GFP) produced in our laboratory by breeding *Cybr*-deficient mice with GFP-transgenic B6 animals.

Adoptive transfer of purified naive T cells from *Cybr*-KO/GFP or B6/GFP animals in M-MSV-injected Rag2-/- γc-/- mice allowed to focus on the study of the T cell compartment. In particular, we investigated the effects of Cybr deletion on CTL priming on the T cell side, since dendritic cells of recipient mice carry a wild type form of this protein. Except for a delay in the onset of the tumor in mice injected with isolated B6/GFP T cells, no significant differences were found in the kinetics of sarcomas development in all groups of mice. Despite the fact that transferred T cells from both animal strains expanded in the host, as assessed by flow cytometry analysis of PBMC, tumors continued to growth without undergoing regression. This suggested that wild type and *Cybr*-deficient transferred T cells were not able to mount a fully effective immune response. We inferred that the Rag2-/- γc-/- mouse did not represent an optimal model for our purposes. Likely, the physical structure of spleen and lymph nodes, found to be hypoplastic, precluded *per se* an efficient recruitment and hence an efficient priming of naive T cells. Therefore, ongoing experiments will involve different animal models. In this regard, reconstitution of nu/nu athymic B6 mice with T cell-depleted bone marrow from either B6 or *Cybr*-KO mice, followed by adoptive transfer of naive or memory T cells from *Cybr*-KO/GFP or B6/GFP animals, will provide the appropriate experimental set up to dissect the role of Cybr in the APC or T cell compartments. In particular, by transferring memory T cells from *Cybr*–KO/GFP or B6/GFP animals we will be able to potentially rule out a pure role in recirculation and homing to the tumor site, thus highlighting the impact that Cybr may have during the priming phases of immune response.

ABBREVIATIONS

Ab: antibody
ADP: adenosine diphosphate
AFP: α-fetoprotein
Ag: antigen
AP-1: activator protein 1
APC: antigen presenting cells
ARF: ADP-ribosylation factor
ARNO: ARF nucleotide binding site opener
BCR: B cell receptor
CALLA: common acute lymphoblastic leukemia antigen
CASP: cytohesin-associated scaffolding protein
CD: clusters of differentiation
CEA: carcinoembryonic antigen
cSMAC: central supramolecular activation complex
CT Ag: cancer/testis antigens
CTL: cytotoxic T lymphocytes
Cybr: Cytohesin binder and regulator
CYTIP: cytohesin interacting protein
DC: dendritic cells
dSMAC: distal supramolecular activation complex
EBV: Epstein-Barr Virus
EGF: epidermal growth factor
Fas-L: Fas ligand
FcγR: fragment crystallizable γ receptor
FoxP3: forkhead box protein 3
gp100: protein
GRASP: GRP1-associated scaffolding protein
GTP: guanosine triphosphate
HBV: Hepatitis B Virus
HCV: Hepatitis C Virus
Her2/Neu: human epidermal growth factor receptor 2
HLA: human leukocyte antigen
HPV: Human Papilloma Virus
HTLV-1: Human T-lymphotropic type I Virus
ICAM-1: intercellular adhesion molecule
IFNR: IFN receptor
IgSF: immunoglobulin superfamily
IL: interleukin
INF-*γ*: interferon-*γ*
ITAM: immunoreceptor tyrosine-based activation motifs
JNK: c-Jun N-terminal kinase
KLRG1: killer cell lectin-like receptor subfamily G member 1
KO: knock-out
KSHV: Kaposi’s Sarcoma Herpes Virus
Lck: lymphocyte specific protein tyrosine kinase

LDA: limiting dilution analysis
LFA-1: leucocyte function associated antigen 1
LMP: large multifunctional protease
MAPK: mitogen-activated protein kinase
MART-1/MELAN-A: melanoma antigen recognized by T cells
MDSC: myeloid-derived suppressors cells
MHC: major histocompatibility complex
M-MSV: Moloney murine sarcoma virus
M-MuLV: Moloney murine leukemia virus
MTOC: microtubule-organizing center
NFAT: nuclear factor of activated T cell
NK cells: natural killer cells
NKT: natural killer T cells
PAMPs: pathogen-associate molecular patterns
PHA: phytohemagglutinin
PK-C: protein kinase
PKCθ: protein kinase C theta
PLC-γ: phospholipase C gamma
PMA: phorbol-12-myristate-13-acetate
PMN: polymorphonuclear cells
PRR: pattern recognition receptor
PSA: prostate-specific antigen
PSCDBP: pleckstrin homology Sec7 and coiled coil domains binding protein
pSMAC: peripheral supramolecular activation complex
SNX27: sorting nexin 27
TAA: Tumor-Associated Antigens
Tap: transporter associated with antigen processing
TCM cells: central memory T cells
TCR: T cell receptor
TEM: effector memory T cells
TGF-β: tumor growth factor-β
TIL: tumor infiltrating leukocytes
TIL: tumor infiltrating leukocytes
TN cells: naive T cells
TNFR: tumor necrosis factor receptor
TNF-α: tumor necrosis factor-α
TSA: Tumor-Specific Antigens
TSCM cells: stem cell memory T cells
VLA-4: very late antigen-4
ZAP-70: zeta-chain-associated protein kinase 70

BIBLIOGRAPHY

[1] C. A. Janeway and R. Medzhitov, “Innate immune recognition.,” *Annual review of immunology*, vol. 20, pp. 197–216, Jan. 2002.

[2] T. Kawai and S. Akira, “The role of pattern-recognition receptors in innate immunity: update on Toll-like receptors.,” *Nature immunology*, vol. 11, no. 5, pp. 373–84, May 2010.

[3] S. C. Eisenbarth and R. A. Flavell, “Innate instruction of adaptive immunity revisited: the inflammasome.,” *EMBO molecular medicine*, vol. 1, no. 2, pp. 92–8, May 2009.

[4] B. Amulic, C. Cazalet, G. L. Hayes, K. D. Metzler, and A. Zychlinsky, “Neutrophil function: from mechanisms to disease.,” *Annual review of immunology*, vol. 30, pp. 459–89, Jan. 2012.

[5] Y. Liu and G. Zeng, “Cancer and innate immune system interactions: translational potentials for cancer immunotherapy.,” *Journal of immunotherapy (Hagerstown, Md. : 1997)*, vol. 35, no. 4, pp. 299–308, May 2012.

[6] S. Ostrand-Rosenberg, “Immune surveillance: a balance between protumor and antitumor immunity.,” *Current opinion in genetics & development*, vol. 18, no. 1, pp. 11–8, Mar. 2008.

[7] J. Banchereau and R. M. Steinman, “Dendritic cells and the control of immunity.,” *Nature*, vol. 392, no. 6673, pp. 245–52, Mar. 1998.

[8] C. A. J. T. P. W. M. et al. Janeway, *Immunobiology: the Immune System in Health and Disease*, 5th ed. Garland Science, 2001.

[9] et al. Alberts B, Johnson A, Lewis J, *Molecular Biology of the Cell*, 4th ed. Garland Science, 2002.

[10] A. H. Abbas, Abul K, Lichtman, *Cellular and Molecular Immunology*, 5th ed. Saunders, 2005.

[11] E. Mougneau, S. Hugues, and N. Glaichenhaus, “Antigen presentation by dendritic cells in vivo.,” *The Journal of experimental medicine*, vol. 196, no. 8, pp. 1013–6, Oct. 2002.

[12] R. M. Steinman, D. Hawiger, and M. C. Nussenzweig, “Tolerogenic dendritic cells.,” *Annual review of immunology*, vol. 21, pp. 685–711, Jan. 2003.

[13] D. Martorelli, E. Muraro, A. Merlo, R. Turrini, A. Rosato, and R. Dolcetti, “Role of CD4+ cytotoxic T lymphocytes in the control of viral diseases and cancer.,” *International reviews of immunology*, vol. 29, no. 4, pp. 371–402, Aug. 2010.

[14] Z. Chen and J. J. O’Shea, “Th17 cells: a new fate for differentiating helper T cells.,” *Immunologic research*, vol. 41, no. 2, pp. 87–102, Jan. 2008.

[15] F. Annunziato, L. Cosmi, V. Santarlasci, L. Maggi, F. Liotta, B. Mazzinghi, E. Parente, L. Filì, S. Ferri, F. Frosali, F. Giudici, P. Romagnani, P. Parronchi, F. Tonelli, E. Maggi, and S. Romagnani, “Phenotypic and functional features of human Th17 cells.,” *The Journal of experimental medicine*, vol. 204, no. 8, pp. 1849–61, Aug. 2007.

[16] T. Duhen, R. Geiger, D. Jarrossay, A. Lanzavecchia, and F. Sallusto, “Production of interleukin 22 but not interleukin 17 by a subset of human skin-homing memory T cells.,” *Nature immunology*, vol. 10, no. 8, pp. 857–63, Aug. 2009.

[17] S. Trifari, C. D. Kaplan, E. H. Tran, N. K. Crellin, and H. Spits, “Identification of a human helper T cell population that has abundant production of interleukin 22 and is distinct from T(H)-17, T(H)1 and T(H)2 cells.,” *Nature immunology*, vol. 10, no. 8, pp. 864–71, Aug. 2009.

[18] S. Eyerich, K. Eyerich, D. Pennino, T. Carbone, F. Nasorri, S. Pallotta, F. Cianfarani, T. Odorisio, C. Traidl-Hoffmann, H. Behrendt, S. R. Durham, C. B. Schmidt-Weber, and A. Cavani, “Th22 cells represent a distinct human T cell subset involved in epidermal immunity and remodeling.,” *The Journal of clinical investigation*, vol. 119, no. 12, pp. 3573–85, Dec. 2009.

[19] H. Fujita, K. E. Nograles, T. Kikuchi, J. Gonzalez, J. A. Carucci, and J. G. Krueger, “Human Langerhans cells induce distinct IL-22-producing CD4+ T cells lacking IL-17 production.,” *Proceedings of the National Academy of Sciences of the United States of America*, vol. 106, no. 51, pp. 21795–800, Dec. 2009.

[20] W. J. Grossman, J. W. Verbsky, W. Barchet, M. Colonna, J. P. Atkinson, and T. J. Ley, “Human T regulatory cells can use the perforin pathway to cause autologous target cell death.,” *Immunity*, vol. 21, no. 4, pp. 589–601, Oct. 2004.

[21] M. Miyara and S. Sakaguchi, “Natural regulatory T cells: mechanisms of suppression.,” *Trends in molecular medicine*, vol. 13, no. 3, pp. 108–16, Mar. 2007.

[22] M. H. Andersen and D. Schrama, “Cytotoxic T Cells,” vol. 126, no. April 2005, 2006.

[23] C. Castelli, L. Rivoltini, G. Andreola, M. Carrabba, N. Renkvist, and G. Parmiani, “T-cell recognition of melanoma-associated antigens.,” *Journal of cellular physiology*, vol. 182, no. 3, pp. 323–31, Mar. 2000.

[24] S. Nagata, “Fas-mediated apoptosis.,” *Advances in experimental medicine and biology*, vol. 406, pp. 119–24, Jan. 1996.

[25] E. J. Blott and G. M. Griffiths, “Secretory lysosomes.,” *Nature reviews. Molecular cell biology*, vol. 3, no. 2, pp. 122–31, Mar. 2002.

[26] J. a Trapani and M. J. Smyth, “Functional significance of the perforin/granzyme cell death pathway.,” *Nature reviews. Immunology*, vol. 2, no. 10, pp. 735–47, Oct. 2002.

[27] E. J. Wherry, “T cell exhaustion.,” *Nature immunology*, vol. 12, no. 6, pp. 492–9, Jun. 2011.

[28] L. Gattinoni, C. a Klebanoff, and N. P. Restifo, “Paths to stemness: building the ultimate antitumour T cell.,” *Nature reviews. Cancer*, vol. 12, no. 10, pp. 671–84, Oct. 2012.

[29] S. C. De Rosa, L. a Herzenberg, and M. Roederer, “11-color, 13-parameter flow cytometry: identification of human naive T cells by phenotype, function, and T-cell receptor diversity.,” *Nature medicine*, vol. 7, no. 2, pp. 245–8, Mar. 2001.

[30] W. Weninger, M. a Crowley, N. Manjunath, and U. H. von Andrian, “Migratory properties of naive, effector, and memory CD8(+) T cells.,” *The Journal of experimental medicine*, vol. 194, no. 7, pp. 953–66, Oct. 2001.

[31] F. Sallusto, D. Lenig, R. Förster, M. Lipp, and A. Lanzavecchia, “Two subsets of memory T lymphocytes with distinct homing potentials and effector functions.,” *Nature*, vol. 401, no. 6754, pp. 708–12, Oct. 1999.

[32] E. W. Newell, N. Sigal, S. C. Bendall, G. P. Nolan, and M. M. Davis, “Cytometry by time-of-flight shows combinatorial cytokine expression and virus-specific cell niches within a continuum of CD8+ T cell phenotypes.,” *Immunity*, vol. 36, no. 1, pp. 142–52, Jan. 2012.

[33] S. M. Henson, O. Franzese, R. Macaulay, V. Libri, R. I. Azevedo, S. Kiani-Alikhan, F. J. Plunkett, J. E. Masters, S. Jackson, S. J. Griffiths, H.-P. Pircher, M. V. D. Soares, and A. N. Akbar, “KLRG1 signaling induces defective Akt (ser473) phosphorylation and proliferative dysfunction of highly differentiated CD8+ T cells.,” *Blood*, vol. 113, no. 26, pp. 6619–28, Jun. 2009.

[34] P. Romero, A. Zippelius, I. Kurth, M. J. Pittet, C. Touvrey, E. M. Iancu, P. Corthesy, E. Devevre, D. E. Speiser, and N. Rufer, “Four functionally distinct populations of human effector-memory CD8+ T lymphocytes.,” *Journal of immunology (Baltimore, Md. : 1950)*, vol. 178, no. 7, pp. 4112–9, Apr. 2007.

[35] T. Kambayashi, E. Assarsson, A. E. Lukacher, H.-G. Ljunggren, and P. E. Jensen, “Memory CD8+ T cells provide an early source of IFN-gamma.,” *Journal of immunology (Baltimore, Md. : 1950)*, vol. 170, no. 5, pp. 2399–408, Mar. 2003.

[36] a. D. Judge, X. Zhang, H. Fujii, C. D. Surh, and J. Sprent, “Interleukin 15 Controls both Proliferation and Survival of a Subset of Memory-Phenotype CD8+ T Cells,” *Journal of Experimental Medicine*, vol. 196, no. 7, pp. 935–946, Sep. 2002.

[37] J. T. Tan, “Interleukin (IL)-15 and IL-7 Jointly Regulate Homeostatic Proliferation of Memory Phenotype CD8+ Cells but Are Not Required for Memory Phenotype CD4+ Cells,” *Journal of Experimental Medicine*, vol. 195, no. 12, pp. 1523–1532, Jun. 2002.

[38] D. Hamann, P. A. Baars, M. H. Rep, B. Hooibrink, S. R. Kerkhof-Garde, M. R. Klein, and R. A. van Lier, “Phenotypic and functional separation of memory and effector human CD8+ T cells.,” *The Journal of experimental medicine*, vol. 186, no. 9, pp. 1407–18, Nov. 1997.

[39] L. Gattinoni, E. Lugli, Y. Ji, Z. Pos, C. M. Paulos, M. F. Quigley, J. R. Almeida, E. Gostick, Z. Yu, C. Carpenito, E. Wang, D. C. Douek, D. a Price, C. H. June, F. M. Marincola, M. Roederer, and N. P. Restifo, “A human memory T cell subset with stem cell-like properties.,” *Nature medicine*, vol. 17, no. 10, pp. 1290–7, Oct. 2011.

[40] A. Grakoui, S. K. Bromley, C. Sumen, M. M. Davis, A. S. Shaw, P. M. Allen, and M. L. Dustin, “The immunological synapse: a molecular machine controlling T cell activation.,” *Science (New York, N.Y.)*, vol. 285, no. 5425, pp. 221–7, Jul. 1999.

[41] C. R. Monks, B. A. Freiberg, H. Kupfer, N. Sciaky, and A. Kupfer, “Three-dimensional segregation of supramolecular activation clusters in T cells.,” *Nature*, vol. 395, no. 6697, pp. 82–6, Sep. 1998.

[42] C. R. Monks, H. Kupfer, I. Tamir, A. Barlow, and A. Kupfer, “Selective modulation of protein kinase C-theta during T-cell activation.,” *Nature*, vol. 385, no. 6611, pp. 83–6, Jan. 1997.

[43] K.-H. Lee, A. D. Holdorf, M. L. Dustin, A. C. Chan, P. M. Allen, and A. S. Shaw, “T cell receptor signaling precedes immunological synapse formation.,” *Science (New York, N.Y.)*, vol. 295, no. 5559, pp. 1539–42, Mar. 2002.

[44] N. Valitutti, S Espagnolle, “Immunological Synapse,” 2006.

[45] M. Iwashima, B. A. Irving, N. S. van Oers, A. C. Chan, and A. Weiss, “Sequential interactions of the TCR with two distinct cytoplasmic tyrosine kinases.,” *Science (New York, N.Y.)*, vol. 263, no. 5150, pp. 1136–9, Mar. 1994.

[46] K. V. Salojin, J. Zhang, C. Meagher, and T. L. Delovitch, “ZAP-70 is essential for the T cell antigen receptor-induced plasma membrane targeting of SOS and Vav in T cells.,” *The Journal of biological chemistry*, vol. 275, no. 8, pp. 5966–75, Mar. 2000.

[47] B. L. Williams, B. J. Irvin, S. L. Sutor, C. C. Chini, E. Yacyshyn, J. Bubeck Wardenburg, M. Dalton, A. C. Chan, and R. T. Abraham, “Phosphorylation of Tyr319 in ZAP-70 is required for T-cell antigen receptor-dependent phospholipase C-gamma1 and Ras activation.,” *The EMBO journal*, vol. 18, no. 7, pp. 1832–44, Apr. 1999.

[48] L. P. Kane, J. Lin, and A. Weiss, “Signal transduction by the TCR for antigen.,” *Current opinion in immunology*, vol. 12, no. 3, pp. 242–9, Jun. 2000.

[49] L. A. Pitcher and N. S. C. van Oers, “T-cell receptor signal transmission: who gives an ITAM?,” *Trends in immunology*, vol. 24, no. 10, pp. 554–60, Oct. 2003.

[50] A. Kupfer and G. Dennert, “Reorientation of the microtubule-organizing center and the Golgi apparatus in cloned cytotoxic lymphocytes triggered by binding to lysable target cells.,” *Journal of immunology (Baltimore, Md. : 1950)*, vol. 133, no. 5, pp. 2762–6, Nov. 1984.

[51] J. R. Kuhn and M. Poenie, “Dynamic polarization of the microtubule cytoskeleton during CTL-mediated killing.,” *Immunity*, vol. 16, no. 1, pp. 111–21, Jan. 2002.

[52] E. K. Haddad, X. Wu, J. A. Hammer, and P. A. Henkart, “Defective granule exocytosis in Rab27a-deficient lymphocytes from Ashen mice.,” *The Journal of cell biology*, vol. 152, no. 4, pp. 835–42, Mar. 2001.

[53] J. Feldmann, I. Callebaut, G. Raposo, S. Certain, D. Bacq, C. Dumont, N. Lambert, M. Ouachée-Chardin, G. Chedeville, H. Tamary, V. Minard-Colin, E. Vilmer, S. Blanche, F. Le Deist, A. Fischer, and G. de Saint Basile, “Munc13-4 is essential for cytolytic granules fusion and is mutated in a form of familial hemophagocytic lymphohistiocytosis (FHL3).,” *Cell*, vol. 115, no. 4, pp. 461–73, Nov. 2003.

[54] J. C. Stinchcombe, G. Bossi, S. Booth, and G. M. Griffiths, “The immunological synapse of CTL contains a secretory domain and membrane bridges.,” *Immunity*, vol. 15, no. 5, pp. 751–61, Nov. 2001.

[55] J. C. Stinchcombe and G. M. Griffiths, “The role of the secretory immunological synapse in killing by CD8+ CTL.,” *Seminars in immunology*, vol. 15, no. 6, pp. 301–5, Dec. 2003.

[56] Y. Sykulev, M. Joo, I. Vturina, T. J. Tsomides, and H. N. Eisen, “Evidence that a single peptide-MHC complex on a target cell can elicit a cytolytic T cell response.,” *Immunity*, vol. 4, no. 6, pp. 565–71, Jun. 1996.

[57] M. E. Anderson and T. J. Siahaan, “Targeting ICAM-1/LFA-1 interaction for controlling autoimmune diseases: designing peptide and small molecule inhibitors.,” *Peptides*, vol. 24, no. 3, pp. 487–501, Mar. 2003.

[58] L. Devine, S. L. Lightman, and J. Greenwood, “Role of LFA-1, ICAM-1, VLA-4 and VCAM-1 in lymphocyte migration across retinal pigment epithelial monolayers in vitro.,” *Immunology*, vol. 88, no. 3, pp. 456–62, Jul. 1996.

[59] T. A. Springer, “Traffic signals for lymphocyte recirculation and leukocyte emigration: the multistep paradigm.,” *Cell*, vol. 76, no. 2, pp. 301–14, Jan. 1994.

[60] D. Wong, R. Prameya, and K. Dorovini-Zis, “In vitro adhesion and migration of T lymphocytes across monolayers of human brain microvessel endothelial cells: regulation by ICAM-1, VCAM-1, E-selectin and PECAM-1.,” *Journal of neuropathology and experimental neurology*, vol. 58, no. 2, pp. 138–52, Mar. 1999.

[61] H. Yusuf-Makagiansar, M. E. Anderson, T. V. Yakovleva, J. S. Murray, and T. J. Siahaan, “Inhibition of LFA-1/ICAM-1 and VLA-4/VCAM-1 as a therapeutic approach to inflammation and autoimmune diseases.,” *Medicinal research reviews*, vol. 22, no. 2, pp. 146–67, Mar. 2002.

[62] J. E. Blanks, T. Moll, R. Eytner, and D. Vestweber, “Stimulation of P-selectin glycoprotein ligand-1 on mouse neutrophils activates beta 2-integrin mediated cell attachment to ICAM-1.,” *European journal of immunology*, vol. 28, no. 2, pp. 433–43, Mar. 1998.

[63] S. I. Simon, Y. Hu, D. Vestweber, and C. W. Smith, “Neutrophil tethering on E-selectin activates beta 2 integrin binding to ICAM-1 through a mitogen-activated protein kinase signal transduction pathway.,” *Journal of immunology (Baltimore, Md. : 1950)*, vol. 164, no. 8, pp. 4348–58, Apr. 2000.

[64] E. C. Butcher and L. J. Picker, “Lymphocyte homing and homeostasis.,” *Science (New York, N.Y.)*, vol. 272, no. 5258, pp. 60–6, Apr. 1996.

[65] P. K. Gopalan, C. W. Smith, H. Lu, E. L. Berg, L. V. McIntire, and S. I. Simon, “Neutrophil CD18-dependent arrest on intercellular adhesion molecule 1 (ICAM-1) in shear flow can be activated through L-selectin.,” *Journal of immunology (Baltimore, Md. : 1950)*, vol. 158, no. 1, pp. 367–75, Jan. 1997.

[66] P. A. Detmers and S. D. Wright, “Adhesion-promoting receptors on leukocytes.,” *Current opinion in immunology*, vol. 1, no. 1, pp. 10–5.

[67] C. S. Elangbam, C. W. Qualls, and R. R. Dahlgren, “Cell adhesion molecules--update.,” *Veterinary pathology*, vol. 34, no. 1, pp. 61–73, Jan. 1997.

[68] J. M. Casasnovas, T. Stehle, J. H. Liu, J. H. Wang, and T. A. Springer, “A dimeric crystal structure for the N-terminal two domains of intercellular adhesion molecule-1.,” *Proceedings of the National Academy of Sciences of the United States of America*, vol. 95, no. 8, pp. 4134–9, Apr. 1998.

[69] M. L. Dustin, O. Carpen, and T. A. Springer, “Regulation of locomotion and cell-cell contact area by the LFA-1 and ICAM-1 adhesion receptors.,” *Journal of immunology (Baltimore, Md. : 1950)*, vol. 148, no. 9, pp. 2654–63, May 1992.

[70] G. H. Hersmann, J. Kriegsmann, J. Simon, C. Hüttich, and R. Bräuer, “Expression of cell adhesion molecules and cytokines in murine antigen-induced arthritis.,” *Cell adhesion and communication*, vol. 6, no. 1, pp. 69–82, Jun. 1998.

[71] F. McLaughlin, B. P. Hayes, C. M. Horgan, J. E. Beesley, C. J. Campbell, and A. M. Randi, “Tumor necrosis factor (TNF)-alpha and interleukin (IL)-1beta down-regulate intercellular adhesion molecule (ICAM)-2 expression on the endothelium.,” *Cell adhesion and communication*, vol. 6, no. 5, pp. 381–400, Jan. 1998.

[72] J. C. Porter and N. Hogg, “Integrin cross talk: activation of lymphocyte function-associated antigen-1 on human T cells alters alpha4beta1- and alpha5beta1-mediated function.,” *The Journal of cell biology*, vol. 138, no. 6, pp. 1437–47, Sep. 1997.

[73] C. Abraham, J. Griffith, and J. Miller, “The dependence for leukocyte function-associated antigen-1/ICAM-1 interactions in T cell activation cannot be overcome by expression of high density TCR ligand.,” *Journal of immunology (Baltimore, Md. : 1950)*, vol. 162, no. 8, pp. 4399–405, Apr. 1999.

[74] B. Salomon and J. A. Bluestone, “LFA-1 interaction with ICAM-1 and ICAM-2 regulates Th2 cytokine production.,” *Journal of immunology (Baltimore, Md. : 1950)*, vol. 161, no. 10, pp. 5138–42, Nov. 1998.

[75] T. Labuda, J. Wendt, G. Hedlund, and M. Dohlsten, “ICAM-1 costimulation induces IL-2 but inhibits IL-10 production in superantigen-activated human CD4+ T cells.,” *Immunology*, vol. 94, no. 4, pp. 496–502, Aug. 1998.

[76] B. J. Burbach, R. B. Medeiros, K. L. Mueller, and Y. Shimizu, “T-cell receptor signaling to integrins.,” *Immunological reviews*, vol. 218, pp. 65–81, Aug. 2007.

[77] T. R. Mempel, S. E. Henrickson, and U. H. Von Andrian, “T-cell priming by dendritic cells in lymph nodes occurs in three distinct phases.,” *Nature*, vol. 427, no. 6970, pp. 154–9, Jan. 2004.

[78] M. J. Miller, A. S. Hejazi, S. H. Wei, M. D. Cahalan, and I. Parker, “T cell repertoire scanning is promoted by dynamic dendritic cell behavior and random T cell motility in the lymph node.,” *Proceedings of the National Academy of Sciences of the United States of America*, vol. 101, no. 4, pp. 998–1003, Jan. 2004.

[79] M. L. Dustin and T. A. Springer, “T-cell receptor cross-linking transiently stimulates adhesiveness through LFA-1.,” *Nature*, vol. 341, no. 6243, pp. 619–24, Oct. 1989.

[80] Y. Shimizu, G. A. Van Seventer, K. J. Horgan, and S. Shaw, “Regulated expression and binding of three VLA (beta 1) integrin receptors on T cells.,” *Nature*, vol. 345, no. 6272, pp. 250–3, May 1990.

[81] T. Kinashi, “Intracellular signalling controlling integrin activation in lymphocytes.,” *Nature reviews. Immunology*, vol. 5, no. 7, pp. 546–59, Jul. 2005.

[82] M. L. Dustin, S. K. Bromley, Z. Kan, D. a Peterson, and E. R. Unanue, “Antigen receptor engagement delivers a stop signal to migrating T lymphocytes.,” *Proceedings of the National Academy of Sciences of the United States of America*, vol. 94, no. 8, pp. 3909–13, Apr. 1997.

[83] J. T. Pribila, A. C. Quale, K. L. Mueller, and Y. Shimizu, “Integrins and T cell-mediated immunity.,” *Annual review of immunology*, vol. 22, pp. 157–80, Jan. 2004.

[84] a. Grakoui, “The Immunological Synapse: A Molecular Machine Controlling T Cell Activation,” *Science*, vol. 285, no. 5425, pp. 221–227, Jul. 1999.

[85] M. Mittelbrunn, A. Molina, M. M. Escribese, M. Yáñez-Mó, E. Escudero, A. Ursa, R. Tejedor, F. Mampaso, and F. Sánchez-Madrid, “VLA-4 integrin concentrates at the peripheral supramolecular activation complex of the immune synapse and drives T helper 1 responses.,” *Proceedings of the National Academy of Sciences of the United States of America*, vol. 101, no. 30, pp. 11058–63, Jul. 2004.

[86] C. W. Cairo, R. Mirchev, and D. E. Golan, “Cytoskeletal regulation couples LFA-1 conformational changes to receptor lateral mobility and clustering.,” *Immunity*, vol. 25, no. 2, pp. 297–308, Aug. 2006.

[87] S. Balkow, S. Heinz, P. Schmidbauer, W. Kolanus, B. Holzmann, S. Grabbe, and M. Laschinger, “LFA-1 activity state on dendritic cells regulates contact duration with T cells and promotes T-cell priming.,” *Blood*, vol. 116, no. 11, pp. 1885–94, Sep. 2010.

[88] P. Bousso and E. Robey, “Dynamics of CD8+ T cell priming by dendritic cells in intact lymph nodes.,” *Nature immunology*, vol. 4, no. 6, pp. 579–85, Jun. 2003.

[89] M. Bajénoff, S. Granjeaud, and S. Guerder, “The strategy of T cell antigen-presenting cell encounter in antigen-draining lymph nodes revealed by imaging of initial T cell activation.,” *The Journal of experimental medicine*, vol. 198, no. 5, pp. 715–24, Sep. 2003.

[90] R. J. Creusot and N. A. Mitchison, “How DCs control cross-regulation between lymphocytes.,” *Trends in immunology*, vol. 25, no. 3, pp. 126–31, Mar. 2004.

[91] P. Reichardt, B. Dornbach, and M. Gunzer, “The molecular makeup and function of regulatory and effector synapses.,” *Immunological reviews*, vol. 218, pp. 165–77, Aug. 2007.

[92] C. Heufler, D. Ortner, and S. Hofer, “Cybr, CYTIP or CASP: an attempt to pinpoint a molecule’s functions and names.,” *Immunobiology*, vol. 213, no. 9–10, pp. 729–32, Jan. 2008.

[93] B. Dixon, B. Sahely, L. Liu, and B. Pohajdak, “Cloning a cDNA from human NK/T cells which codes for an unusual leucine zipper containing protein.,” *Biochimica et biophysica acta*, vol. 1216, no. 2, pp. 321–4, Nov. 1993.

[94] H. KIM, “Assignment of the human B3-1 gene (PSCDBP) to chromosome 2 band q11.2 by radiation hybrid mapping.,” *Cytogenet Cell Genet.*, pp. 84(1–2):95, 1999.

[95] M. Mansour, S. Y. Lee, and B. Pohajdak, “The N-terminal coiled coil domain of the cytohesin/ARNO family of guanine nucleotide exchange factors interacts with the scaffolding protein CASP.,” *The Journal of biological chemistry*, vol. 277, no. 35, pp. 32302–9, Aug. 2002.

[96] T. Boehm, S. Hofer, P. Winklehner, B. Kellersch, C. Geiger, A. Trockenbacher, S. Neyer, H. Fiegl, S. Ebner, L. Ivarsson, R. Schneider, E. Kremmer, C. Heufler, and W. Kolanus, “Attenuation of cell adhesion in lymphocytes is regulated by CYTIP, a protein which mediates signal complex sequestration.,” *The EMBO journal*, vol. 22, no. 5, pp. 1014–24, Mar. 2003.

[97] Q. Chen, A. Coffey, S. G. Bourgoin, and M. Gadina, “Cytohesin binder and regulator augments T cell receptor-induced nuclear factor of activated T Cells.AP-1 activation through regulation of the JNK pathway.,” *The Journal of biological chemistry*, vol. 281, no. 29, pp. 19985–94, Jul. 2006.

[98] A. J. MacNeil and B. Pohajdak, “Getting a GRASP on CASP: properties and role of the cytohesin-associated scaffolding protein in immunity.,” *Immunology and cell biology*, vol. 87, no. 1, pp. 72–80, Jan. 2009.

[99] A. J. MacNeil, M. Mansour, and B. Pohajdak, “Sorting nexin 27 interacts with the Cytohesin associated scaffolding protein (CASP) in lymphocytes.,” *Biochemical and biophysical research communications*, vol. 359, no. 4, pp. 848–53, Aug. 2007.

[100] S. Hofer, K. Pfeil, H. Niederegger, S. Ebner, V. A. Nguyen, E. Kremmer, M. Auffinger, S. Neyer, C. Fürhapter, and C. Heufler, “Dendritic cells regulate T-cell deattachment through the integrin-interacting protein CYTIP.,” *Blood*, vol. 107, no. 3, pp. 1003–9, Feb. 2006.

[101] P. Tang, T. P. Cheng, D. Agnello, C. Wu, B. D. Hissong, W. T. Watford, H. Ahn, J. Galon, J. Moss, M. Vaughan, J. J. O. Shea, and M. Gadina, “Cybr , a cytokine-inducible protein that binds cytohesin-1 and regulates its activity,” 2001.

[102] A. a Theodoridis, C. Eich, C. G. Figdor, and A. Steinkasserer, “Infection of dendritic cells with herpes simplex virus type 1 induces rapid degradation of CYTIP, thereby modulating adhesion and migration.,” *Blood*, vol. 118, no. 1, pp. 107–15, Jul. 2011.

[103] W. T. Watford, D. Li, D. Agnello, L. Durant, K. Yamaoka, Z. J. Yao, H.-J. Ahn, T. P. Cheng, S. R. Hofmann, T. Cogliati, A. Chen, B. D. Hissong, M. R. Husa, P. Schwartzberg, J. J. O’Shea, and M. Gadina, “Cytohesin binder and regulator (cybr) is not essential for T- and dendritic-cell activation and differentiation.,” *Molecular and cellular biology*, vol. 26, no. 17, pp. 6623–32, Sep. 2006.

[104] V. Coppola, C. a Barrick, S. Bobisse, M. C. Rodriguez-Galan, M. Pivetta, D. Reynolds, O. M. Z. Howard, M. E. Palko, P. F. Esteban, H. a Young, A. Rosato, and L. Tessarollo, “The scaffold protein Cybr is required for cytokine-modulated trafficking of leukocytes in vivo.,” *Molecular and cellular biology*, vol. 26, no. 14, pp. 5249–58, Jul. 2006.

[105] V. Heib, F. Sparber, C. H. Tripp, D. Ortner, P. Stoitzner, and C. Heufler, “Cytip regulates dendritic-cell function in contact hypersensitivity.,” *European journal of immunology*, vol. 42, no. 3, pp. 589–97, Mar. 2012.

[106] F. M. Burnet, “The concept of immunological surveillance.,” *Progress in experimental tumor research*, vol. 13, pp. 1–27, Jan. 1970.

[107] J. B. Swann and M. J. Smyth, “Immune surveillance of tumors.,” *The Journal of clinical investigation*, vol. 117, no. 5, pp. 1137–46, May 2007.

[108] C. M. Southam, “Immunologic tolerance to human cancer transplants in rats.,” *Cancer research*, vol. 26, no. 12, pp. 2496–502, Dec. 1966.

[109] C. M. Southam, A. Brunschwig, A. G. Levin, and Q. S. Dizon, “Effect of leukocytes on transplantability of human cancer.,” *Cancer*, vol. 19, no. 11, pp. 1743–53, Nov. 1966.

[110] J. Galon, A. Costes, F. Sanchez-Cabo, A. Kirilovsky, B. Mlecnik, C. Lagorce-Pagès, M. Tosolini, M. Camus, A. Berger, P. Wind, F. Zinzindohoué, P. Bruneval, P.-H. Cugnenc, Z. Trajanoski, W.-H. Fridman, and F. Pagès, “Type, density, and location of immune cells within human colorectal tumors predict clinical outcome.,” *Science (New York, N.Y.)*, vol. 313, no. 5795, pp. 1960–4, Sep. 2006.

[111] L. Zhang, G. Widera, S. Bleecher, D. A. Zaharoff, B. Mossop, and D. Rabussay, “Accelerated immune response to DNA vaccines.,” *DNA and cell biology*, vol. 22, no. 12, pp. 815–22, Dec. 2003.

[112] C. Bottino, L. Moretta, and A. Moretta, “NK cell activating receptors and tumor recognition in humans.,” *Current topics in microbiology and immunology*, vol. 298, pp. 175–82, Jan. 2006.

[113] M. H. Manjili, N. Egilmez, K. L. Knutson, S. R. Selvan, and J. R. Ostberg, “Tumor Escape and Progression under Immune Pressure.,” *Clinical & developmental immunology*, vol. 2012, p. 641079, Jan. 2012.

[114] G. P. Dunn, A. T. Bruce, H. Ikeda, L. J. Old, and R. D. Schreiber, “Cancer immunoediting: from immunosurveillance to tumor escape.,” *Nature immunology*, vol. 3, no. 11, pp. 991–8, Nov. 2002.

[115] G. P. Dunn, L. J. Old, and R. D. Schreiber, “The immunobiology of cancer immunosurveillance and immunoediting.,” *Immunity*, vol. 21, no. 2, pp. 137–48, Aug. 2004.

[116] G. P. Dunn, L. J. Old, and R. D. Schreiber, “The three Es of cancer immunoediting.,” *Annual review of immunology*, vol. 22, pp. 329–60, Jan. 2004.

[117] D. Pardoll, “Does the immune system see tumors as foreign or self?,” *Annual review of immunology*, vol. 21, pp. 807–39, Jan. 2003.

[118] J. P. Medema, J. de Jong, L. T. Peltenburg, E. M. Verdegaal, A. Gorter, S. A. Bres, K. L. Franken, M. Hahne, J. P. Albar, C. J. Melief, and R. Offringa, “Blockade of the granzyme B/perforin pathway through overexpression of the serine protease inhibitor PI-9/SPI-6 constitutes a mechanism for immune escape by tumors.,” *Proceedings of the National*

Academy of Sciences of the United States of America, vol. 98, no. 20, pp. 11515–20, Sep. 2001.

[119] H. T. Khong and N. P. Restifo, “Natural selection of tumor variants in the generation of ‘tumor escape’ phenotypes.,” *Nature immunology*, vol. 3, no. 11, pp. 999–1005, Nov. 2002.

[120] L. Zitvogel, A. Tesniere, and G. Kroemer, “Cancer despite immunosurveillance: immunoselection and immunosubversion.,” *Nature reviews. Immunology*, vol. 6, no. 10, pp. 715–27, Oct. 2006.

[121] P. Matzinger, “The danger model: a renewed sense of self.,” *Science (New York, N.Y.)*, vol. 296, no. 5566, pp. 301–5, Apr. 2002.

[122] T. J. Curiel, “Tregs and rethinking cancer immunotherapy.,” *The Journal of clinical investigation*, vol. 117, no. 5, pp. 1167–74, May 2007.

[123] J. P. Higgins, M. B. Bernstein, and J. W. Hodge, “Enhancing immune responses to tumor-associated antigens.,” *Cancer biology & therapy*, vol. 8, no. 15, pp. 1440–9, Aug. 2009.

[124] O. Yaprak, M. Akyildiz, M. Dayangac, B. T. Demirbas, N. Guler, G. B. Dogusoy, Y. Yuzer, and Y. Tokat, “AFP level and histologic differentiation predict the survival of patients with liver transplantation for hepatocellular carcinoma.,” *Hepatobiliary & pancreatic diseases international : HBPD INT*, vol. 11, no. 3, pp. 256–61, Jun. 2012.

[125] H.-L. Tong, Z.-N. Dong, X.-Y. Wen, J. Gao, B. Wang, and Y.-P. Tian, “Impact of chronic kidney disease on serum tumor markers concentrations.,” *Chinese medical journal*, vol. 126, no. 2, pp. 274–9, Jan. 2013.

[126] M. J. Scanlan, A. O. Gure, A. A. Jungbluth, L. J. Old, and Y.-T. Chen, “Cancer/testis antigens: an expanding family of targets for cancer immunotherapy.,” *Immunological reviews*, vol. 188, pp. 22–32, Oct. 2002.

[127] J. Xiao and H.-S. Chen, “Biological functions of melanoma-associated antigens.,” *World journal of gastroenterology : WJG*, vol. 10, no. 13, pp. 1849–53, Jul. 2004.

[128] M. Aris, M. R. Zubieta, M. Colombo, J. M. Arriaga, M. Bianchini, M. Alperovich, A. I. Bravo, M. M. Barrio, and J. Mordoh, “MART-1- and gp100-expressing and -non-expressing melanoma cells are equally proliferative in tumors and clonogenic in vitro.,” *The Journal of investigative dermatology*, vol. 132, no. 2, pp. 365–74, Mar. 2012.

[129] B. Lenormand, M. C. Béné, J. F. Lesesve, C. Bastard, H. Tilly, M. P. Lefranc, G. C. Faure, R. Garand, A. Falkenrodt, G. Kandel, E. Solary, M. Maynadié, M. P. Callat, F. Thouret, M. Monconduit, and J. P. Vannier, “PreB1 (CD10-) acute lymphoblastic leukemia: immunophenotypic and genomic characteristics, clinical features and outcome in 38 adults and 26 children. The Groupe dEtude Immunologique des Leucémies.,” *Leukemia & lymphoma*, vol. 28, no. 3–4, pp. 329–42, Jan. 1998.

[130] J. Placer and J. Morote, “[Usefulness of prostatic specific antigen (PSA) for diagnosis and staging of patients with prostate cancer].,” *Archivos españoles de urología*, vol. 64, no. 8, pp. 659–80, Oct. 2011.

[131] M. Yanuck, D. P. Carbone, C. D. Pendleton, T. Tsukui, S. F. Winter, J. D. Minna, and J. A. Berzofsky, “A mutant p53 tumor suppressor protein is a target for peptide-induced CD8+ cytotoxic T-cells.,” *Cancer research*, vol. 53, no. 14, pp. 3257–61, Jul. 1993.

[132] W. J. Gullick, M. S. Berger, P. L. Bennett, J. B. Rothbard, and M. D. Waterfield, “Expression of the c-erbB-2 protein in normal and transformed cells.,” *International journal of cancer. Journal international du cancer*, vol. 40, no. 2, pp. 246–54, Aug. 1987.

[133] R. T. Javier and J. S. Butel, “The history of tumor virology.,” *Cancer research*, vol. 68, no. 19, pp. 7693–706, Oct. 2008.

[134] A. C. Prats, G. De Billy, P. Wang, and J. L. Darlix, “CUG initiation codon used for the synthesis of a cell surface antigen coded by the murine leukemia virus.,” *Journal of molecular biology*, vol. 205, no. 2, pp. 363–72, Jan. 1989.

[135] L. Chieco-Bianchi, D. Collavo, and G. Biasi, “Immunologic unresponsiveness to murine leukemia virus antigens: mechanisms and role in tumor development.,” *Advances in cancer research*, vol. 51, pp. 277–306, Jan. 1988.

[136] D. Collavo, A. Colombatti, G. Biasi, L. Chieco-Bianchi, and A. J. Davies, “Immune reactivity in the Moloney strain of murine sarcoma virus oncogenesis: requirement of thymus-derived lymphocytes for in vivo protection.,” *Journal of the National Cancer Institute*, vol. 56, no. 3, pp. 603–8, Mar. 1976.

[137] W. Chen, H. Qin, B. Chesebro, M. A. Cheever, W. E. I. Chen, H. Qin, and B. Chesebro, “Identification of a gag-encoded cytotoxic T-lymphocyte epitope from FBL-3 leukemia shared by Friend , Moloney , and Rauscher murine leukemia virus-induced tumors . Identification of a gag-Encoded Cytotoxic T-Lymphocyte Epitope from FBL-3 Leukemia Shared b,” 1996.

[138] a J. Sijts, M. L. De Bruijn, M. E. Ressing, J. D. Nieland, E. a Mengedé, C. J. Boog, F. Ossendorp, W. M. Kast, and C. J. Melief, “Identification of an H-2 Kb-presented Moloney murine leukemia virus cytotoxic T-lymphocyte epitope that displays enhanced recognition in H-2 Db mutant bm13 mice.,” *Journal of virology*, vol. 68, no. 9, pp. 6038–46, Sep. 1994.

[139] G. Milan, a Zambon, M. Cavinato, P. Zanovello, a Rosato, and D. Collavo, “Dissecting the immune response to moloney murine sarcoma/leukemia virus-induced tumors by means of a DNA vaccination approach.,” *Journal of virology*, vol. 73, no. 3, pp. 2280–7, Mar. 1999.

[140] K. Schepers, M. Toebes, G. Sotthewes, F. a Vyth-Dreese, T. a M. Dellemijn, C. J. M. Melief, F. Ossendorp, and T. N. M. Schumacher, “Differential kinetics of antigen-specific CD4+ and CD8+ T cell responses in the regression of retrovirus-induced sarcomas.,” *Journal of immunology (Baltimore, Md. : 1950)*, vol. 169, no. 6, pp. 3191–9, Sep. 2002.

[141] G. Milan, A. Zambon, M. Cavinato, A. Rosato, and D. Collavo, “Dissecting the Immune Response to Moloney Murine Sarcoma / Leukemia Virus-Induced Tumors by Means of a DNA Vaccination Approach Dissecting the Immune Response to Moloney Murine Sarcoma / Leukemia Virus-Induced Tumors by Means of a DNA Vaccination Approach,” 1999.

[142] X. Cao, E. W. Shores, J. Hu-Li, M. R. Anver, B. L. Kelsall, S. M. Russell, J. Drago, M. Noguchi, a Grinberg, and E. T. Bloom, “Defective lymphoid development in mice lacking

expression of the common cytokine receptor gamma chain.," *Immunity*, vol. 2, no. 3, pp. 223–38, Mar. 1995.

[143] Y. Shinkai, G. Rathbun, K. P. Lam, E. M. Oltz, V. Stewart, M. Mendelsohn, J. Charron, M. Datta, F. Young, and A. M. Stall, "RAG-2-deficient mice lack mature lymphocytes owing to inability to initiate V(D)J rearrangement.," *Cell*, vol. 68, no. 5, pp. 855–67, Mar. 1992.

[144] D. Collavo, A. Colombatti, and L. Chieco-Bianchi, "T lymphocyte requirement for MSV tumour prevention or regression.," *Nature*, vol. 249, no. 453, pp. 169–70, May 1974.

[145] G. Biasi, M. Mazzocchi, A. Facchinetti, M. Panozzo, P. Zanovello, D. Collavo, and L. Chieco-bianchi, "Induction of Moloney Murine Sarcoma Virus Tolerance in Adult Mice by Anti-CD4 Monoclonal Antibody Treatment Induction of Moloney Murine Sarcoma Virus Tolerance in Adult Mice by Anti-CD4 Monoclonal Antibody Treatment1," 1990.

[146] S.-L. Chang, C. L.-T. Chang, P.-I. Huang, M.-H. Tao, and W.-C. Yang, "Role of Cybr, a cytohesin binder and regulator, in CD4(+) T-cell function and host immunity.," *Molecular immunology*, vol. 46, no. 16, pp. 3218–23, Oct. 2009.

[147] A. Rosato, S. Mandruzzato, V. Bronte, A. Zambon, B. Macino, F. Calderazzo, P. Zanovello, and D. Collavo, "Role of anti-LFA-1 and anti-ICAM-1 combined MAb treatment in the rejection of tumors induced by Moloney murine sarcoma virus (M-MSV).," *International journal of cancer. Journal international du cancer*, vol. 61, no. 3, pp. 355–62, May 1995.

[148] A. Rosato, V. Bronte, S. Mandruzzato, A. Zambon, F. Calderazzo, G. Biasi, P. Zanovello, and D. Collavo, "Role of adhesion molecules in the immune reaction to M-MSV-induced tumors.," *International journal of cancer. Supplement = Journal international du cancer. Supplement*, vol. 7, pp. 24–7, Jan. 1992.

RINGRAZIAMENTI

Ringrazio la **Prof.ssa Zanovello** e il **Prof.Amadori**
per avermi dato l’opportunità di svolgere l’attività di ricerca presso il
Dipartimento di Scienze Chirurgiche, Oncologiche e Gastroenterologiche
Dell’Università di Padova.

Un ringraziamento particolare al **Dott.Antonio Rosato**,
per il contributo teorico, professionale e umano a questo progetto.